Development of Dual Energy X-ray Absorptiometry Techniques for Bone Mineral Measurement

Mohammad Reza Salamat

Thesis Submitted for the Degree of PhD

University of Edinburgh

December 1998

DECLARATION

The composition of this thesis and, except where stated, the research described therein, are entirely my own work.

M R Salamat

To my wife, my children and my parents

Acknowledgements

I would like to thank my supervisor Dr J Hannan for his kind advice, guidance, criticism and encouragement throughout the course of this project. I also would like to thank Dr D Smith and Dr P Tothill for their useful comments and suggestions on the presentation of this thesis.

Thanks to Ms C Millar and Mr S Cowen for their initial help with using the equipment. I am grateful to Mr C Ferrington for his kind assistance with the computing needs. I also wish to thank Mrs C Ness, the secretary for her kind attitude. I am delighted with Mr G Campbell from the Mechanical and Electronics workshop for making the necessary items for various experiments.

I am thankful to staff in the Department of Medical Physics and Medical Engineering in the Western General Hospital, some neighbouring staff and friends for being my control volunteers. I also very much appreciate the head of department professor W N McDicken for his kindness and advice.

I wish to thank my wife for her tireless patience, encouragement and supportive attitude throughout the entire programme.

The financial support of the government of the Islamic Republic of Iran is also gratefully acknowledged.

INDEX

List of Figures

List of Tables

Abbreviations

A	Area
Al	aluminium
ANOVA	Analysis of variance
BMC	Bone mineral content
BMD	Bone mineral density
BMI	Body mass index (weight/height^2, kg/m^2)
BUA	Broadband ultrasound attenuation
CaHA	Calcium hydroxyapatite
CV	Precision
CoV	Coefficient of variation
DPA	Dual photon absorptiometry
DXA	Dual energy x-ray absorptiometry
F	Fast Spine acquisition protocol
FA	Forearm acquisition protocol
HH	Hologic Hand protocol, new software
MR	Magnetic resonance
P	Performance Spine acquisition protocol
pQCT	Peripheral quantitative computed tomography
QCT	Quantitative computed tomography
QDR	Quantitative digital radiography
QMR	Quantitative magnetic resonance
r	Correlation coefficient
RA	Rheumatoid arthritis patient
ROI	Region of interest
SD	Standard deviation
SOS	Speed of sound
SPA	Single photon absorptiometry
SXA	Single x-ray absorptiometry
Sv	Sievert
TBBMC	Total body bone mineral content
TBBMD	Total body bone mineral density
US	Ultrasound
W	Weight
*	Build up plate used
-	Scans analysed with default linearity correction coefficients

Definition of Some Terms

Auto-scan facility: A scanner facility that allows repeat measurements without the intervention of the operator.

Linearity: A proportional relationship between the measured BMD and correct BMD.

Linearity correction coefficients: The software environment variables that correct for non-linearity with BMD.

Line spacing setting: This measurement shows how much the scanning arm steps between each pass of the scanning arm. The line spacing (or space between the lines) in the Fast Spine acquisition protocol is 0.2007 cm and the line spacing in the Performance Spine acquisition protocol is approximately one half as large as in the Fast Spine protocol. The line spacing in the Forearm acquisition protocol is the same as in the Performance Spine protocol. The line spacing for Whole Body scans is fixed at 1.303 cm.

Resolution: This is the scan line width divided by the number of samples. It has the standard values of 1 mm for the Performance and the Fast Spine acquisition protocols. The resolution for the Forearm acquisition protocol is 0.5 mm. The scan resolution for the Whole Body acquisition protocol is fixed at 2 mm.

Sub-regional analysis: The scanner has a sub-regional body composition facility that allows the measurement of regional body composition.

Threshold: A threshold selects which density values are identified as bone or soft tissue.

Abstract

Osteoporosis is a skeletal disease, reflected by the progressive reduction of bone mass and increased bone fragility which affects 1 in 4 women and 1 in 12 men. One in 5 people sustaining a hip fracture die within 6 months and many more become highly dependent.

Due to the role of bone mineral contribution to the skeletal integrity, quantitative methods of its evaluation are required to assess fracture risk, follow progression of disease and evaluate the effects of treatment. Although there are several risk factors for the prediction of fractures, reduced bone mineral density (BMD) is the strongest predictor. There are several methodologies available for bone mineral measurement. Dual energy x-ray absorptiometry (DXA) has an overall advantage in terms such as precision and radiation exposure. It is a well-established method and has the potential of multi-site measurement. Although DXA is widely used to assess bone mineral of the spine and hip, little use of the technique has been made to investigate other sites of the body. Therefore, appropriate methods were developed to measure the hand, os calcis and tibia. Anomalies of total body DXA were investigated and an alternative method of measurement was developed. A Hologic QDR-1000W DXA system was used for the investigations.

Hand bone mineral measurement is of particular interest in rheumatoid arthritis patients (RA). A hand phantom which provided a convenient means of evaluating various protocols and assessing long term precision was developed and used for the investigations. The conventional protocols differ in factors such as scan speed, linearity, tissue depth dependence and precision. Therefore, four DXA protocols were developed and evaluated for various factors. A new protocol was also evaluated to establish the optimum method of measuring hand bone mineral. The new protocol and the optimum 'developed' method showed no significant difference in terms of precision, linearity, soft tissue, posture dependency or separation of RA and normal subjects. The RA patients had significantly lower hand bone mineral ($P \leq 0.01$) than the normal subjects.

A technique was developed for the assessment of os calcis. An os calcis phantom was constructed and used to assess precision and the effect of size of region of interest (ROI) on precision. In-vitro precise (CV = 0.4%) and linear measurements were achieved independent of the size of ROI and soft tissue. Two different ways of subject positioning and two ROIs for the measurements were established, using a group of subjects. In-vivo precise measurements ($CV \leq 1.1\%$) were achieved for both ROIs. The BMD of the os calcis was measured in a group of normal subjects and also in patients who were diagnosed as osteopenic/osteoporotic based on the spine and/or femur BMD. T-scores for the os calcis were calculated for both ROIs and compared with the spine and femur T-scores in the patient group. There was no significant difference between the patients' T-scores for the spine, os calcis and the femur.

A method was developed for the assessment of the various sections of the lower leg (tibia/fibula). Measurements were linear and soft tissue independent. Precise measurements ($CV \leq 1.4\%$) were achieved for the proximal and total lower leg. The rotation of the legs showed the least effect on BMD measurement of the proximal lower leg. Two groups of normal and osteopenic/osteoporotic patients were compared for the BMD T-score of the various sites of the body. The difference between the groups was more significant at the spine. However, the bone loss at the proximal/distal lower leg was as significant as the bone loss at the femur neck/total femur. Excellent correlation ($r = 0.92$, $p < 0.0001$) was found between the proximal lower leg T-score and the total femur T-score. This correlation was as close as the correlation between the femur neck/total femur and the proximal/distal lower leg BMD T-score.

Anomalies in total body bone mineral have been observed during weight change. A total body index (TBI) was therefore developed which related total bone mineral content to stature. In-vitro and in-vivo effects of changes in weight and soft tissue composition and positioning were investigated, using a whole body phantom and a control group. Two groups of anorexic and normal subjects were compared for the TBI, total body BMD and the spine BMD. TBI showed a higher difference between the anorexic and normal groups than total body BMD and as high as the spine BMD. Precisions of TBI and total body BMD measurements were comparable.

The development of the above methods should also apply to fan beam systems.

Chapter 1

General Introduction

1.1 Osteoporosis

Osteoporosis is a crippling and painful disease which affects 1 in 4 women and 1 in 12 men (National Osteoporosis Society (NOS), 1995a). The progressive decrease in bone mass leads to an increased susceptibility to fractures, which result in substantial morbidity and mortality (Consensus Development Conference, 1993).

Bone mineral areal density (BMD) expressed in units of g/cm^2 is defined as the ratio of BMC/Area, where BMC (g) is the bone mineral content and Area (cm^2) is the bone cross sectional area. Although there are several risk factors for fractures, reduced bone mineral density is the strongest predictor (Leichter et al., 1982; Wasnich et al., 1987; Cummings et al., 1992). Figure 1.1 compares a normal bone with an osteoporotic one.

The first sign that one is suffering from osteoporosis may be a broken bone, often caused by only a minor bump or fall. Any bone may be affected but the forearm, hip, spine and ribs are more at risk of fracture. Very fragile bones may break just by coughing or stretching.

Another sign is loss of height caused by the bones in the spine becoming weak and crushing together. If several are squashed then the spine will start to curve. Dramatic loss of height is more common in male than in female sufferers, with 10% of osteoporotic men suffering a height loss of 5 to 10 inches (NOS 1995b).

If the spine becomes severely deformed, one may have breathing difficulties due to loss of space under the ribs; the head may protrude forward and the stomach may start to bulge. This may reduce mobility and cause changes in lifestyle.

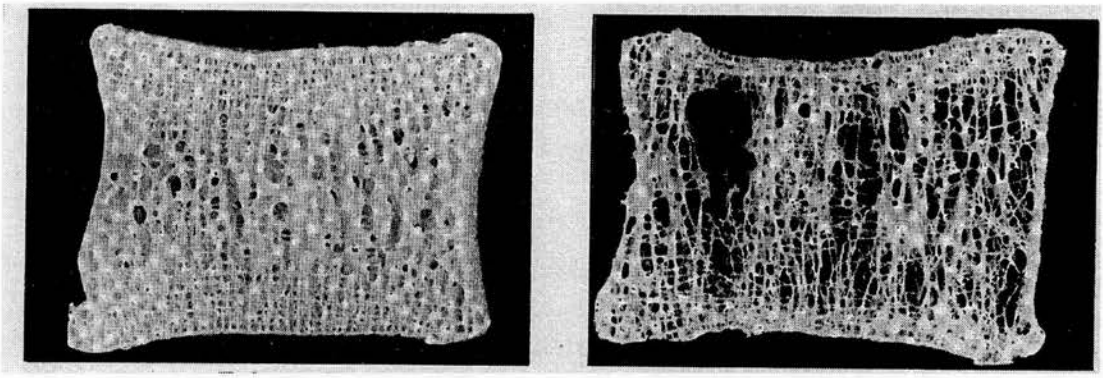

Figure 1.1 Enlarged sections of normal and osteoporotic bone (From NOS, 1995b).

1.2 Health-related and economic costs

1.2.1 Mortality

In Britain substantial evidence is now available that osteoporotic fractures may lead to significant disability and death. Every year there are over 60,000 hip fractures resulting in more than 40 premature deaths a day (NOS, 1995a). Hip fractures are associated with a 20% excess mortality in the initial six months following fracture (Cummings et al., 1985). Recent data suggests that vertebral fractures are also associated with significantly increased mortality (Cooper et al., 1993).

1.2.2 Morbidity

Osteoporotic fractures are associated with serious disability (Cooney, Marottoli 1993). Complications adding to the rehabilitation problems include pneumonia, pressure sores and urinary tract infections. According to the Department of Health, around 50% of hip fracture victims may become totally dependent upon help from others (Minister of Health, 1987).

The annual incidences of morbidity and mortality from the main causes in post-menopausal females are compared in Figure 1.2. The annual incidence of morbidity is

considerably higher in women with osteoporotic fractures than in women having either breast cancer or endometrial cancer or even a combination of both kinds of cancers.

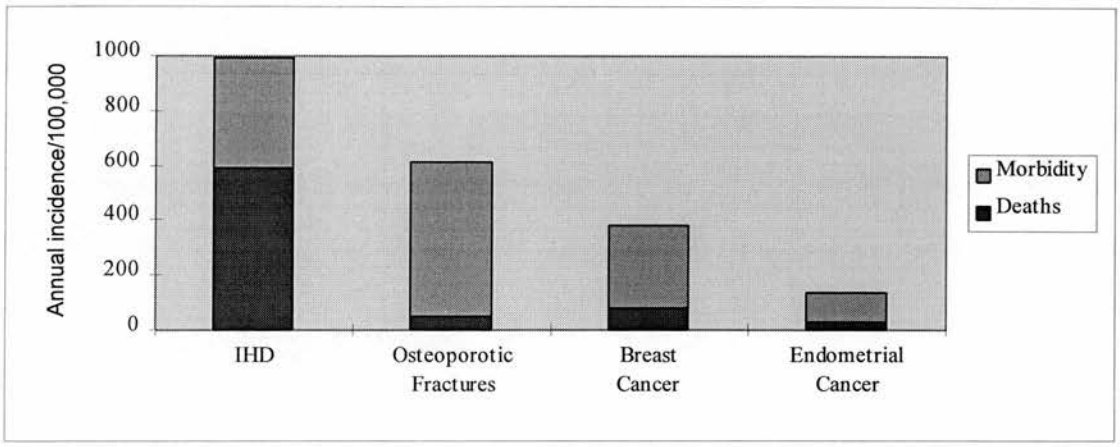

Figure 1.2 Annual incidences of morbidity and death from major causes in post-menopausal women (From Henderson et al., 1986). IHD, Ischemic heart disease.

1.2.3 Economic costs

Osteoporosis causes more than 150,000 fractures each year in the United Kingdom (Compston et al., 1995). Over 10,000 men in the UK suffer fractures of the spine, and 12,000 fractures of the hip (NOS, 1994a). The resulting cost to the National Health Service (NHS) is estimated to be £750 million a year (NOS, 1995b).

1.3 Risk factors

Due to cost and the limited number of bone scanners mass scanning of the population is not possible, so in clinical practice selection of patients for bone assessment should be carried out. People with the following criteria are at high risk of bone loss.

- Women who have had an early menopause (before 45) or an early hysterectomy.
- Women who have suffered in the past from anorexia nervosa or bulimia.
- Women who have over exercised, as do competitive runners.

- Men and women who have already had a fracture after a minor fall.
- Men and women who have lost height due to fracturing vertebrae in the spine.
- People who have been treated with corticosteroids for a long time.
- Patients with a strong family history of osteoporotic fracture. Smokers and heavy drinkers.
- Patients with rheumatoid arthritis, malabsorption, male hypogonadism.
- Patients with cardiac, liver and other transplants as well as immobilising diseases.
- Patients with chronic gastrointestinal disease, liver disease, diabetes, paget's disease or renal lithiasis.
- Hyperthyroidism and over-treatment with thyroxine, renal disease and adrenal disorders.

Race and sex are two of the factors known to affect bone density, so it is necessary to obtain normative data for every population. In order to construct a normal range people with the above criteria should be excluded, because of being at high risk of suffering from the osteoporosis.

1.4 Methodologies for the assessment of bone

Non-invasive techniques for the determination of BMD have been available since the discovery of x-rays by Roentgen in 1895. In the past decade, considerable progress has been made to develop methods to evaluate the skeleton non-invasively to detect osteoporosis at its early stages, its progression and its response to treatment. Clinicians are now able to assess the peripheral, central and entire skeleton as well as trabecular or cortical bone envelopes with a high degree of precision and fairly good accuracy.

The performance of a bone densitometer is characterised by its precision, accuracy and diagnostic sensitivity. Precision reflects the ability of a system to reproduce the same results in repeated measurements. Accuracy means the ability of an instrument to measure the same bone mineral of a subject as measured by another independent 'gold standard' method such as ashing. Diagnostic sensitivity refers to the ability of a system

to differentiate between normal and osteoporotic individuals and to measure age and disease-related bone loss.

1.4.1 Radiographic absorptiometry

Also known as radiographic photodensitometry, radiographic absorptiometry depends upon measuring the optical density of x-ray films of bones and it is the oldest quantitative technique for assessing bone mineral. Although radiographic absorptiometry is an inexpensive and readily available technique its application was initially imprecise. A coefficient of variation (CV) of 9 to 10% was reported by Morgan et al. (1967). Recently developed computer-assisted methods have improved precision (Matsumoto et al., 1994). Yang et al. (1994) performed radiographic absorptiometry for bone mineral measurement of the phalanges; short term precision errors of 1% for BMC and 0.6% for BMD and an accuracy error of 4.8% were reported. Metacarpal, radius, ulna, femur and tibia have all been studied, but measurements of the phalanges where the overlying soft tissue is thinnest, have been more successful.

1.4.2 Single photon and x-ray absorptiometry

Single photon absorptiometry (SPA) was introduced by Cameron and Sorensen (1963). The technique was widely used until recently and then replaced by single x-ray absorptiometry (SXA) due to improved precision and spatial resolution and the shorter scanning time (Bjarnason et al., 1995). Both methods offer measurements of bone at peripheral sites of the skeleton such as distal, ultradistal radius and os calcis. A radionuclide source such as ^{125}I, or small x-ray tube, with a highly collimated photon beam is used to measure radiation attenuation at the measurement site. In addition to these sites, SPA has been applied to the femur, humerus and finger. Nicoll et al. (1987) developed a method to measure bone mineral in the whole hand. SPA/SXA requires a uniform soft tissue thickness and can therefore only measure peripheral sites which can be inserted in a water bath.

Very promising results have recently been published, showing the value of the os calcis (as well as radius) in predicting osteoporotic fractures (Vogel et al., 1988). Both methods provide low exposure to radiation.

1.4.3 Neutron activation analysis

Application of neutron activation analysis to bone mineral determination relies on the fact that 99% of the calcium in the body is in the skeleton. When the body is irradiated with neutrons, many of its constituent elements become radioactive and can be quantified by examining the characteristic gamma ray emission. Anderson et al. (1964) pioneered the technique to show that sodium and chlorine could readily be measured. Chamberlain et al. (1968) pursued the possibility of measuring calcium by this method.

Accuracies based on phantom measurements of about 5% were reported (Tothill 1989). Cohn et al. (1972) found a precision of 1% for anthropomorphic phantoms. Nicoll et al. (1987) found in-vitro and in-vivo precisions of 1.8% and 2.9%, respectively. The original technique for estimation of total body calcium, neutron activation analysis, is largely unavailable, technically difficult, and rarely used, principally because of the high radiation exposure.

For neutron irradiation of part of the body radionuclide sources are used, with a reasonably inexpensive system. Sites studied were the hand (Maziere et al., 1979), forearm and the spine (Smith and Tothill, 1979).

1.4.4 Quantitative computed tomography

Quantitative computed tomography (QCT) determines the true volumetric density (mg/cm^3) of trabecular, cortical or integral bone at any skeletal site. The technique has been employed for the assessment of vertebral fracture risk (Cann et al., 1980), measurement of age-related bone loss (Kalender et al., 1987) and osteoporosis and other metabolic bone diseases (Genant et al., 1987). The validity of QCT for spinal cancellous bone measurement is widely accepted. The typical automatic analysis time for a spine

measurement is a few seconds, and the total imaging time is several minutes. The technique can be performed in single or dual energy modes, which differ in accuracy, precision and radiation (Genant, Boyd 1977). In-vivo precision errors of 2% to 4%, and accuracy errors of 5% to 15% for spinal QCT have been reported (Table 1.1).

Peripheral QCT (pQCT) bone scanners have been used to assess the peripheral skeleton. Initially a radionuclide source (typically ^{125}I) was used. However, more recently x-ray sources are employed (Rüegsegger et al., 1991). pQCT allows for a true volumetric density measurement of appendicular bone. Ease of use and the ability to measure cortical and trabecular bone separately, make the method an ideal alternative to SPA or SXA. In-vivo precisions of 1.7% for the trabecular, 0.8% for the total and 0.9% for the cortical BMD measurements have been reported (Butz et al., 1994). In-vitro accuracy of the method was calculated to be 2% (Durand et al., 1991).

1.4.5 Quantitative ultrasound

The use of quantitative ultrasound (QUS) to estimate skeletal strength has increased in recent years. Its low cost, portability, ease of use and freedom from ionising radiation are its advantages. These benefits, combined with preliminary clinical reports showing good diagnostic sensitivity for fracture discrimination, have encouraged further basic investigation and commercial development. Several QUS systems are now commercially available. These devices measure ultrasound parameters mainly in spongy bone at the calcaneus and patella, cortical bone at the tibia and integral bone at the phalanges. The measured parameters are speed of sound (SOS) and/or the frequency dependency of the attenuation of the ultrasound signal, called broadband ultrasound attenuation (BUA). SOS is measured at the os calcis, tibia, patella and phalanges. More recently, a QUS system that measures SOS along the tibia has become commercially available (SoundScan 2000, 1994). The precisions of SOS and BUA measurements are about 0.3% to 1.2% and 1.3% to 3.8%, respectively (Table 1.1). SOS and BUA can be used together to calculate stiffness. Precision of stiffness is about 2% (Lunar News June 1994). However, it is more appropriate to normalise precision by comparing it with the difference between young normal subjects and osteoporotic patients or the annual decrease in post-menopausal women (Lunar News April 1996).

1.4.6 Quantitative magnetic resonance

Magnetic resonance (MR) has developed considerably since its introduction to clinical science in the early 1970s. Its application is based on high magnetic fields, transmission of radiofrequency (RF) waves and the detection of RF signals from exited hydrogen protons. The MR technique has revolutionised medical imaging. Recently, the potential of quantitative magnetic resonance (QMR) and magnetic resonance microscopy (μMR) for the assessment of osteoporosis has been investigated. Until now, MR imaging techniques have been mostly limited to the study of soft tissue or of gross skeletal structure, because compact bone does not generate any detectable MR signal. However, newly developed QMR techniques have been used to study spongy bone. An in-vivo precision of ~3.5% for trabecular bone has been reported (Ouyang et al., 1995).

1.4.7 Dual photon and x-ray absorptiometry

SPA/SXA measurements are not possible at sites with non-uniform soft tissue thickness such as the axial skeleton, spine, hip or entire body. Therefore, dual photon absorptiometry (DPA) techniques were introduced. The method uses a radionuclide source, typically ^{153}Gd, at two effective energy levels (Mazess, Barden 1987). Dual x-ray absorptiometry (DXA) was introduced commercially as the direct successor to DPA (Stein et al., 1987). DXA uses the same principles as DPA, but in DXA an x-ray tube replaces the radionuclide source. Beams of two distinct energies are either produced by alternately pulsing the x-ray generator at two different voltages or by selectively filtering an x-ray spectrum. The main advantages of an x-ray system over a DPA radionuclide system are improved accuracy and precision due to better resolution and the removal of errors caused by source decay correction. Another advantage is shorter scanning time due to an increased photon flux of the x-ray tube (Kelly et al., 1988).

1.4.8 Comparison of different techniques

Precision, accuracy, radiation dose and the worldwide distribution of different types of bone scanners are shown in Table 1.1. DXA bone densitometers have the highest world wide distribution of over 6000 systems, because they have many advantages, such as the ability to measure the various sites.

Table 1.1 Precision, accuracy and radiation dose of the various techniques (Genant et al., 1996). The main measurement sites and the world wide distribution sites are also shown.

Technique (World distribution) Measurement site	Precision error (%)	Accuracy error (%)	Effective dose (μSv)
Radiographic absorptiometry (500)			
phalanx/metacarpal	1-2	5	~5
SXA/DXA (3000)			
radius/os calcis	1-2	4-6	<1
DXA (6000)			
antero-posterior spine	1-1.5	4-10	~1
lateral spine	2-3	5-15	~3
proximal femur	1.5-3	6	~1
forearm	~1	5	<1
whole body	~1	3	~3
QCT (4000)			
spine trabecular	2-4	5-15	~50
spine integral	2-4	4-8	~50
pQCT (1000)			
radius trabecular	1-2	?	~1
radius total	1-2	2-8	~1
QUS (2000)			
SOS os calcis/tibia	0.3-1.2	?	0
BUA os calcis	1.3-3.8	?	0

Dose for annual background ~2000 μSv, for abdominal radiograph ~500 μSv, for abdominal CT ~ 4000 μSv (Kalender 1992).

1.5 Operating principles of SPA/SXA and DPA/DXA

Figure 1.3 shows the operating principles of SPA in both air (A) and water (B). The absorption is a function of the medium density. It is zero in air and increases as the beam travels through the increasing thickness of soft tissue. As the beam hits a bone, the attenuation increases much more quickly. When the arm is surrounded with soft tissue equivalent material of constant thickness, such as water, attenuation through non-bone

areas becomes constant (Figure 1.3B). The bone mineral content within the scanned path is then proportional to the additional attenuation caused by bone.

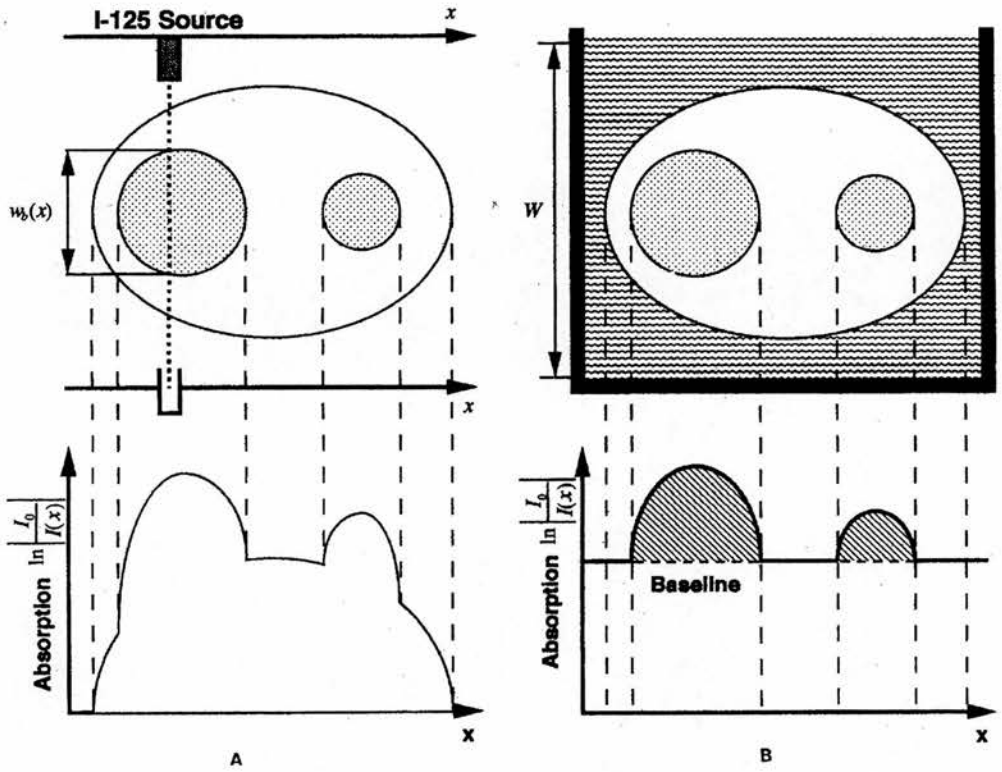

Figure 1.3 Attenuation profiles for (A) a simulated forearm in air and the detector-source (above). (B) the arm surrounded in a water bath with a constant soft tissue thickness around it. The effect on the baseline is evident. (From Wahner and Fogelman 1994).

The soft tissue needs to be of a homogeneous material of constant thickness for the SPA to work; otherwise, an acceptable baseline could not be defined. It is assumed that the measurement site is composed only of bone, muscle and other types of soft tissue that can be closely simulated by water. This condition is not completely met in the forearm. The uniform appearance of the baseline is affected by both the fat surrounding the bone and the subcutaneous fat. For certain measurement conditions, it is essential to correct for this fat.

Figure 1.4 illustrates three types of energy distributions used in DPA/DXA. The attenuation characteristics differ for bone and soft tissue as a function of x-ray photon energy which is the basis for the operating principle of DPA and DXA. These methods register attenuation profiles at two distinct energies. By multiplying the soft tissue attenuation at one energy by a constant so that the difference between the two profiles becomes zero over soft tissue areas, the algorithm creates the same effect as introducing a water bath in SPA.

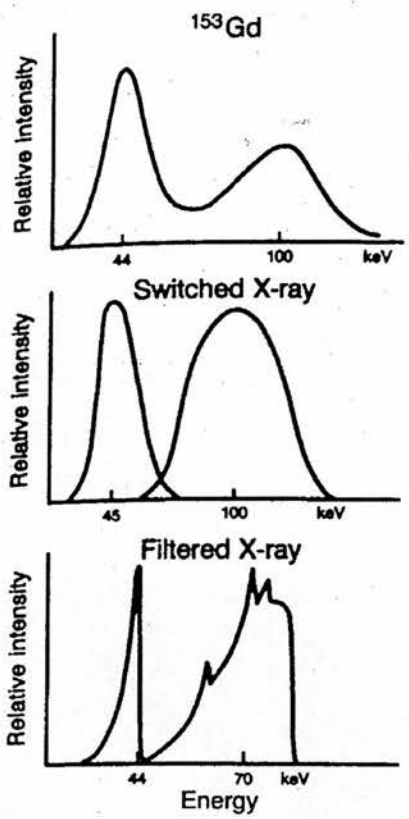

Figure 1.4 Energy spectra for radiation sources used in different bone scanners. (From Wahner and Fogelman 1994).

1.5.1 Different implementations of DXA

There are two types of DXA scanners: the first available one was based on an energy switching x-ray source as introduced by Hologic (1987), and the second type incorporates rare earth filters into a constant-potential x-ray source as introduced by both Lunar (1988)

and Norland (1988) and by Sopha (1989). Both implementations are briefly discussed below.

1.5.1.1 Energy switching

The only widely available system that incorporates energy switching implementation is the Hologic system (Figure 1.5). In this system the x-ray tube potential is rapidly switched between 70 and 140 kVp synchronously with the line frequency. Known amounts of bone and soft-tissue equivalent material need to be interposed into the beam to achieve simultaneous calibration. These materials are mounted on a wheel which has different segments to represent the bone, a soft tissue standard and an empty segment for air values and rotates synchronously with the x-ray pulses.

DXA uses the energy dependence of bone and soft tissue attenuation to estimate bone mineral content. X-ray based systems must account for an effect known as "beam hardening". Beam hardening is due to the absorption of the low-energy photons by the patient's body when subjected to a polychromatic x- ray beam (one composed of many different energies). As a result the proportion of higher energy photons increases with depth inside the body and the x-ray spectrum is said to be "harder". The attenuation coefficient is, therefore, depth-dependent and corrections may be required to compensate for the beam hardening. This phenomenon is reduced in Hologic systems by narrowing the width of the high-energy spectrum with a 2 mm thick brass and aluminium filter. Furthermore, the simultaneous calibration also compensates for beam hardening, because rays travelling through adjacent segments of the calibration wheel are equally affected by it. Finally, corrections are applied during image analysis.

1.5.1.2 Filtered x-ray

In this implementation, the output of a constant-potential x-ray tube is filtered by a rare earth filter (called k-edge filter) to separate the x-ray distribution into two separate high

and low energy components. In comparison to energy switching systems, these systems produce somewhat lower beam hardening due to the narrower spectra.

This system requires pulse counting detectors. Two common problems are associated with this system, namely detector pile-up and energy cross-over. The electronics cannot keep up with the continuous incoming x-ray photons which need to be processed individually in order to determine whether the pulse should be counted in the high or low-energy window. Therefore, some photons may be missed if they hit the detector while the electronics are still engaged in processing a previous pulse. Higher pulse rates encountered in thin body parts or air require to be adjusted by appropriate correction algorithms. Energy cross-over is another phenomenon that influences the pulse counting detector and is caused by high-energy photons erroneously being counted as low-energy photons. This phenomenon is corrected by assigning a fraction of the low-energy counts to the high energy channel.

1.5.2 Total body composition measurements

The DXA technique is also applied successfully to measure both fat mass and lean mass quantities of the whole body. The physical basis for the measurement is that the attenuations of the high and low-energy x-ray beams are dependent upon the composition of the material through which they pass. By using known standards of various effective fat to lean ratios to calibrate the attenuations of the high and low-energy beams, it is possible to measure the fat, lean and total masses as well as the bone mineral values. This involves analysing the "non-bone" pixels using the attenuation coefficients for lean soft tissue and fat, and then interpolating the results for the pixels which contain bone.

1.5.3 Pencil-beam scanners

The main parts of the Hologic QDR-1000W DXA system are illustrated in Figure 1.5. This is the system on which the investigations reported in this thesis were made. In this system photons are emitted from an x-ray source and then are collimated into a beam and pass through the subject's soft tissue and bone, continue the same path and enter a detector where the intensity of the incoming beam is registered. The detector consists of a Nal(Tl) crystal coupled to a photomultiplier operated in current mode. The source collimator and detector are exactly aligned and mechanically coupled. Different size collimators are automatically selected for different scan modes. They move across the subject's body to register a single projection to represent the attenuation profile of a single image line. Choice of speed is effectively obtained by using different inter-line spacing. Data acquisition protocols may employ rectilinear scanning to cover a larger area.

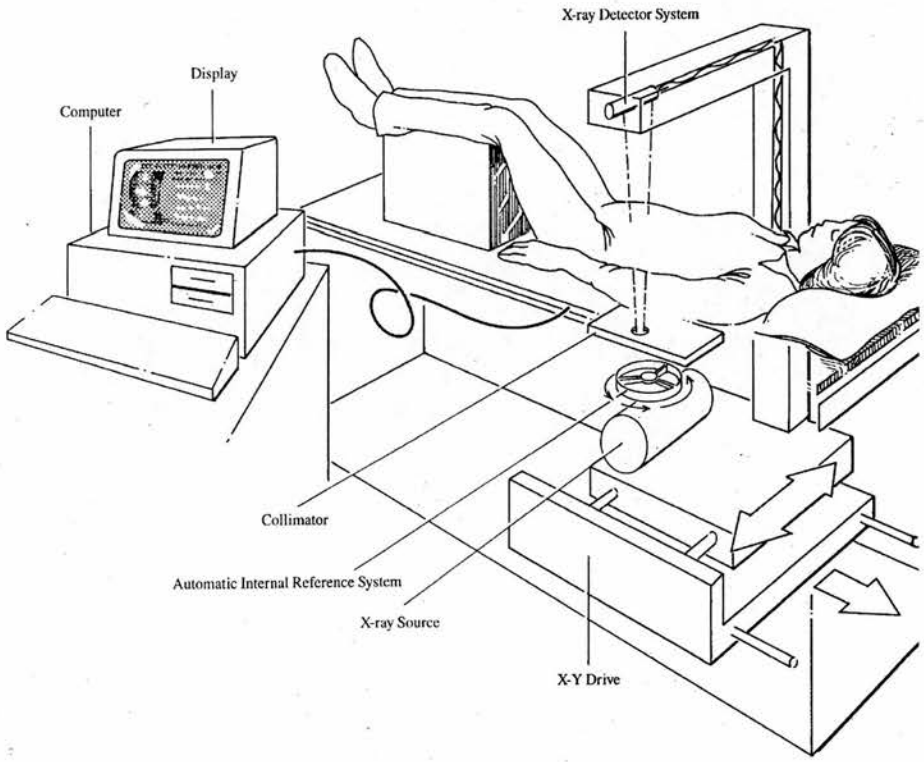

Figure 1.5 Schematic illustration of components of a DXA pencil beam system (Hologic QDR 1000W) capable of scanning the entire body or smaller parts. (From the manufacturer's manual).

1.5.4 Fan-beam scanners

Fan-beam DXA systems use a narrow "slit" x-ray collimator with a multi-element detector array. Both the detector array and x-ray fan beam extend across the width of the region being scanned, requiring the scanning motion to take place only along the length of the scanned region. For the scanning of the hip and spine only a single pass is required, but for the total body three passes are required. The main advantages of fan beam systems are reduced scanning time and improved image resolution; precise hip and spine images can be acquired in typically 1 minute. However, some fan beam systems can also rotate through 90 degrees allowing lateral imaging of the supine spine. The lateral imaging helps to identify artifacts which may influence the anterior-posterior images in many elderly patients. Moreover, the lateral spine imaging can be used to perform vertebral morphometry. Fan beam systems allow a faster and more convenient vertebral morphometry than conventional x-ray morphometry, and result in a lower radiation dose to the patients.

1.6 Aims and outline of the thesis

Initially when DXA scanners became commercially available for bone assessment they had the ability to measure the hip and the lumbar spine. Later, appropriate software was supplied for the measurement of the forearm, whole body and small animals. DXA is an established method with the potential of multi-site bone quality assessment with very low radiation dose. Although DXA is widely used to assess bone mineral of the spine and hip little use of the technique has been made to investigate other sites. This thesis investigates the potential use of DXA in the hand, os calcis and tibia. Total body DXA is used by many centres but anomalies have been reported. These anomalies have been investigated and an alternative method of assessing total body bone mineral has been developed.

The thesis is organised into six chapters. The first chapter discusses the health and economic aspects of osteoporosis. It gives a brief discussion of the various methods of assessing bone mineral, a more detailed description of DXA and describes the aims and outline of the thesis. The studies on individual bone measurement sites are described in chapter 2 to 5, which each contain an introduction section, followed by a materials and methods section, results, discussion and conclusions.

Chapter 2 describes the significance of hand bone mineral assessment and the problems associated with the measurements of the hand in rheumatoid arthritis patients (RA). A hand phantom was developed and used to study how changes in soft tissue and hand posture affect the measured bone mineral. Six methods of measurements, including software recently released by the manufacturer were assessed. In-vitro and in-vivo precisions were also assessed. The optimum method was used to compare hand bone mineral in RA patients and normals.

Chapter 3 explains the need for the assessment of os calcis bone density. In this chapter a method for the measurement of the os calcis bone mineral was established. The in-vitro and in-vivo precisions and the factors that might affect the measurements were assessed. Two groups of osteopenic/osteoporotic and normal women were compared. The difference in os calcis bone density between the patient and control groups was compared with the corresponding differences for the spine and hip.

Chapter 4 describes the development of a method to measure bone mineral of the lower leg (tibia/fibula). The effect of rotation of the leg was investigated and precision for various sections of the leg were measured. Correlations between BMD T-scores at different sites of the body and sections of the lower legs were also assessed. Two groups of normal and osteopenic/osteoporotic patients were compared for the various sections of the lower leg, spine, femur neck/total femur and total body using the World Health Organisation (WHO) criteria of normal, osteopenia and osteoporosis.

Chapter 5 investigates an anomaly in total body bone mineral measurements. In order to find a possible explanation for the observed anomaly in-vitro and in-vivo measurements were carried out. Appropriate measures were made to establish an alternative index for the total body bone mineral measurements (TBI). Precision and the difference in TBI, total body bone mineral content/density and spine BMD were compared for two groups of anorexic and normal subjects.

Chapter 6 summarises the findings of the preceding chapters and makes recommendations for future work.

Chapter 2

Development of Hand Bone Mineral Measurements by DXA

2.1 Introduction

One of the earliest radiological changes in rheumatoid arthritis (RA) is that of juxta-articular bone loss, or osteopenia, affecting the hands and feet (Bywaters 1960). However, radiological osteopenia does not become apparent until a considerable proportion of bone is lost.

Tothill (1986) showed that the mean hand bone mineral content (BMC) in a group of 56 patients with RA was 82 percent of normal, confirming the importance of peri-articular loss. Most of the patients with established RA will have disease localised to the small joints of the hand; for example in patients who had active disease for two years the loss of BMC was 33% (Nicoll et al., 1987a)

Using SPA Reid et al. (1988) compared two groups of controls (20M / 58F) and RA patients (18M / 40F). Hand BMC was significantly reduced in female (24.1%, $P < 0.001$) and male (13.5%, $P = 0.002$) patients with RA receiving non-steroidal anti-inflammatory drugs.

Cartilage and bone resorption are typical features of early RA which are traditionally recognised by radiological signs of joint space narrowing, peri-articular osteoporosis and marginal joint erosions (North et al., 1994). Peri-articular bone mass has been found to be decreased in RA using metacarpal indices (Reid et al., 1986).

Quantification of juxta-articular bone loss could be a sensitive index of joint damage (Peel et al., 1994). Since the hand has a large number of such sites compared with its bone mass, it may be a more sensitive indicator of disease status than other sites of the

body.

Measurement of forearm BMC by SPA using ^{125}I as the isotope source was an established technique (Cameron et al., 1968). Neutron activation analysis to measure bone in-vivo has been applied to the hand (Catto et al., 1973 and Maziere et al., 1979). Maziere et al. (1979) compared activation analysis of hand calcium using ^{252}Cf (132 controls, 45 osteoporotics) with SPA in radial epiphyses (37 controls, 13 osteoporotics) and found a strong correlation between the two. They preferred the NAA technique, which gave a coefficient of variation of 2.4% for repeated measurements of ten controls compared with 3.6% for the SPA. Some SPA measurements were abandoned because results could not be reproduced. Maziere's preference for NAA of the hand was based upon the site of the measurement rather than upon the technique. The technique was cumbersome and involved a high radiation dose to the hand of 7.5 mSv. Nicoll et al. (1987b) developed a method for hand BMC measurement using SPA, finding a measurement precision error of 1.9% in control population. The drawbacks of the technique are the poor resolution of the images and the inclusion of the distal radius and ulna in the hand region of interest.

DXA could potentially offer many advantages for the assessment of hand bone mineral. The equipment is widely available and the precision obtained for other sites suggests that adequate precision for the hand could be achieved to allow progression and treatment of RA to be monitored. The effective dose for the measurement of hand bone mineral by DXA has been shown to be only 0.06 μSv (Pye and Law, 1990). However, there are particular problems associated with the measurement of hand bone mineral in RA patients which must be thoroughly evaluated. RA is a progressive disease characterised by inflammation and swelling of the joints and the hand may become progressively more distorted. It is therefore important to assess how changes in soft tissue and hand posture affect the measured bone mineral. The optimum technique should be linear, precise and relatively independent of soft tissue thickness and hand posture. The time required to acquire the scan is another important factor.

Six DXA protocols have been evaluated to establish the optimum method of measuring hand bone mineral in patients with RA. The available protocols differ in terms of pixel size, scan speed, line spacing, linearity correction factors and bone density threshold. The linearity correction factors are used to correct for beam hardening effects and the factors used by the manufacturer are appropriate for particular ranges of bone density and tissue thickness. The linearity factors for the range of bone density and tissue thickness appropriate to the hand were established using known amounts of calcium hydroxyapatite (CaHA). The effects of bone density threshold and hand posture on BMC and BMD were evaluated using aluminium tubes embedded in perspex. Aluminium was used to simulate bone because it is a low density material with an atomic number close to average atomic number of the CaHA. The effects of soft tissue thickness were assessed using an aluminium step wedge. A hand phantom was constructed and used to assess the precision of the various protocols. The effects of using a build up plate were evaluated. In-vivo precision and the effect of hand posture were assessed in a group of normal subjects. Prediction equations for hand BMD and BMC in normal subjects were used to derive indices of hand bone mineral which were then used to compare normal subjects and patients with RA. From the combination of the in-vitro results and the measurements in normal subjects and patients with RA the optimum technique for the measurement of hand bone mineral has been established. The precision of the method and therefore its ability to monitor changes with disease progression or treatment has been assessed.

2.2 Methods and materials

2.2.1 Derivation of linearisation values

Measurements of BMD by the standard Hologic Spine and Forearm software are dependent on the soft tissue thickness (Tothill and Avenell, 1994), and non- linear in the hand BMD range. This non-linearity, i.e. a non-proportional relationship between the measured BMD and correct BMD values, leads to errors in the estimation of hand BMD.

To overcome the dependency of soft tissue thickness, the method of Pye and Law (1990) was used to determine the appropriate linearity correction factors. Measurements were performed with and without a build up plate. These linearity correction coefficients are the software environment variables that correct for non-linearity with BMD. Therefore, the current Forearm and Spine protocol linearity correction coefficients were over-written by the acquired linearity correction coefficients for hand bone mineral measurements.

2.2.2.1 Spine acquisition method with and without the use of a build up plate

The first step was to produce a calibration for the CaHA equivalence of an aluminium step wedge. Four dishes of CaHA, 5cm diameter and 2.5 mm, 5 mm, 10 mm and 15 mm depths with known weights of CaHA were used. They were scanned three times through a build up plate, consisting of 4.5 mm aluminium alloy (EH30) and 20 mm Poly-methyl-methacrylate (Perspex). An aluminium step wedge (0.8, 1.6, 3.2, 5.6, 8.0 mm) was scanned under the same conditions.

To derive linearisation values for Spine mode without the use of the build up plate, the same procedure was followed but a 20mm "perspex plate" for the soft tissue was used. The reason for using the perspex plate for acquiring the appropriate linearisation values was because the software did not recognise any bone without enough soft tissue adjacent to it.

2.2.2.2 Forearm acquisition method with and without the use of a build up plate

The same procedure as above was used to obtain the linearity correction values for the Forearm method with and without the use of the build up plate.

2.2.3 In-vivo measurements

The hands of five healthy male and female subjects were scanned in Forearm mode to detect the percentage change in BMC and BMD from a reference point (ulna radius junction). 10 subjects (7M/3F) of different ages (25 - 55 y) had scans of hands in two postures of relaxed flat and loose-clenched in Forearm acquisition method to find the most appropriate bone threshold with the least BMC change between the two hand postures. The hand was held in two different postures of relaxed flat and loose-clenched alongside the manufacturer's forearm support to minimise the precision error due to positioning. Precision was from duplicate measurements in 11 healthy subjects (7M / 4F) of both sexes, for modified Forearm, Spine (performance and fast), as well as the newly developed Hand software in both speeds.

To find how patients with established RA can be separated from controls, age, height, weight and body mass index (BMI = weight/height^2) were matched. The previously acquired scans (Table 2.1) from Scothern et al. (1993) were reanalysed using *HH (P). They measured BMC, BMD and hand function and pain in both the dominant and non-dominant hand in two groups of RA patients (n = 42) and controls (n = 25). In that study a Hologic QDR-1000W scanner and modified spine protocol were used.

The details of healthy control subjects and RA for both sexes are shown in Table 2.1. The control subjects were all active, in good health with no known history of disease that might influence bone metabolism.

Table 2.1 Physical characteristics of control subjects and RA patients. The number of subjects is shown in brackets. The results are expressed as the mean ± SD and the range.

		Age (y)	Height (m)	Weight (kg)	BMI (kgm^{-2})
F	Control	56.1 ± 10.7	1.61 ± .06	64.3 ± 9.2	24.2 ± 3.2
e	(24)	39.7 - 71.8	1.49 - 1.69	39.1 - 78.0	16.5 - 31.1
m					
a					
l	RA	61.1 ± 9.5	1.61 ± .06	63.1 ± 11.0	24.3 ± 3.6
e	(26)	43.1 - 80.1	1.49 - 1.70	43.0 - 86.7	19.3 - 30.4
s					
M	Control	43.0 ± 19.0	1.73 ± .05	85.4 ± 21.7	28.0 ± 5.9
a	(15)	19.8 - 74.1	1.68 - 1.82	61.8 - 125	21.5 - 37.6
l					
e	RA	54.7 ± 11.8	1.72 ± .05	71.6 ± 12.4	24.2 ± 3.8
s	(12)	26.5 - 66.1	1.65 - 1.79	46.3 - 90.0	17.0 - 30.8

Figure 2.1a shows a photograph of the DXA bone mineral assessment of a volunteer's hand.

2.2.4 In-vitro measurements

The typical range of BMDs for a human hand was obtained using the Forearm sub-region protocol. A set of 4 aluminium tubes were made having equivalent BMDs close to those of fingers and equal external diameters of 8.0 mm and internal diameters of 7.0, 6.7, 6.3 and 6.0 mm. The tubes weighed 1.54, 1.96, 2.41 and 2.85 grams, respectively. All tubes had the same length of 50 mm and were covered with perspex tubes with wall thicknesses of 2.5 mm.

To assess the effect on the bone mineral of threshold, bone wall thickness, height above the scanner couch and angle of inclination, the same aluminium tubes were used. For every experiment a mean of 3 measurements was taken. To investigate the linearity and the effect of soft tissue depth on bone mineral the aluminium step wedge was used.

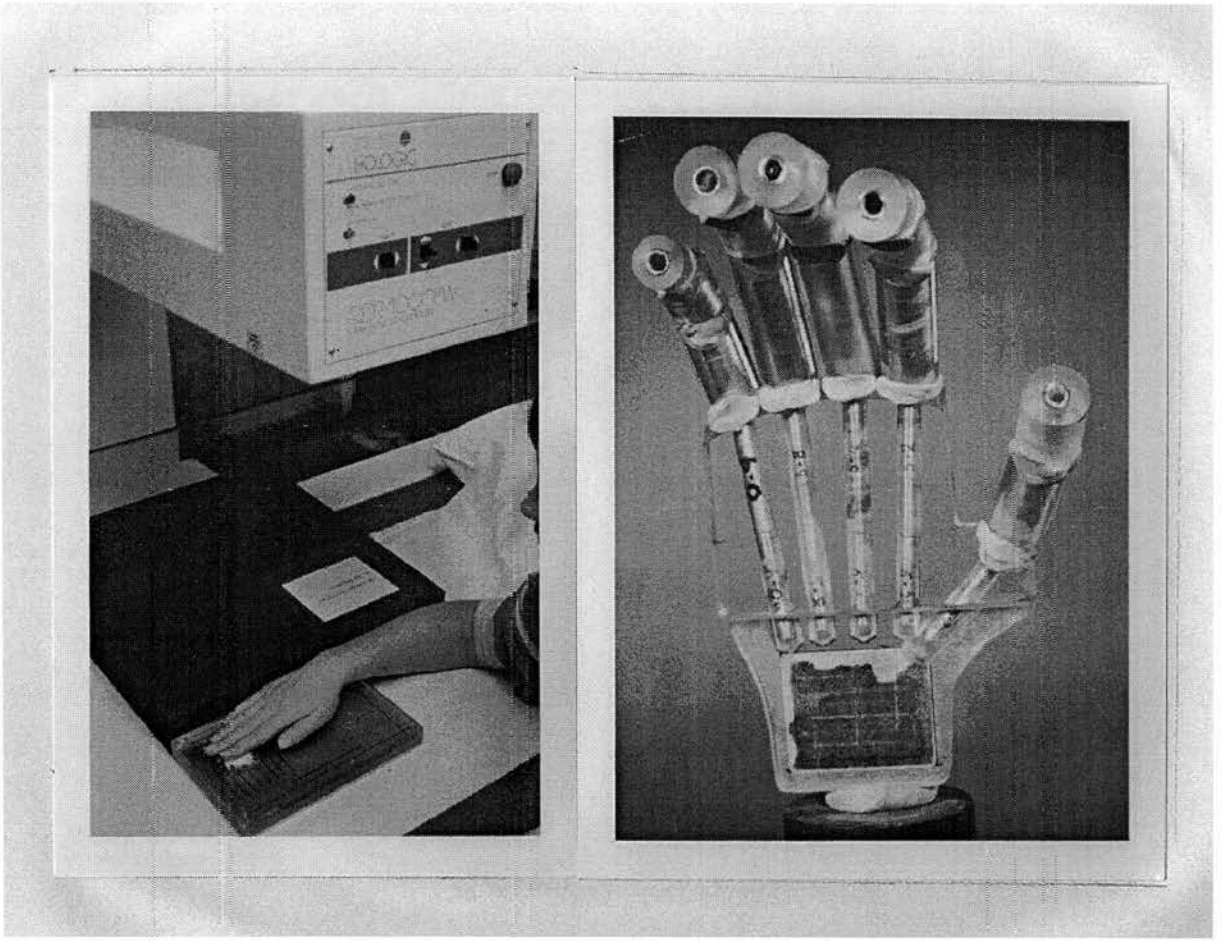

Figure 2.1a DXA bone mineral assessment of a volunteer's hand.

Figure 2.1b Hand phantom for investigation of various protocols and assessing the long term precision.

To provide a convenient means of investigating various protocols and assessing long term precision, a hand phantom was designed (Figure 2.1b). The hand phantom was made out of aluminium tubes and a rectangular aluminium slab to mimic the fingers and bones in the wrist. They were covered with perspex to simulate the soft tissue.

2.2.5 Statistics

Linear regression analysis was used to find the correlation between BMC and BMD measured by different protocols. Linear regression analysis was also used to find the correlation of BMC and BMD with age, height and weight.

Bland and Altman's (1986) statistical method was used for assessing agreement between two methods of bone mineral measurements. This method was used wherever a correlation coefficient was obtained, to reassure that there was good agreement between two methods or two variables over the entire range. Analysis of variance (ANOVA) was performed to determine any significant difference among different protocols for precision.

A paired t-test was performed to find the significance of the reduction in the mean percentage change for two different hand postures using different thresholds. An un-paired t-test was performed to examine if the difference between the healthy controls and RA was significant. A paired t-test was used to determine whether there was a significant difference in BMC or BMD for the control subjects when the new linearity correction factors were used rather than the original factors. For the above analysis Origin™ Graphical Package (1994) was used.

Due to the correlation of hand bone mineral variables with age and size, the biological variance in BMC and BMD could be reduced by expressing the subjects' results as ratios of BMC/BMC_p and BMD/BMD_p, where BMC_p and BMD_p were predicted values obtained using equations derived from the multiple regression analysis. For this analysis Unistat® Statistical Package (1995) was used.

2.3 Results

2.3.1 Linearity

2.3.1.1 CaHA and aluminium step wedge

Figure 2.2(a) compares the BMD measured for the CaHA dishes with the known BMD, using the standard performance Spine method with the use of the build up plate ('P method). The line of identity is also shown and it can be seen that the slope is significantly greater than unity (B = 1.13). Figure 2.2(b) shows the BMD of the aluminium step wedge as a function of thickness for both the default and modified 'P protocols. This shows that the default protocol was unable to detect the first step which had a BMD of Approximately 0.18 g/cm^2. The modified protocol detected the first step and gave a response which was linear over the range 0.18 - 0.7 g/cm^2.

Figure 2.2(c) shows the corresponding results for the aluminium tubes. Again the default protocol failed to detect the first three tubes, whereas the modified protocol identified all four tubes, with values of BMD which were linear over the entire range. This emphasises the importance of using linearity correction factors which are appropriate to the ranges of bone mineral density and soft tissue thickness in a particular anatomical site.

Figure 2.3a shows the measured aluminium step wedge BMD as a function of thickness for the various protocols. The Figure shows a slope of 0.216 ± 0.005 (g/cm^2)/mm wedge thickness and a significant intercept of 0.07 ± 0.02 for the Forearm acquisition mode with the default linearity correction coefficients ('FA). The 'FA technique was improved when the scans were reanalysed with the appropriate linearity correction coefficients (FA) showing an insignificant intercept of 0.008 ± 0.01 and the same slope of 0.216 ± 0.003

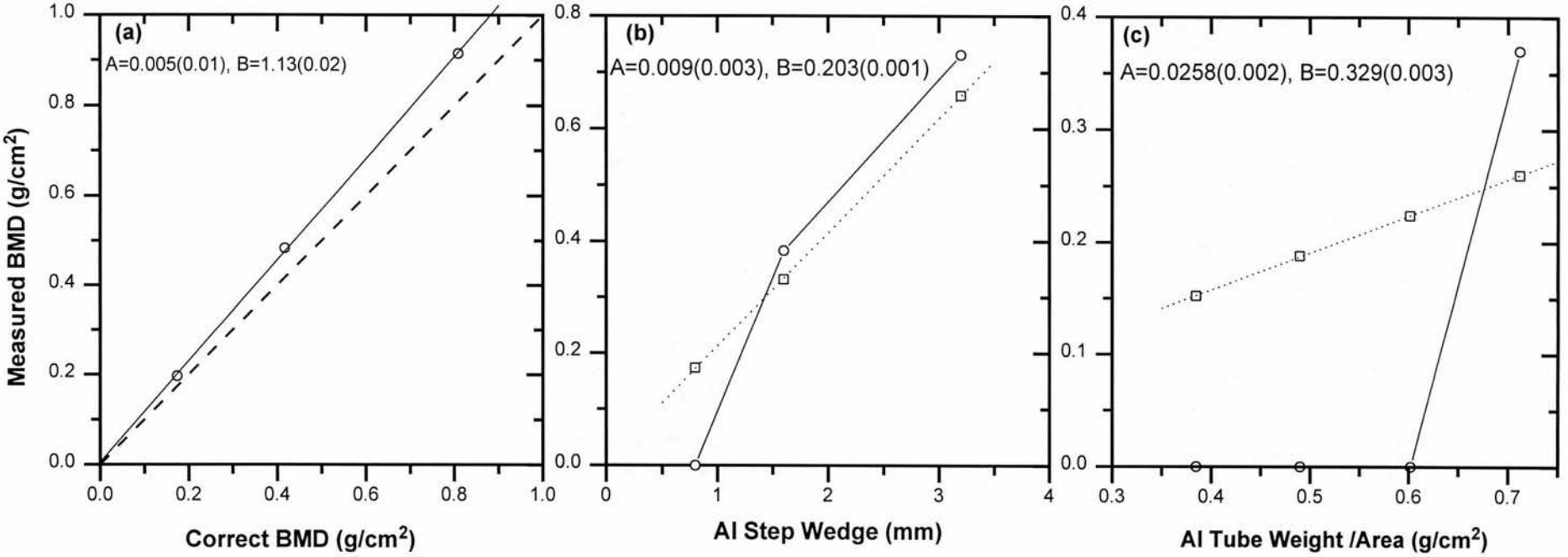

Figure 2.2 Linearity for the measurement of hand, using a 'developed' protocol. (a) DXA scans of CaHA dishes with the *P method, analysed with the default software. The dashed line is the line of identity. (b) BMD of Al step wedge as a function of thickness. (c) BMD of Al tube for different wall thickness. N.B. in (b) and (c) the solid lines are the default trends and the dotted lines are the least square fits to the data obtained with the modified software.

Hologic's newly developed Hand software (*HH i.e. scans taken under the performance spine (P) mode using the build up plate) gave a significant offset of -0.037 ± 0.01 and a gradient of 0.237 ± 0.003. Reanalysing the scans and applying the appropriate linearity correction coefficients in the Spine analysis software gave a non-significant intercept of 0.025 ± 0.012 and slope of 0.193 ± 0.004.

However, the differences in slope and intercept between the different protocols can be appreciated more easily by considering the percentage changes in BMD corresponding to a 10% change from an initial thickness of 1.25 mm, equivalent to 0.26 g/cm^2 of CaHA and are shown in bold in Figure 2.3. The changes varied from 7.9 to 11.4%.

Figure 2.3b shows the plots of measured CaHA BMDs versus the correct values for different methods. The -FA showed a significant intercept of 0.080 ± 0.107. When the scans were reanalysed using the acquired linearity correlation coefficients (FA), the intercept was significantly improved to 0.022 ± 0.021.

The *HH method yielded a considerably higher slope than 1.00 by almost 11% with an insignificant offset. Scans performed under the Performance Spine method (P) using the build up plate analysed with the appropriate linearity correction coefficients (*P) showed an intercept of 0.031 ± 0.029 and 0.926 ± 0.034 which would be improved if the results of the first three dishes were plotted (A = 0.0009 ± 0.011 and B = 1.008), i.e. having a BMD range of 0.17 - 0.80 g/cm^2. This BMD range is within low RA patients' hand BMD and high normal subjects' hand BMD.

To appreciate the real differences between the slopes and intercepts and assuming a 10% increase in BMD with an initial value of 0.24 g/cm^2, different methods show different estimates of 7.5%, 9.2%, 10.3% and 8.8% for the -FA, FA, *HH and *P protocols, respectively (Figure 2.3b).

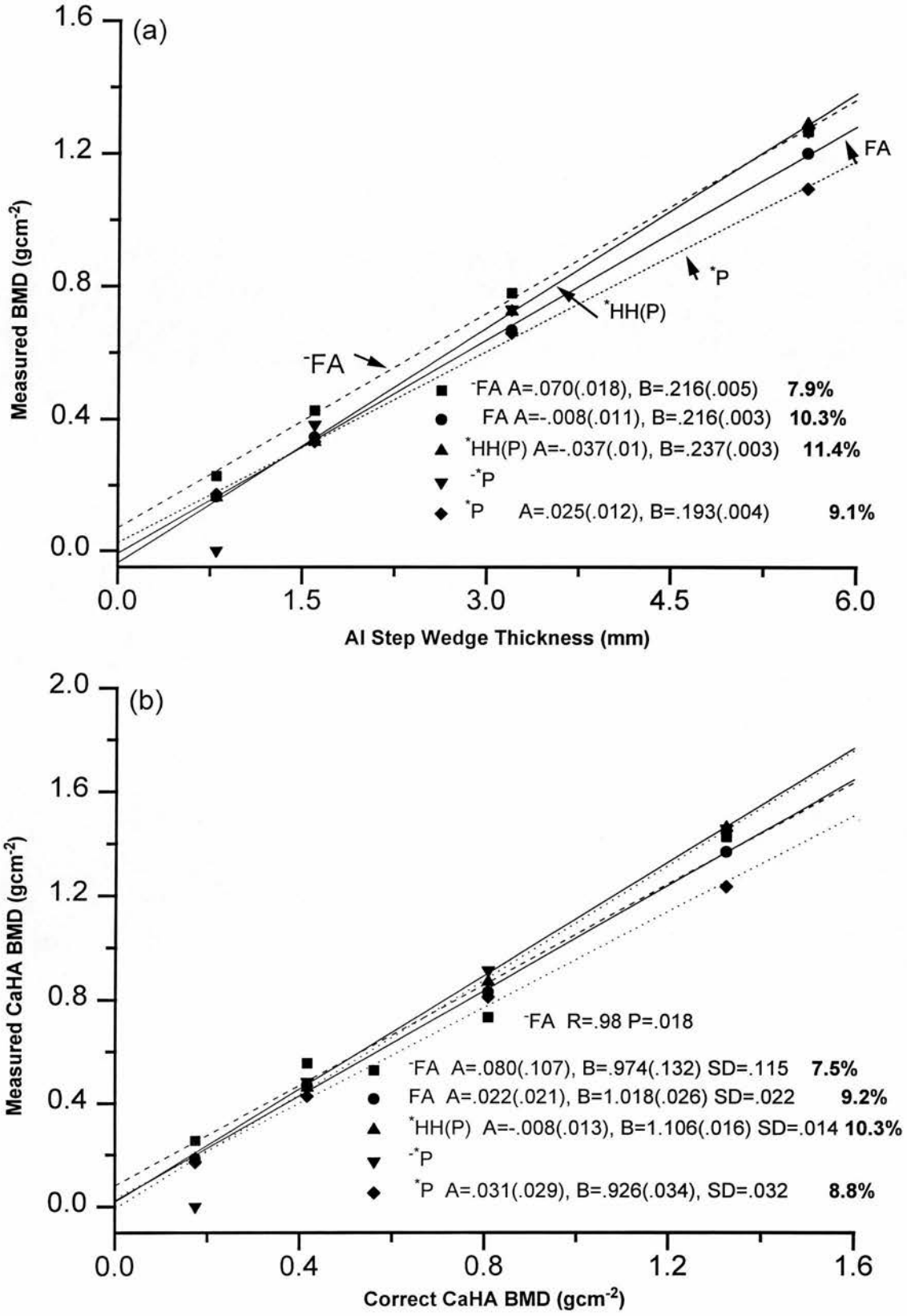

Figure 2.3 Linearity for the various protocols, (a) between the measured Al step wedge BMD and the Al step wedge thickness, (b) between the measured CaHA BMD and the correct CaHA BMD. The numbers shown in bold are the % change in BMD for an increase of 10% in the correct CaHA BMD. In all cases R>0.999, P 0.003.

2.3.1.2 Aluminium tubes

Figure 2.4 shows the regression of BMD on weight/area (W/A) for the aluminium tubes, for the FA (as an example) with and without use of the build up plate. The data was obtained with the tubes held in different positions, i.e. on the plane surface, 8cm above and inclined at 40° to the bone densitometer table.

Table 2.2 tabulates the results obtained from Figure 2.4 and other graphs for the various protocols. The Table shows the BMD gain for a 10% increase in the tube W/A for different methods and positions. For an initial value of W/A = 0.7g/cm^2, there were no significant differences in the predicted BMD for similar conditions. There was an exception that a significant difference between the *HH and *P protocols was observed when the tubes were inclined with respect to the densitometer couch plane surface.

Table 2.3 summarises the corresponding linearity results for BMC. In this case, the changes in measure BMC for a true change of 10% were calculated for an initial weight of 2.8g. For the FA protocol there were no significant differences in linearity with or without the build up plate when the tubes were in any particular position or orientation. The *P method showed almost the same 10% gain in BMC with a 10% increase in tubes weight, unless the tubes were at an inclined angle. *HH (P) and *HH (F) the recent Hologic's hand software showed similar results for all tubes' positions. When tubes were at an inclined angle, both protocols showed a higher variance from the mean results compared to the other two positions.

2.3.2 Effect of threshold

The 'threshold' is used to select which density values are identified as bone and which are considered to be soft tissue. The effect of threshold on BMD and BMC was assessed by re-analysing the scans of the aluminium tubes.

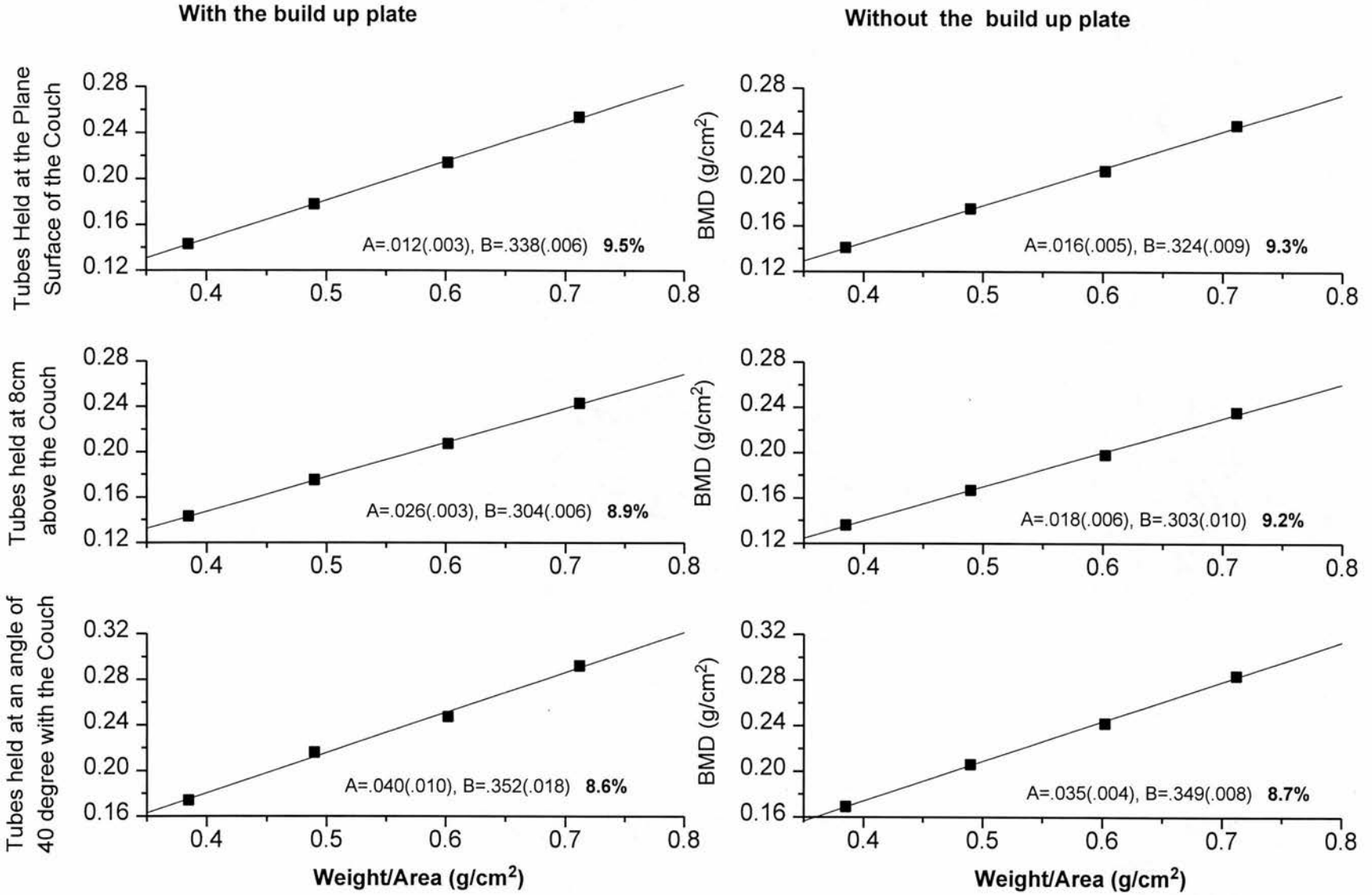

Figure 2.4 Linearity for the FA acquisition mode, using Al tubes. The numbers shown in bold are the gains in BMDs due to an increase of 10% in Weight/Area. In all conditions R>0.999 and p<0.001. A = intercept and B = slope of the regression lines.

Table 2.2 The change in measured BMD for a 10% increase in aluminium tube areal density for different methods.

Method	Tube position	Intercepts (A), Slopes (B) and the estimated percentage change for 10% increase in tube (BMD)									
		With the build up plate					Without the build up plate				
		A	sd	B	sd	+%	A	sd	B	sd	+%
FA	A	.012	.003	.338	.006	9.5 ± .1	.016	.005	.324	.009	9.3 ± .2
	B	.026	.003	.304	.006	8.9 ± .1	.018	.006	.303	.010	9.2 ± .2
	C	.040	.010	.352	.018	8.6 ± .2	.035	.004	.349	.008	8.7 ± .1
P	A	.026	.002	.329	.003	9.0 ± .1	.025	.001	.327	.002	9.0 ± .03
	B	.028	.002	.307	.004	8.8 ± .1	.030	.004	.304	.007	8.8 ± .1
	C	.056	.011	.331	.020	8.1 ± .2	.025	.015	.399	.027	9.2 ± .4
*HH (P)	A	.032	.014	.265	.024	8.5 ± .4					
	B	.019	.005	.275	.010	9.1 ± .2					
	C	.023	.024	.348	.043	9.1 ± .6					
*HH (F)	A	.032	.009	.260	.016	8.5 ± .3					
	B	.026	.010	.261	.017	8.8 ± .3					
	C	.022	.027	.369	.049	9.2 ± .6					

Thresholds for the FA and *P methods were set at 10,10,10 and 8,8,8, respectively.
In all conditions $R > 0.99$, $P<0.01$. NB a value of $W/A = 0.7 g/cm^2$ is taken to estimate the increase in BMD.
A: The tubes held on the plane surface, B: 8cm above and C: at an angle 40° to the densitometer couch.

Table 2.3 The change in measured BMC for a 10% increase in aluminium tube mass for different methods.

Method	Tube position	Intercepts (A), Slopes (B) and the estimated percentage change for 10% increase in tube (BMC)									
		With the build up plate					Without the build up plate				
		A	sd	B	sd	+%	A	sd	B	sd	+%
FA	A	-.177	.035	.408	.016	11.8 ± .5	-.135	.023	.397	.010	11.4 ± .3
	B	-.197	.035	.408	.016	12.1 ± .5	-.152	.035	.385	.015	11.6 ± .5
	C	-.157	.031	.413	.014	11.6 ± .4	-.081	.052	.376	.023	10.8 ± .6
P	A	-.032	.071	.472	.032	10.2 ± .5	-.161	.062	.449	.027	11.5 ± .7
	B	-.052	.037	.482	.016	10.4 ± .3	-.231	.102	.458	.045	12.2 ± 1.2
	C	.234	.061	.394	.027	8.2 ± .2	.021	.05	.374	.023	9.8 ± .4
*HH (P)	A	-.120	.045	.356	.020	11.4 ± .6					
	B	-.212	.039	.395	.017	12.4 ± .6					
	C	-.069	.14	.358	.062	10.7 ± 1.3					
*HH (F)	A	-.147	.089	.341	.040	11.8 ± 1.2					
	B	-.265	.016	.389	.007	13.2 ± .3					
	C	-.072	.10	.340	.045	10.8 ± 1.1					

Threshold for the FA and *P mode were set to 10,10,10 and P = 8,8,8, respectively.
In all conditions $R > 0.99$, $P<0.01$. NB a value of W = 2.8 g is taken to estimate the increase in BMC.
A: The tubes held on the plane surface, B: 8cm above and C: At an angle 40° to the densitometer couch.

Figure 2.5 shows an example of the effect of altering the threshold. Increasing the threshold results in failure to detect the edge regions because they have lower areal density. Since the reduction in area is more significant than the reduction in mass, the net effect is to overestimate the BMD. The effects of altering threshold on BMD are summarised in Table 2.4 for the FA and P protocols, with and without the use of a build up plate.

The slopes and intercepts from the least-square fits were used to calculate the measured changes for true changes of 10%, using an initial value for tube weight/area of 0.7 g/cm^2 (corresponding to 0.25 g/cm^2 CaHA). For the default protocol the default threshold gave changes varying from 8.7% to 9.3% without the build up plate; this was improved slightly to 9.2% to 9.3% using threshold 8,8,8. The build up did not have a significant effect. Varying the threshold over the range shown in Table 2.4 had no significant effect on the P protocol.

Table 2.5 shows the effects of threshold on BMC. To appreciate the significance of the differences in slopes and intercepts the measured changes for a true change in weight of 10% were calculated. It can be seen from Table 2.5 that for any particular protocol the effect of threshold on the change in BMC is relatively small. Since patients have a wide range of hand BMD, there cannot be a standard threshold appropriate for every individual. However, the actual hand phantom was also reanalysed with the appropriate linearity correction coefficients and different thresholds and the best threshold for each technique giving the closest area value to the actual 80.0 cm^2 has been established. Table 2.6 and Figures 2.5a and b also reveal the influence of threshold set on the image area, BMC and BMD for the Hand phantom and the aluminium tubes, respectively. Figure 2.5 shows the scan analysed with the threshold set at 5, 5, 5 which will cause thicker tubes to appear. When the same scan is reanalysed with threshold 12, 12, 12 tubes appeared narrower with lower BMC, but a higher BMD was estimated (Figure 2.5b).

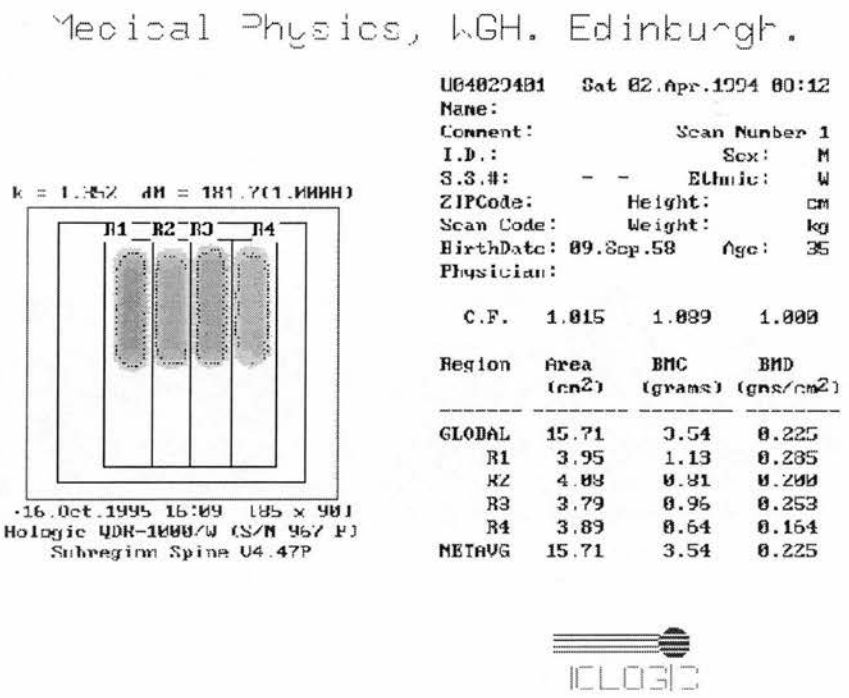

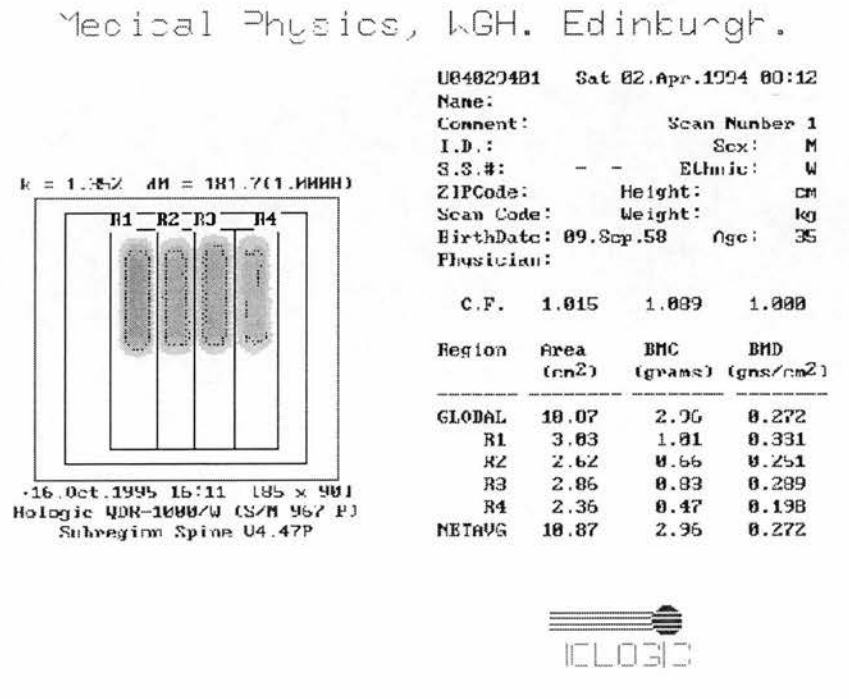

Figure 2.5 The effect of threshold change on edge detection, the above image (a) has been analysed with acquired linearity correction coefficients and threshold set at 5,5,5 (tubes are wider). The below image (b) with threshold =12,12,12 (the thinnest tube R4 has not been fully detected).

Table 2.4 The influence of threshold change on BMD and the estimate of BMD for a 10% increase in tube BMD (shown below each line) for different protocols with different thresholds.

Protocol	Tubes position	Intercepts (A), Slopes (B) and the Estimated % Change for 10% increase in tube BMD (W/A) for different thresholds					
		With the build up plate			Without the build up plate		
		8,8,8	Default		6,6,6	8,8,8	Default
	A	.014, .320	.012, .338		.016, .288	.017, .300	.016, .324
		9.4	9.5		9.3	9.3	9.3
FA	B	.022, .295	.026, .304		.013, .278	.017, .285	.018, .303
		9.0	8.9		9.4	9.2	9.2
	C	.030, .352	.040, .352		.026, .327	.019, .358	.035, .349
		8.9	8.6		9.0	9.3	8.7
		With the build up plate			Without the build up plate		
		5,5,5	7,7,7	10,10,10	6,6,6	8,8,8	
	A	.025, .326	.026, .336	.026, .329	.025, .332	.025, .327	
		9.0	9.0	9.0	9.0	9.0	
P	B	.030, .294	.032, .312	.028, .307	.031, .297	.030, .304	
		8.7	8.7	8.8	8.7	8.8	
	C	.058, .317	.059, .345	.056, .331	.023, .387	.025, .399	
		7.9	8.0	8.1	9.2	9.2	

Default threshold for the FA method = 10, 10, 10. In all cases $R > 0.95$, $P<0.03$.
A: The tubes held on the plane surface, B- 8 cm above and C- at an angle 40° to the densitometer couch.

Table 2.5 The influence of threshold change on BMC and the estimate of BMC for a 10% increase in tube weight (shown below each line) for different methods with different thresholds.

Method		Tube position Intercepts (A), Slopes (B) and the Estimated % Change for 10% increase in tube BMC (Weight) for different thresholds				
		With the build up plate		Without the build up plate		
		8,8,8	Default	6,6,6	8,8,8	Default
	A	-.095, .397	-.177, .408	-.002, .381	-.004, .385	-.135, .397
		10.6	11.2	10.0	10.0	10.9
FA	B	-.064, .385	-.197, .408	-.012, .367	-.072, .381	-.152, .385
		10.4	11.4	10.1	10.5	11.1
	C	-.034, .388	-.157, .413	.005, .370	.003, .358	-.081, .376
		10.2	11.1	10.0	10.0	10.6
		With the build up plate		Without the build up plate		
		5,5,5	7,7,7	6,6,6	8,8,8	10,10,10
	A	-.012, .427	-.107, .451	-.069, .420	-.161, .449	-.032, .472
		10.1	10.6	10.4	11.0	10.2
P	B	-.027, .422	-.099, .438	-.159, .438	-.231, .458	-.052, .482
		10.2	10.9	11.0	11.4	10.3
	C	.087, .391	.038, .397	.058, .367	.021, .374	.234, .394
		9.5	9.8	9.6	9.9	8.7

Default threshold = 10, 10, 10. In all cases $R > 0.95$, $P<0.03$.
A: The tubes held on the plane surface, B- 8cm above and C- at an angle 40° to the densitometer couch.

Table 2.6 The influence of threshold change on hand phantom area, BMC and BMD and comparison with the values obtained from the *HH protocols.

Method		With the build up plate		Without the build up plate		
Threshold		8,8,8	Default	8,8,8		10,10,10
	Area	87.6	77.9	85.1		78.7
FA	BMC	18.9	17.8	25.6		18.8
	BMD	0.216	0.228	0.301		0.239
	Area		84.4			
*HH (P)	BMC		18.7			
	BMD		0.222			
	Area		81.6			
*HH (F)	BMC		17.8			
	BMD		0.218			
Threshold		8,8,8	10,10,10,	6,6,6	8,8,8	10,10,10
	Area	95.2	82.9	87.8	79.5	72.8
P	BMC	21.8	20.3	21.1	20.2	19.1
	BMD	0.230	0.245	0.240	0.254	0.262

2.3.3 Influence of soft tissue thickness

To assess how the bone mineral variables are affected by soft tissue changes, which typically involves the joints of the RA patients fingers and causes them to inflame, the aluminium step wedge was used. For each method different water depths (simulating soft tissue) of 0, 2 and 6 cm were used. Images were analysed using a fixed area away

from the edges to eliminate the edge detection deficiencies in order to compare the effect of soft tissue on bone mineral determination. Normalised values of measured aluminium step wedge BMD versus depths of water were plotted. Figure 2.6 shows the results for some of the methods as examples. All results are tabulated in Table 2.7 for comparison.

Table 2.7 The influence of soft tissue thickness on hand BMD.

Method	With the build up plate				Method	Without the build up plate			
	A	sd	B	sd		A	sd	B	sd
	.161	.003	-.0024	.0011		.165	.001	-.0047	.00019
*FA	.319	.003	-.0050	.0012	FA	.341	.001	-.0058	.00032
	.636	.001	-.0092	.00043		.670	.001	-.0056	.00023
	.163	.002	-.0033	.00058		.165	.003	-.0045	.0010
*P	.327	.003	-.0040	.0077	P	.329	.007	-.0066	.0023
	.651	.004	-.0047	.0019		.657	.010	-.0083	.0025
	.159	.003	-.0022	.0013					
*HH	.333	.001	-.0020	.0001		Not Relevant			
	.716	.0002	-.0024	.0003					

For each protocol the slope and intercept of the BMD versus water depth are shown. The three lines for each protocol correspond to the first three steps of the aluminium step wedge.

Considering the standard deviations of the slopes for the two methods of P and FA with and without the use of the build up plate on average for the three steps the slopes for the aluminium step wedge BMD versus soft tissue thickness do not significantly differ. For the second step of the wedge which has the closest value to hand, the slope is -0.005 $(g/cm^2)cm^{-1}$ (H_2O). The protocol *HH results in the smallest variation in BMD with variation in soft tissue and the effect is independent of BMD.

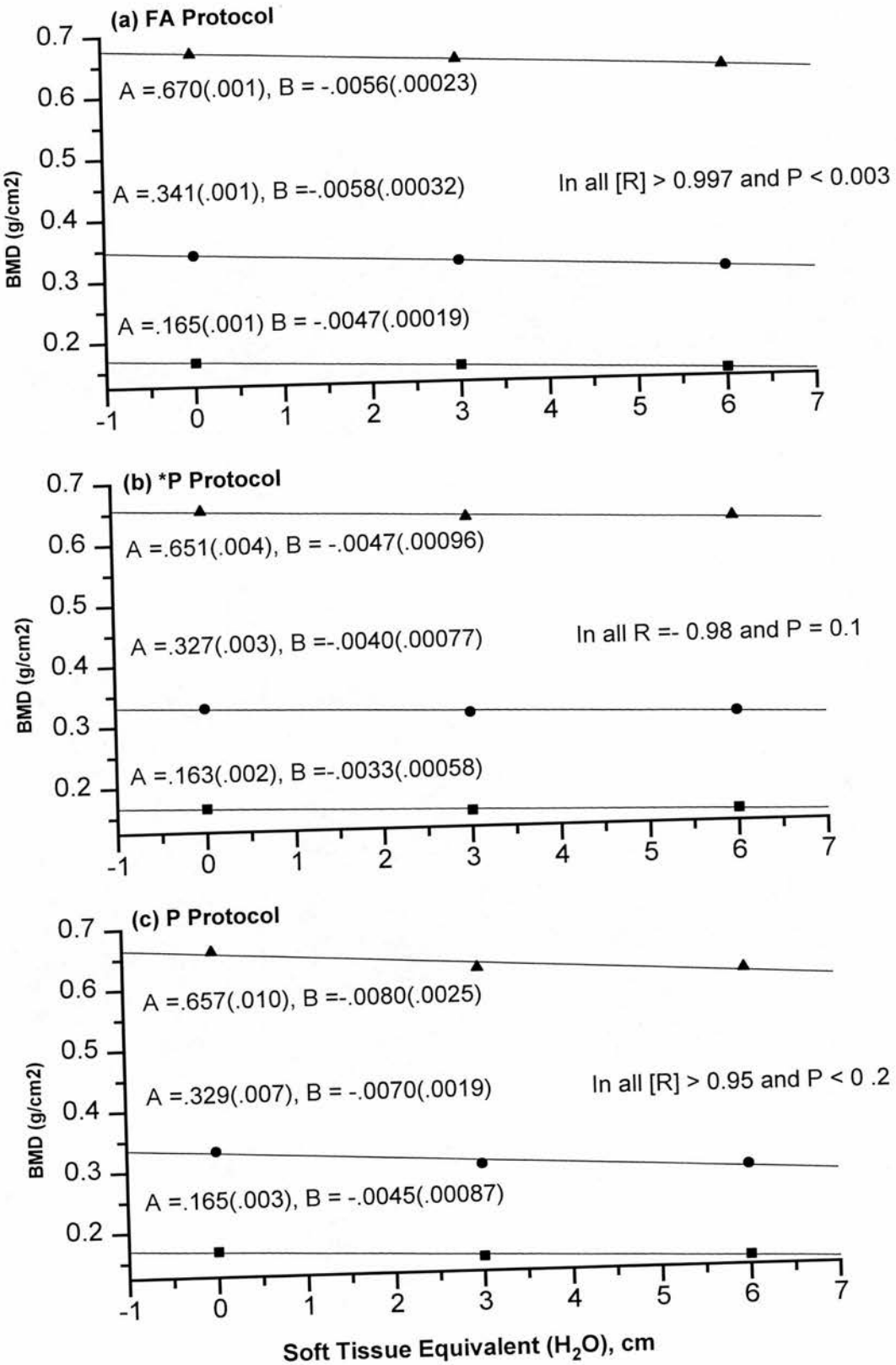

Figure 2.6 Variation of measured BMD with soft tissue thickness, for three of the protocols summarised in Table 2.7. An Al step wedge having steps equivalent to 0.16, 0.32 and 0.64 g/cm^2 of CaHA was used to mimic bone.

2.3.4 Effect of bone wall thickness

To find whether the image area depends upon the bone thickness, the results from the aluminium tubes used in the previous sections were plotted in Figure 2.7. Aluminium tubes' BMDs covered the range 0.13 - 0.26 g/cm^2. The Figure illustrates the plots of aluminium measured area versus the tubes wall thicknesses. Scans were acquired in the P mode and analysed with the sub-region spine protocol (default) to separate each tube from the adjacent ones. On scans analysed with the default threshold, the thinnest tube was not detected, and even for the tubes having thicker walls the areas were very much underestimated in comparison to the actual 4.0 cm^2.

- The FA method underestimated the area for the first two thinner tubes and obtained correct estimates for the thicker tubes.

- The *P method analysed with the threshold set at 10,10,10 overestimated the area even for the thinnest tubes (approximately 5% for the first two tubes), to a maximum of 5 cm^2 for the thickest ones.

- The *HH (P) and *HH (F) acquisition methods have parallel trends for the graphs of measured area versus tube wall thickness. The *HH (F) protocol found a mean 10% underestimate compared to the *HH (P) protocol which gave areas of 3.4, 3.5, 3.7, 4.2 cm^2, respectively for each tube compared with the actual area of 4.0cm^2.

- As Figure 2.7 reveals, excluding the -P, *HH (F) and *P techniques, there are only small difference between the other techniques, although values calculated using the FA and the P acquisition modes (with threshold set at 8,8,8 and default threshold for the FA method) are closest to the actual area.

- Figure 2.7 clearly shows the reasons for artifacts in BMD due to variation in area with thickness variation, in particular for the default Spine protocol (-P).

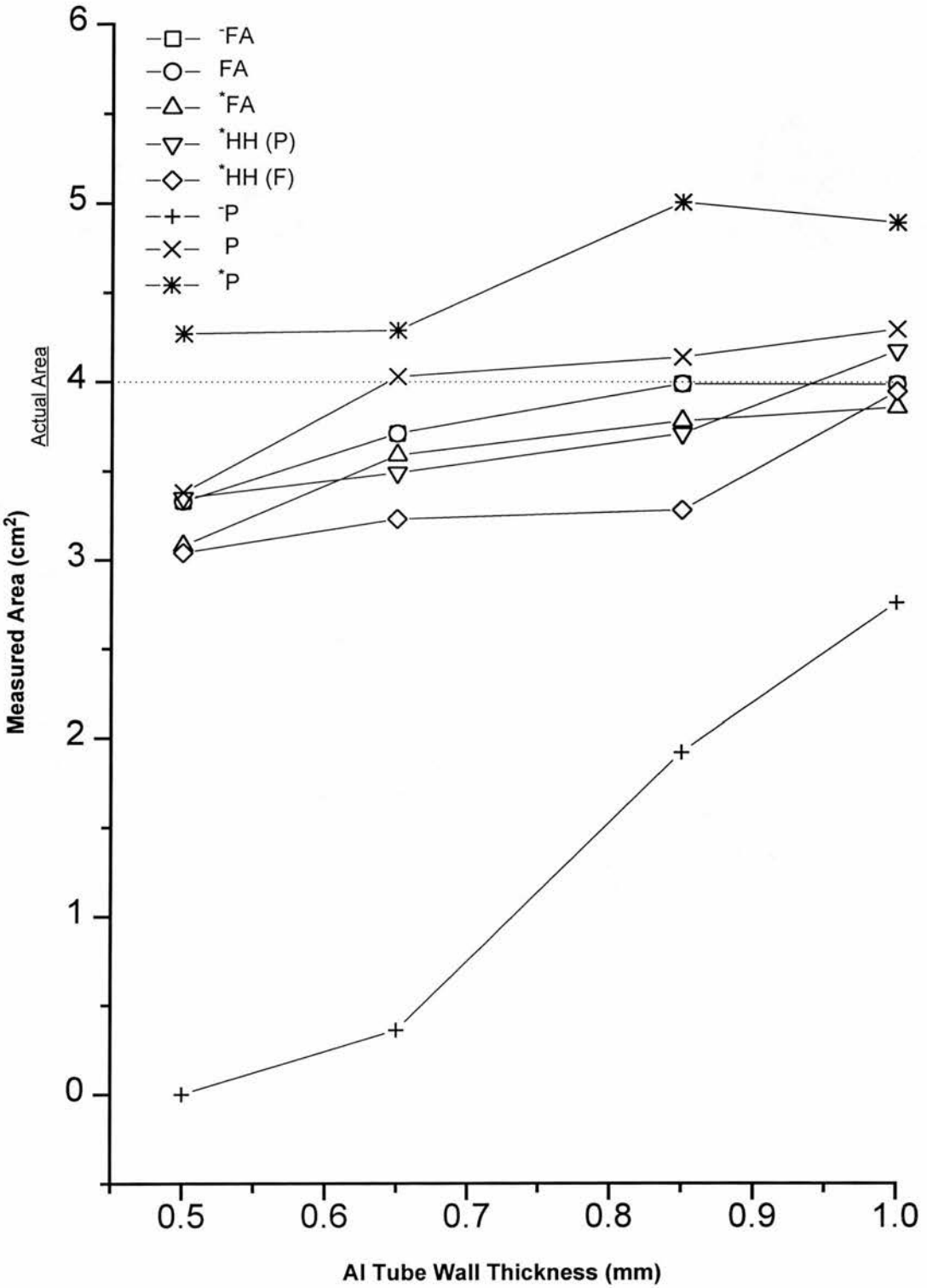

Figure 2.7 The effect of tube wall thickness on measured Area for all techniques, analysed with the appropriate linearity correction coefficients and default Threshold for the FA mode scans, 10,10,10 and 8,8,8 for *P and P, respectively.

2.3.5 Effect of height above the scanner couch on apparent bone mineral density

Patients with RA may not often place their hand flat on the scanner couch. To examine the influence of height on hand BMD, two aluminium tubes with average BMDs of 0.15 and 0.25 g/cm^2 were scanned at various heights from 0 to 8 cm. Measurements were performed for the FA and P protocols with and without a build up plate. Least square fits to the BMD versus height data were performed. The results are summarised in Table 2.8 in terms of the change in BMD per cm change in height. It can be seen from this Table that the effect of possible differences in height is negligible.

Table 2.8 The effect of height above the scanner couch on measured hand BMD.

Method	Tube BMD g/cm^2	+build up plate Slope (gcm^{-2}/cm above the couch)	-build up plate
FA	0.15	-0.0000	-0.0006
	0.25	-0.0014	-0.0015
P	0.15	-0.0007	-0.0004
	0.2	-0.0016	-0.0012

2.3.6 Effect of an angle between the bone and the scanner couch

In section 2.3.1.3 (Table 2.2) the changes in measured BMD corresponding to true changes of 10% were evaluated using aluminium tubes in various positions and orientations. In order to consider the effect of 'changes' in orientation, the regression equations were used to calculate the measured BMC and BMD for particular tube weight(2.8 g) and weight/area (0.7 g/cm^2), respectively.

The values of BMC and BMD for the tubes positioned on the surface of the scanner couch and at an angle of 40° to it are shown in Table 2.9. The measurements at an angle of 40° simulate the position of the proximal metacarpal phalanges or distal phalanges when the patient's hand is in a semi-clenched posture. The percentage changes between the two tube orientations are also shown in Table 2.9. It can be seen that the changes in BMD are significantly greater than the changes in BMC for all protocols as expected. However, there are significant differences between the protocols particularly in terms of the changes in BMD. The changes in the manufacturer's protocol (*HH) are in fact significantly greater than either the FA or P protocols. The smallest effect on BMD is with the P protocol using a build up plate. However, the FA protocol produces a similar effect even without a build up plate and gives the smallest change in BMC.

2.3.7 Hand region of interest selection

In following the course of bone mineral measurements in a patient over time, the precision of the measurements is greatly improved if the same ROI is used from one scan to the next. Figure 2.8a shows the hand ROI selection. At the distal ulna radius junction the ends of the bones are excluded from the hand ROI to prevent any variations due to positioning of the hand and the interference of those bones in the hand area. To find the effect of hand ROI selection on percentage BMD and BMC changes with respect to the distance from the reference point (the distal ulna radius junction), the scans of five control volunteers (3M+2F) taken in FA mode were reanalysed with two line intervals (1 line interval = 2.0 mm) above and below the reference point (in steps of one). Figure 2.9 shows the percentage change of BMD and BMC versus the number of line intervals with regard to the reference. The BMD varies from subject to subject, but the change in BMD is less than the BMD precision error. The effect of changing the region at the distal ulna radius junction on BMC is much more significant and results in a change of approximately 1% per line. Therefore, if the BMC is being measured, it is vital to use a fixed reference point when selecting the hand region.

Table 2.9 The effect of angle of inclination on bone mineral measurement.

Method	Tube position	with the build up plate				without the build up plate			
		BMD gcm^{-2}	% BMD increase	BMC g	%BMC change	BMD gcm^{-2}	%BMD increase	BMC g	%BMC change
FA	A	.249 ± .007		.965 ± .080		.242 ± .011		.977 ± .051	
	B	.286 ± .023	14.9 ± 5.8	.999 ± .070	+3.5 ± 1.2	.279 ± .010	15.3 ± 34.5	.972 ± .116	-.5 ± .603
P	A	.256 ± .004		1.29 ± .161		.254 ± .002		1.096 ± .138	
	B	.288 ± .025	12.5 ± 7.9	1.34 ± .137	+3.9 ± 2.1	.304 ± .034	19.7 ± 12.3	1.068 ± .114	-2.5 ± 1.7
*HH (P)	A	.217 ± .031		.877 ± .101					
	B	.267 ± .054	23.0 ± 6.4	.933 ± .314	+6.5 ± 21.1				
*HH (F)	A	.214 ± .020		.808 ± .201					
	B	.280 ± .061	30.8 ± 14.9	.880 ± .226	+8.9 ± .07				

A: The tubes held on the plane surface, B: At an angle of 40° to the densitometer couch. BMCs and BMDs are calculated from the regression equations of plots of BMC versus tube weight and BMD versus tube W/A (Tables 2.2 and 2.3) at 2.8g aluminium tube weight and 0.7 g/cm^2 aluminium tube weight/area. The *HH scans were taken with the build up plate according to the manufacturer's recommendation.

(a)

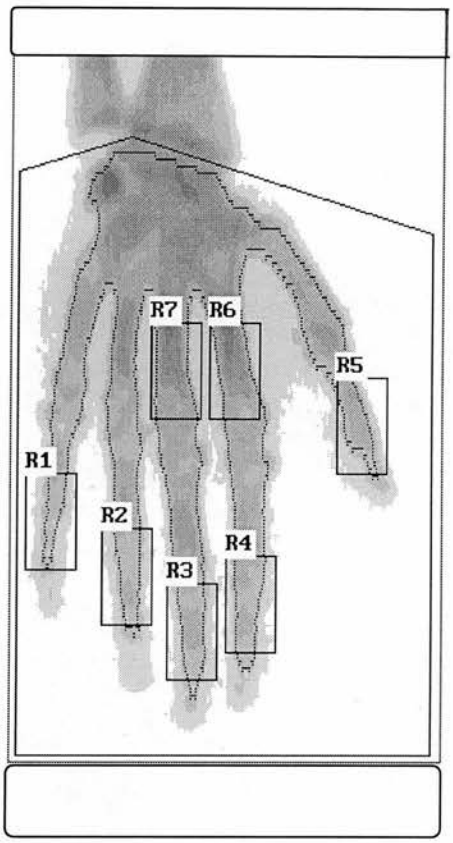

WGH. Edinburgh.

U0721930E Wed 21.Jul.1993 16:34
Name:
Comment:
I.D.: CTL0079 Sex: F
S.S.#: - - Ethnic: W
ZIPCode: Height: 158.00 cm
Scan Code: CM Weight: 51.20 kg
BirthDate: 21.Oct.48 Age: 44
Physician:
Image not for diagnostic use

C.F. 1.014 1.088 1.000

Region	Area (cm2)	BMC (grams)	BMD (gms/cm2)
GLOBAL	54.62	15.80	0.289
R1	1.06	0.16	0.149
R2	1.75	0.30	0.169
R3	1.91	0.40	0.207
R4	2.11	0.43	0.204
R5	1.67	0.39	0.235
R6	2.97	1.07	0.361
R7	3.06	1.06	0.346
NETAVG	14.53	3.80	0.262

HOLOGIC

(b)

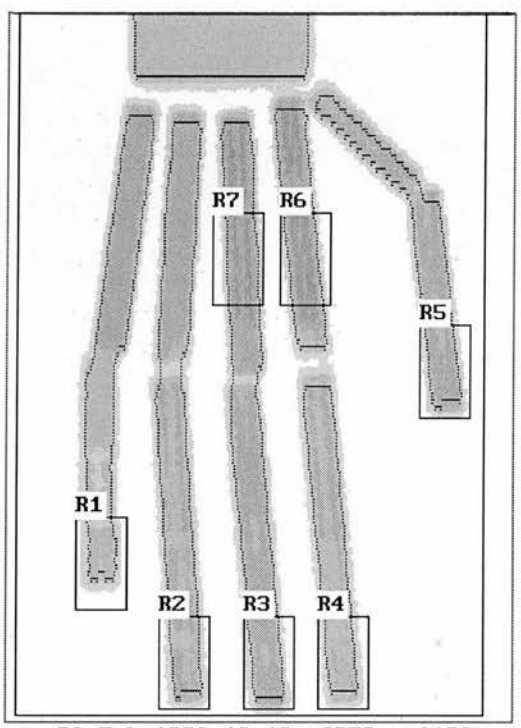

WGH. Edinburgh.

U04269502 Wed 26.Apr.1995 08:30
Name: Hand Phantom #121 QC
Comment: Scan Number 3
I.D.: 121 Sex: F
S.S.#: - - Ethnic:
ZIPCode: Height: cm
Scan Code: MRS Weight: kg
BirthDate: / / Age:
Physician:
Image not for diagnostic use

C.F. 1.017 1.108 1.000

Region	Area (cm2)	BMC (grams)	BMD (gms/cm2)
GLOBAL	78.73	19.98	0.254
R1	1.47	0.22	0.148
R2	2.03	0.47	0.231
R3	2.29	0.63	0.273
R4	1.97	0.40	0.205
R5	2.08	0.51	0.246
R6	2.71	0.99	0.366
R7	2.68	0.93	0.346
NETAVG	15.25	4.15	0.272

HOLOGIC

Figure 2.8 DXA scans of volunteer's hand (a) and the phantom (b), analysed with the sub-region protocol to calculate the hand bone mineral variables for distal, some metacarpal phalanges and the global.

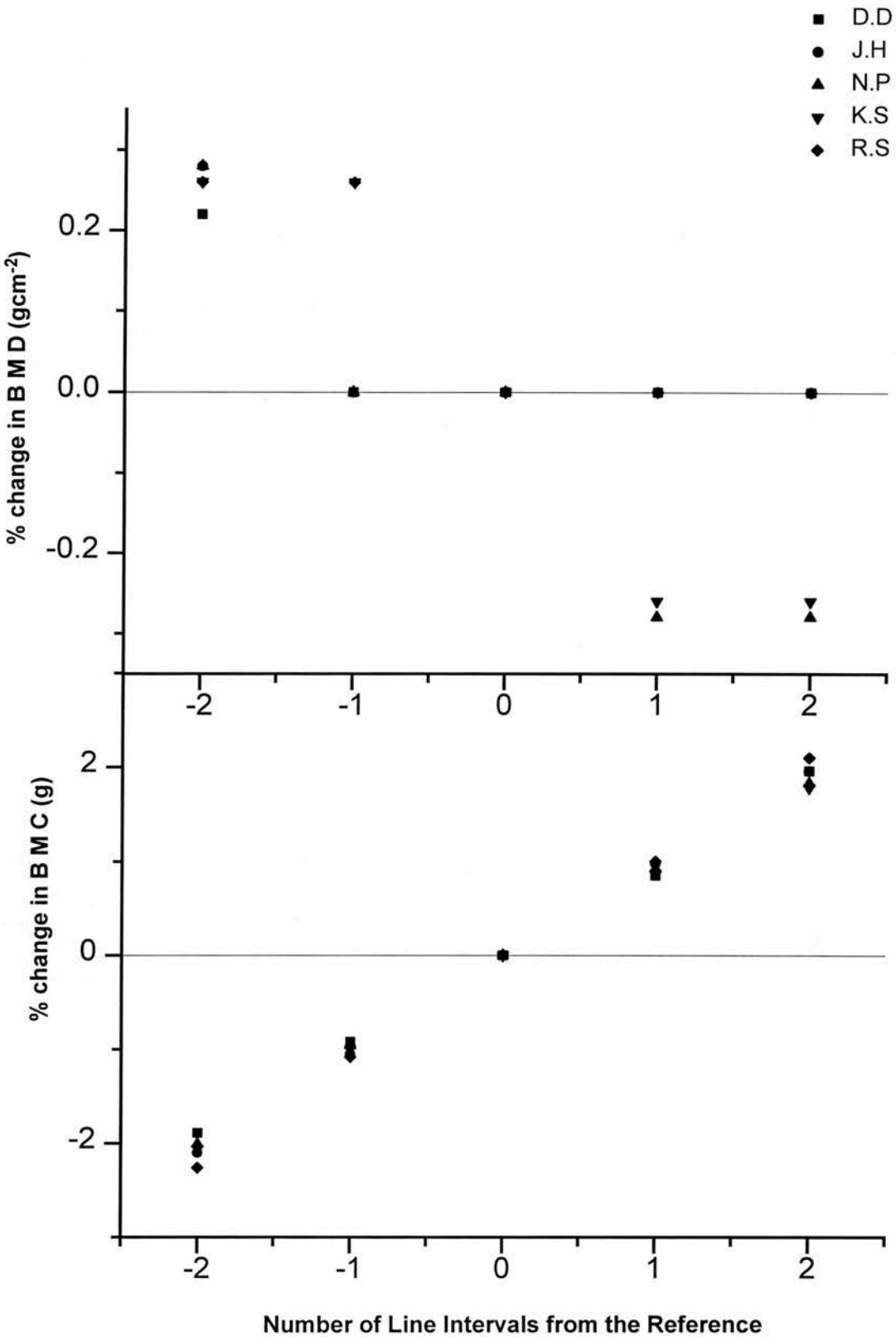

Figure 2.9 The percentage change in BMC and BMD with respect to the distance from the reference point (the distal junction of ulna and radius). The scans were taken in the -FA mode.

The use of BMD effectively eliminates the differences cause by a slight differences in the region at the distal ulna radius junction.

2.3.8 Hand phantom design

To establish the typical range of BMC and BMD in different parts of the hand the sub-region facility of the FA protocol was used to analyse the image of a control female. Measurements were made in the distal phalanges, metacarpal phalanges and the total hand. Figure 2.8a shows an example of the use of the sub-region analysis.

The hand phantom was constructed from aluminium and perspex. It was considered desirable to be able to alter the orientation of the individual phalanges. Therefore, separate phalanges were constructed from aluminium tubes inserted in perspex tubes. Each diameter tube had an outer diameter of 8.0 mm which is similar to the dimensions of the phalanges of a human hand. The inner diameter was varied from 5.2 to 7.0 mm to cover the range of bone density 0.15 to 0.35 g/cm^2. Each aluminium tube was inserted in a perspex tube with an outer diameter of 13 to 19 mm. An aluminium slab was used to simulate the wrist and the metacarpal phalanges and the wrist was covered with a 20 mm perspex palate. The DXA image of the hand phantom is shown in Figure 2.8b. The average BMD and the BMD of the individual regions are also shown.

2.3.9 Effect of angle of deviation in the horizontal plane

To investigate the importance of the position of the hand in relation to the axis of the scanner couch measurements were made with the hand phantom in different orientations. The mean of three measurements for each protocol and each angle were taken.

Table 2.10 summarises the results when the hand phantom was aligned with the long axis of the couch. There were significant differences in the measured BMC and BMD

using the various protocols. No image was detected by the default Spine protocol (-P).

The -FA protocol, i.e. the default Forearm method gave considerably higher BMC and BMD compared to the developed methods. Although there were differences in BMC measured by the performance and fast Spine developed methods due to small differences in the measured area, there were no significant differences in the measured BMD. Figure 2.10 also shows the plots of measured areas and BMC versus angle of deviation from the longitudinal axis of the scanner table for a range of angles of 0 - 15° in 5° increments.

Table 2.10 Hand phantom measurement results for different methods.

Method	Area (cm^2)	BMC (g)	BMD (g/cm^2)
*HH (P)	84.4 ± 0.2	18.7 ± 0.1	0.222 ± 0.001
*HH (F)	81.3 ± 0.6	17.7 ± 0.1	0.218 ± 0.001
*P	80.6 ± 0.2	20.0 ± 0.1	0.248 ± 0.001
*F	80.6 ± 0.2	20.3 ± 0.1	0.252 ± 0.002
P	82.1 ± 0.2	20.7 ± 0.1	0.252 ± 0.001
F	78.5 ± 0.2	19.8 ± 0.1	0.252 ± 0.002
FA	78.9 ± 0.2	19.0 ± 0.1	0.241 ± 0.001
*FA	75.2 ± 0.2	16.9 ± 0.1	0.225 ± 0.001
-FA	78.3 ± 0.2	24.3 ± 0.1	0.310 ± 0.001
-P	No image was detected		

Actual hand phantom area for a length of 22.5 cm from the fingers' tip = 80.0 cm^2.

Table 2.11 compares the data obtained for the hand phantom area and BMC for all techniques for the percentage difference between the hand phantom known 80.0 cm^2 area. Table 2.11 also shows the percentage differences for the first 5° angle deviation from the longitudinal axis of the scanner couch compared with no angle deviation

values. All the developed techniques (except the *FA) measured the area very close (± 1%) to the known hand phantom area of 80.0cm^2. The areas measured by the FA and -FA techniques were identical. The *HH (P) and *HH (F) protocols gave an overestimate of +5% and +2%, respectively. The P and F protocols also estimated +3% and -2% from the true value. It can be seen that there is a 5% overestimate in the measured area for the hand phantom for the first 5° angle deviation that has a true 80.0 cm^2 for the *P method.

The *HH (P) and *HH (F) protocols underestimated 3% and 5% for area and BMC, respectively. Taking the scans in *F mode reduced the measured area and BMC by 1%. The -FA acquisition technique measured with 2% decrease in area and BMC while the *FA method estimated a 2% and 1.5% decrease in area and BMC, respectively, for the 5° deviation.

Table 2.11 The effect of angle of deviation on bone mineral measurement.

	% Difference form 80.0 cm^2 with no angle deviation	% Difference for 5° angle deviation from the initial values		
Method	Area	Area	BMC	BMD
*HH (P)	+5	-3	-3	0
*HH (F)	+2	-5	-5	0
*P	+1	+5	+6	0
*F	+1	-1	-1	0
P	+3	+2	+1	0
F	-2	+2	+1	0
-FA	-1	-2	-2	0
FA	-1	-2	-1.5	0
*FA	-6	-3	-3	0

Thresholds were set at 10, 10, 10 and 8, 8, 8 for the *P and *F protocols, respectively.

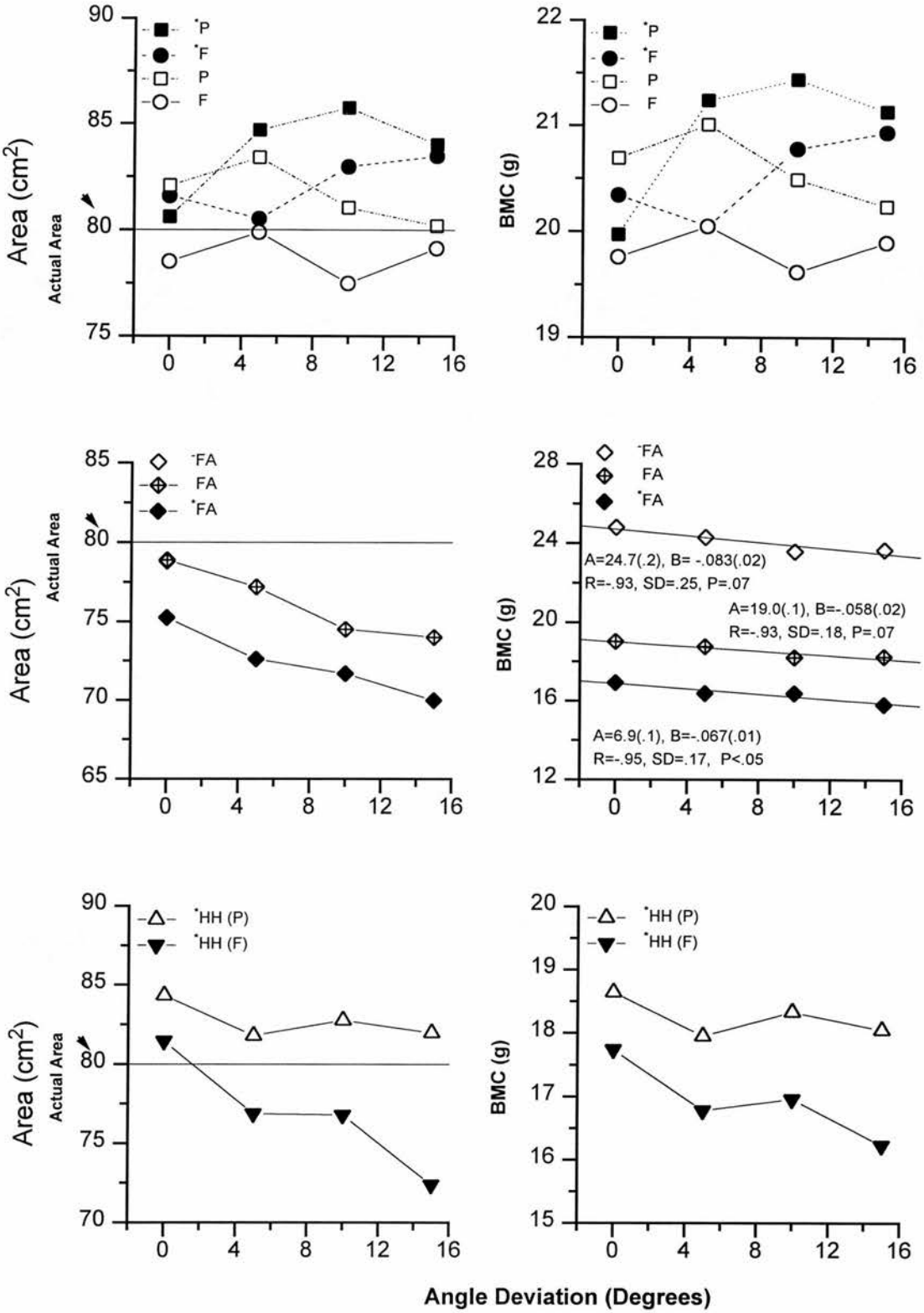

Figure 2.10 Investigation of effect of Hand phantom angle of deviation (from the long axis of the couch) on Area and BMC.

There were no BMD variations more than the reproducibility of the measurements for each technique for a 5° angle change and a maximum of 2% for 15° angle variation. It can be seen from the plots (Figure 2.10) that there is no pattern to the measured area and BMC for the different techniques. There were linearities for the FA technique for either area or BMC with respect to angle deviation, yielding a negative correlation of r = -0.93 and P = 0.07 (though it is not significant) and a slope of -0.058 g/degree angle deviation (which is close to precision of BMC measurements of the method) and an intercept of A = 19.0 g.

The *HH (F) protocol found a significantly (t = -13.8, p = $5x10^{-11}$) smaller phantom area than the *HH (P) protocol, i.e. 81.3 cm^2 as compared to 84.4 cm^2. The hand phantom BMD measurements were found to be the same for the *P, P, *F and F protocols (0.252 g/cm^2). It can be seen from the angle deviation data that the *HH (F) and *P protocols gave a -5% and +5% area change with the first 5° angle deviation, which were the worst cases for both area and BMC.

2.3.10 Minimising hand posture BMC variations

It has been shown previously using aluminium tubes that the threshold setting has an effect on the variation in BMD when the tubes are inclined at an angle to the plane of the scanner couch. To assess the effect of threshold in a more realistic situation measurements were made with the phantom, with the joints positioned to simulate the hand in a flat, intermediate and loose-clenched position. Table 2.12 shows the results (mean ± SD) for the hand phantom bone variables and the precision for the scans taken under the performance spine protocol (*P) with the use of the build up plate. Images were analysed with the new hand analysis, i.e. using the appropriate linearity correction coefficients and the threshold set at 10,10,10; 8,8,8 and 6,6,6, for the phantom postures of flat, intermediate and loose-clenched, respectively. As can be seen from the Table, by reducing the threshold set, the area increases (knowing the true hand phantom = 80 cm^2). In a flat posture the image area increases from 87.5 to 104 cm^2 (a 19%

overestimation), and the BMC increases from 22.9 to 24.0 g (a 4.8% overestimation). As a consequence, the BMD decreases by 12.6% (0.262 - 0.229 gcm^{-2}). By setting the threshold at 8,8,8 and applying the appropriate linearity correction coefficients there was negligible change in BMD between the two postures of flat and intermediate. The overall measurement reproducibility was not significantly different for any posture or any threshold set. The % reduction in area for any threshold between intermediate and flat posture was the same and equal to 4%, except the threshold set at 6,6,6 which was within the precision. A 3% reduction in BMC between the two hand postures for threshold sets 8,8,8 and 6,6,6 and negligible BMC percent change between intermediate and loose-clenched posture, were calculated. The BMD changes for threshold <10,10,10 between flat and intermediate phantom posture were also negligible.

It can be concluded that by setting the threshold at 8,8,8 and applying the appropriate linearity correction coefficients, the minimum variations for hand bone mineral variables between the intermediate and flat or the intermediate and loose-clenched postures are obtained. When a comparison between intermediate and loose-clenched hand postures was made, a BMC change within the measurement precision was observed.

Table 2.13 shows the results for the FA acquisition mode for hand phantom images, analysed with different thresholds for varied phantom postures. As it can be seen with the previous results, by decreasing threshold the area and BMC increased. When a comparison between the new hand analysis using default threshold and threshold set at 6,6,6 (for the flat posture) was made, area and BMC showed an 11% and a 5% increase, respectively resulting in a 6% decrease in BMD. The minimum overall change in area, BMC and BMD was found for the default threshold between the intermediate and the flat phantom postures as well as having the closest area detected compared to the true value.

Table 2.12 Results of hand phantom analysis with change of threshold and varied phantom positions for the *P acquisition protocol. The three lines for each protocol show the results for flat, intermediate and loose-clenched postures, respectively.

Protocol	Area ± SD, CV%	BMC ± SD, CV%	BMD ± SD, CV%	% change in hand bone mineral (between intermediate & flat; intermediate & loose-clenched)		
				Area	BMC	BMD
New	87.5 ± .40, .5	22.9 ± .08, .4	.262 ± .001, .4			
analysis &	84.0 ± .18, .2	21.3 ± .08, .4	.254 ± .001, .6	-4	-7	-3
Thresh = 10,10,10	77.5 ± .78, 1	21.3 ± .18, .8	.276 ± .001, .5	-8	~CV	+9
New	95.7 ± .52, .6	23.1 ± .09, .4	.241 ± .002, .8			
analysis &	91.9 ± .15, .2	22.4 ± .12, .5	.243 ± .001, .4	-4	-3	~CV
Thresh = 8,8,8	83.8 ± .59, .7	22.3 ± .14, .6	.266 ± .002, .8	-9	~CV	+9
New	104 ± .82, .8	24.0 ± .14, .6	.229 ± .002, .9			
analysis &	103 ± .37, .4	23.2 ± .17, .7	.231 ± .001, .4	~CV	-3	~CV
Thresh = 6,6,6	90.5 ± .34, .4	23.1 ± .12, .5	.255 ± .002, .8	-12	~CV	+10

Hand phantom A = 80 cm^2, CV: Precision

Table 2.13 Results of hand phantom analysis with change of threshold and varied phantom positions for the FA acquisition technique. The three lines for each protocol show the results for flat, intermediate and loose-clenched postures, respectively.

Protocol	Area ± SD, CV%	BMC ± SD, CV%	BMD ± SD, CV%	% change in hand bone mineral (between intermediate & flat; intermediate & loose-clenched)		
				Area	BMC	BMD
Default	81.8 ± .10, .1	24.4 ± .09, .4	.299 ± .001, .3			
	80.8 ± .29, .4	25.4 ± .13, .5	.315 ± .001, .3	-1	+4	+5
	70.5 ± .19, .3	24.1 ± .05, .2	.342 ± .001, .3	-13	-5	+9
New analysis & default Thresh	85.8 ± .01, .01	18.6 ± .07, .4	.217 ± .001, .5			
	80.8 ± .29, .4	19.0 ± .11, .6	.235 ± .001, .3	-1	+2	+8
	70.5 ± .19, .3	18.4 ± .04, .2	.261 ± .001, .4	-13	-3	+11
New analysis & Thresh = 8,8,8	90.3 ± .20, .2	19.1 ± .05, .3	.211 ± .001, .5			
	87.3 ± .28, .3	19.7 ± .09, .5	.226 ± .001, .4	-3	+3	+7
	76.6 ± .19, .2	19.2 ± .04, .2	.250 ± .001, .4	-12	-3	+11
New analysis & Thresh = 6,6,6	95.6 ± .15, .2	19.6 ± .07, .4	.204 ± .001, .5			
	92.2 ± .24, .3	20.2 ± .10, .5	.219 ± .001, .5	-3	+3	+7
	81.4 ± .03, .4	19.6 ± .04, .2	.241 ± .001, .4	-12	-3	+10

Hand phantom A = 80 cm^2, CV: Precision

Table 2.14 In-vivo comparison of BMC/BMD percent change in two different hand postures of relaxed flat and loose-clenched (using the appropriate linearity correction coefficients and different threshold) with the FA protocol.

Subject	Protocol	Relaxed Flat Position (RF)			Loose-clenched Position (LC)			BMC % change in two diff postures 100*(RF-LC)÷LC	BMD % change in two diff postures 100*(RF-LC)÷LC
		Area (cm^2)	BMC (g)	BMD (g/cm^2)	Area	BMC	BMD		
AGM	*	71.1	27.8	.391	53.5	26.3	.492	5.7	-20.5
	**	69.6	23.5	.338	53.5	23.5	.438	0.0	-22.8
	***	70.8	23.6	.334	54.0	23.5	.436	0.4	-23.4
	****	75.6	24.2	.320	56.4	23.9	.424	1.3	-24.5
SGF		67.4	24.9	.369	55.5	23.5	.424	6.0	-13.0
		66.3	20.9	.315	55.0	20.4	.371	2.5	-15.1
		67.5	21.0	.312	55.8	20.5	.368	2.4	-15.2
		73.1	21.6	.296	58.83	20.8	.354	3.8	-16.4
IDM		87.7	37.9	.433	65.3	35.1	.538	8.0	-19.5
		83.9	33.3	.397	64.7	31.3	.483	6.4	-17.8
		87.1	32.9	.378	65.4	31.4	.480	4.8	-21.3
		92.9	33.6	.362	68.7	31.8	.463	5.7	-21.8
DDM		84.2	37.7	.448	68.7	35.6	.518	5.9	-13.5
		83.9	33.3	.397	69.0	32.2	.466	3.4	-14.8
		85.2	33.5	.393	69.6	32.3	.464	3.7	-15.3
		90.2	34.2	.377	73.0	32.8	.449	4.3	-16.0
JHM		70.9	25.0	.353	59.7	23.7	.397	5.5	-11.1
		69.4	20.8	.300	64.1	20.8	.324	0.0	-7.4
		70.6	21.0	.297	59.8	20.3	.340	3.4	-12.6
		76.0	21.5	.284	64.1	20.8	.325	3.4	-12.6

Table 2.14 continued

JM	75.6	29.2	.386	59.9	27.9	.466	4.7	-17.2
M	76.2	25.5	.335	60.3	24.7	.410	3.2	-18.3
	77.4	25.7	.332	60.9	24.8	.407	3.6	-18.4
	82.8	26.3	.318	65.5	25.3	.387	4.0	-17.8
GM	78.5	33.1	.422	59.8	29.8	.498	11.1	-15.3
M	78.1	28.9	.371	60.2	26.9	.446	7.4	-16.8
	79.0	29.1	.368	60.8	27.0	.444	7.8	-17.1
	83.8	29.6	.353	64.1	27.4	.428	8.0	-17.5
CS	65.2	26.6	.407	53.7	23.8	.443	11.8	-8.1
F	65.4	23.1	.353	53.2	20.8	.391	11.1	-9.7
	65.7	23.1	.352	53.8	20.9	.388	10.5	-9.3
	72.5	23.8	.329	57.8	21.3	.369	11.7	-10.8
KS	61.2	22.7	.371	47.9	20.5	.428	10.7	-13.3
F	60.3	19.1	.317	47.5	17.8	.375	7.3	-15.5
	61.3	19.3	.314	48.0	17.9	.373	7.8	-15.8
	66.1	19.8	.300	51.5	18.3	.356	8.2	-15.7
MRS	79.7	30.0	.376	60.5	27.7	.459	8.3	-18.1
M	77.8	25.0	.321	59.3	24.0	.404	4.2	-20.5
	79.1	25.2	.318	59.8	24.1	.402	4.6	-20.9
	84.9	25.8	.304	63.2	24.5	.388	5.3	-21.6

Results are expressed for the FA method with the default protocol (*), with threshold set at 12,12,12, and appropriate linearity correction coefficients (**), with default threshold and appropriate linearity correction coefficients (***), with threshold set at 8,8,8 and appropriate linearity correction coefficients (****), respectively.

Table 2.14 shows in-vivo scans results taken under the FA method and compares BMC percent change in two different hand postures of relaxed flat and loose-clenched as well as showing area and BMD variations, when the threshold and the appropriate linearity correction coefficients are changed. For this study ten healthy volunteers, seven males and three females of different ages (25 - 55 y) were scanned. Table 2.14 illustrates the results in five main columns showing the sex, protocol, the hand bone mineral variable for relaxed flat position, loose-clenched position, BMC % and BMD% change in two different positions. It reveals how the change of posture considerably decreases for every subject by modifying the software algorithms. However, there was no significant change with posture for BMD using the new hand analysis.

Table 2.15 summarises the data and shows the BMC percent change between two different postures of relaxed flat and loose-clenched for the ten subjects for each protocol. The mean percent change of 7.7% ± 2.6 for the unmodified default method has reduced significantly to 4.9 ± 3.0 (P = 0.0001). However, by modifying the software and changing the threshold to 12,12,12 or 10,10,10 or finally 8,8,8, significant reductions in the mean percent change have been achieved.

Table 2.15 BMC percent change between two different hand postures for the FA, and FA methods analysed with different thresholds.

Subject	Sex	Method			
		*	**	***	****
1	M	5.7	0.0	0.4	1.3
2	F	6.0	2.5	2.4	3.8
3	M	8.0	6.4	4.8	5.7
4	M	5.9	3.4	3.7	4.3
5	M	5.5	0.0	3.4	3.4
6	M	4.7	3.2	3.6	4.0
7	M	11.1	7.4	7.8	8.0
8	F	11.8	11.1	10.5	11.7
9	F	10.7	7.3	7.8	8.2
10	M	8.3	4.2	4.6	5.3
Mean % change		7.7 ± 2.6	4.6 ± 3.5	4.9 ± 3.0	5.6 ± 3.0

Paired t-test results for the significance of the reduction in the mean percent change are shown in Table 2.16. Significant improvement in BMC reduction between the two hand postures was obtained.

Table 2.16 Paired t-test results for the significance of the reduction in the mean percent change in two different hand postures for the FA protocols, using different thresholds.

Paired t-test on column (*) and columns (**), (***) and (****)				
Protocol	mean	variance	t-value	p-value
*	7.7	6.8		
**	4.6	12	5.8	0.0003
***	4.9	8.9	6.9	0.0001
****	5.6	8.9	5.3	0.0005

*: The default protocol. All other protocols were analysed with the appropriate linearity correction coefficients and threshold set at 12,12,12 (**), default (***) and 8,8,8 (****).

It should be mentioned that there are some limits to changing the threshold. For example by setting the threshold above 12,12,12 some less dense bones in the hand, like the finger tips, were not detected either in-vivo or in-vitro. By setting the threshold below 8,8,8, some artifacts were introduced, i.e. between the fingers some extra bones were shown or the phantom area increased. Moreover, there is no single threshold to suit all subjects with a variety of BMD and hand structures. As an example, it can be seen from Table 2.15 that the FA method with the threshold set at 12,12,12 (**) minimised the effect of posture for the first two subjects but with the default threshold and appropriate linearity correction coefficients (***) minimised the effect for the third subject.

2.3.11 In-vitro and in-vivo comparison of hand bone mineral precision for different techniques

Repeat, short term and long term precision for area, BMC and BMD are shown in Table 2.17. The hand phantom was used for this assessment. The precision error is less than 1% in all cases.

Table 2.17 In-vitro hand bone mineral measurements precisions for different protocols.

Method	N	BMD CV, %	BMC CV, %	Area CV, %
FA, repeat	10	0.26	0.37	0.19
FA, daily	90	0.41	0.74	0.43
*HH (P), repeat	10	0.42	0.55	0.30
*HH (P), daily	13	0.34	0.70	0.59
*HH (F), repeat	10	0.53	0.75	0.80
*HH (F), daily	10	0.53	0.86	0.78

To determine if there is any significant difference between hand bone mineral measurement reproducibility (CV) between different protocols, 11 control subjects of both sexes had repeated scans in the FA, P and F acquisition modes. The images were analysed using different methods. ANOVA was performed and the results are tabulated in Table 2.18, showing hand bone mineral measurements precision means were NOT significantly different.

Table 2.18 ANOVA results to determine if there are significant differences between the in-vivo means of the hand bone mineral variables precisions for different protocols.

	BMD CV(%)		BMC CV(%)		Area CV(%)	
Method	mean	variance	mean	variance	mean	variance
FA	0.41	0.06	0.63	0.16	0.61	0.36
-FA	0.30	0.05	0.74	0.37	0.57	0.29
*HH (P)	0.51	0.25	0.87	0.38	0.82	0.97
*HH (F)	0.71	0.31	0.97	0.49	0.89	0.59
*P	0.32	0.13	1.2	0.37	1.0	0.40
*F	0.35	0.12	1.3	1.0	1.2	0.61
F value	1.71		1.80		1.16	
P value	0.15		0.12		0.33	

2.3.12 Prediction of hand bone mineral variables from age and size

Variations in hand bone mineral variables with age and physical sizes are shown in Table 2.19. Female hand bone mineral values showed a significant correlation ($r = 0.46$, $P < 0.05$) for BMC with age, and a more negative correlation of BMD with age ($r = -0.73$, $P < 0.001$) but no correlation between area and age ($r = -0.15$, $P > 0.05$). The correlations between area, BMC and BMD for females with height were $r = 0.55$, $P < 0.01$; $r = 0.70$, $P < 0.001$ and $r = 0.63$, $P < 0.001$, respectively. The hand bone mineral variables showed no correlation for females for BMD with weight but moderate correlations of $r = 0.52$ $P < 0.05$ for BMC and $r = 0.51$ $P < 0.01$ for area.

Table 2.19 Correlation (r) of hand bone mineral variables with age, height and weight for the control subjects.

	Females			Males		
	Age	Ht	Wt	Age	Ht	Wt
Area	-0.15	**0.55	**0.51	*0.46	*0.34	**0.52
BMC	*-0.46	***0.70	*0.52	0.34	0.34	*0.57
BMD	***-0.73	***0.63	0.38	0.17	0.30	0.49
	BMC	BMD		BMC		BMD
Area	***0.90	***0.60		***0.82		*0.58
BMC		***0.88				***0.94

no * (not significant) $^{*}P < 0.05$ $^{**}P < 0.01$ $^{***}P < 0.001$

For men, only area versus age showed a significant correlation of $r = 0.46$ $P < 0.05$. BMC and BMD showed no significant correlations with age ($r = 0.34$ $P = 0.06$) and ($r = 0.17$ $P = 0.38$), respectively.

Males' hand area was also correlated significantly with physical sizes of height and weight with $r = 0.34$, $P < 0.05$ and $r = 0.52$, $P < 0.01$, respectively. Males BMC showed a positive correlation with weight $r = 0.57$, $P < 0.05$. A significant correlation was not obtained between weight and BMD ($r = 0.49$, $P > 0.05$).

It should be mentioned that in the multiple stepwise regression considering BMC for control females as the dependent variable and dominant or non-dominant hand, height, weight, BMI and age as variables, only age came into the multiple stepwise regression. This is due to the very high correlations of right and left hand ($r_F = 0.98$, $r_M = 0.96$ at $P < 0.0001$) and a moderate correlation of BMC and weight $r = 0.52$, $P < 0.05$ (Table 2.19).

Table 2.20 compares the right and the left hand BMC for both sexes for the controls. The mean right BMCs were significantly higher, $P < 0.0005$ for men and $P < 0.0001$ for women. Therefore it is important for RA patients follow up or for acquisition of normal data that the same side hands are used.

Table 2.20 Comparison between right and left-hand mean BMC for control males (n=15) and females (n=24).

variable	Male Mean ± SD	Female Mean ± SD
Left Hand	29.0 ± 6.6	20.7 ± 4.5
Right Hand	30.4 ± 6.6	22.0 ± 4.6
Mean	29.7 ± 6.6	21.4 ± 5.4

Knowing the above hand bone mineral variable correlations with age, height and weight, attempts were made to reduce the biological variations in BMC by expressing the subjects results as a ratio of $BMC_i = BMC/BMC_P$ and $BMD_i = BMD/BMD_P$. BMC_P and BMD_P were predictive values. Variables entered in the stepwise regression analysis were age, weight, height, BMI and dominant or non-dominant hand. Table 2.21 shows the details.

Table 2.21 Prediction of BMC and BMD from age and body size.

Variable	Predictive equation	SE	r
BMC			
F	29.54-0.1638*Age	2.28	0.62
M	12.88+0.5761*BMI	6.06	0.49
	7.293+0.5850*BMI+0.1282*Age	5.70	0.60
BMD			
F	0.3701-0.0010*Age	0.0436	0.33
M	0.2427+0.0007*Age+0.0033*BMI	0.0530	0.41

Age (y), Wt = weight (kg), Ht = height (m), BMI (kg/m^2), SE = standard error of prediction and r = multiple correlation.

Figure 2.11a illustrates the BMC as a function of age for the control females. There was a significant negative correlation of r = -0.46, P = 0.02. A coefficient of variation (CoV) (standard deviation of the mean value (age regression of hand bone mineral variable) ÷ hand bone mineral value at age 50 years as an example) of CoV_{50y}=21% was obtained. Figure 2.11b compares the BMC of the RA females with the controls.

Z-score compares the patient's measured bone mineral density with age matched reference value.

$$Z\text{-score} = (P - M_{AM})/SD_{AM}$$

P is the measured patients value, M_{AM} is the mean value for sex and age matched controls and SD_{AM} is the standard deviation of the mean value for the age and sex matched controls. A mean Z-score of -0.80 ± 0.70 was calculated.

Figure 2.12a Shows the regression of BMD on age for the control females. A significant P = 0.0001 negative correlation of r = -0.73 and a CoV_{50y}=10% was calculated. Figure 2.12b compares the BMD of the RA females with the control females. A mean Z-score of - 1.44 ± 1.10 was calculated. The difference between the controls and RA patients Z-scores and the CoV for both genders are shown in Table 2.22.

Table 2.22 Comparison of the Z-scores and CoV for normals and RA patients.

	Control CoV (%), Z (± SD)		RA Patients Z (± SD)		Diff in mean Z-score (P)	
	Female	Male	Female	Male	Female	Male
BMC	21,.00 ± .98	21, .02 ± .86	-.84 ± .70	-.72 ± .68	-.84(.0005)	-.70(.002)
BMC_i	20, -.03 ± .98	19,.01 ± .96	-.97 ± .70	-.64 ± .66	-.94($2x10^{-22}$)	-.63(.01)
*BMC	14, .01 ± .99		-1.2 ± 1.4		-1.2($5x10^{-6}$)	
BMD	10, -.07 ± .98	14,.00 ± .98	1.4 ± 1.1	-.78 ± .74	-1.3($1x10^{-6}$)	-.78(.002)
BMD_i	10, -.07 ± .98	10,-.04 ± .98	1.4 ± 1.1		-1.3($8x10^{-7}$)	

*The BMC has been normalised by height. The rest of the hand bone mineral variables have been plotted against age. BMC_i and BMD_i were defined in section 2.3.12. CoV, coefficient of variation as defined in section 2.3.12.

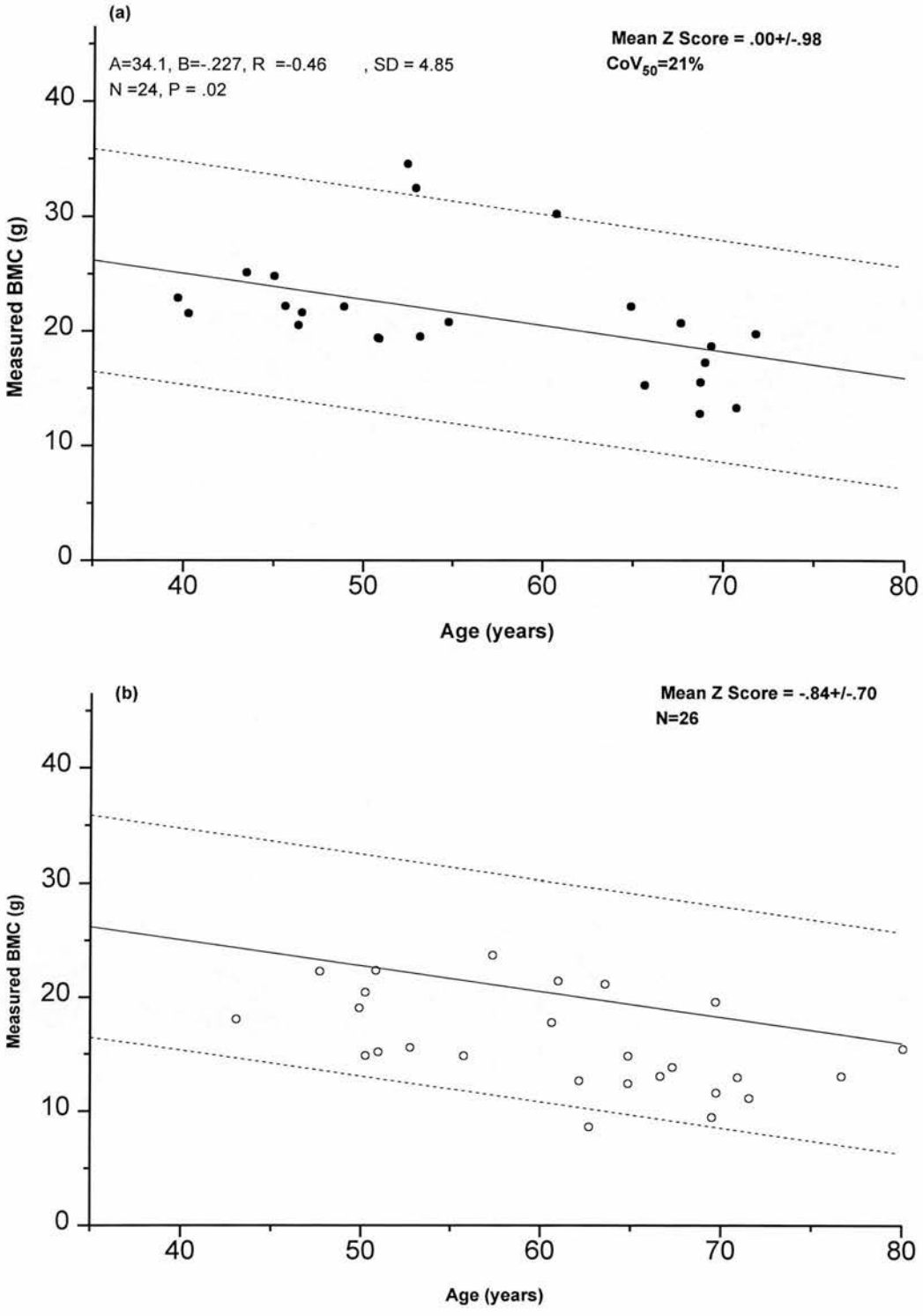

Figure 2.11 (a) Hand BMC as a function of age for the control females. (b) Comparison of the hand BMC of the RA with the normals. The solid line is the least square fit and the broken lines are the 95% confidence intervals for the normal females.

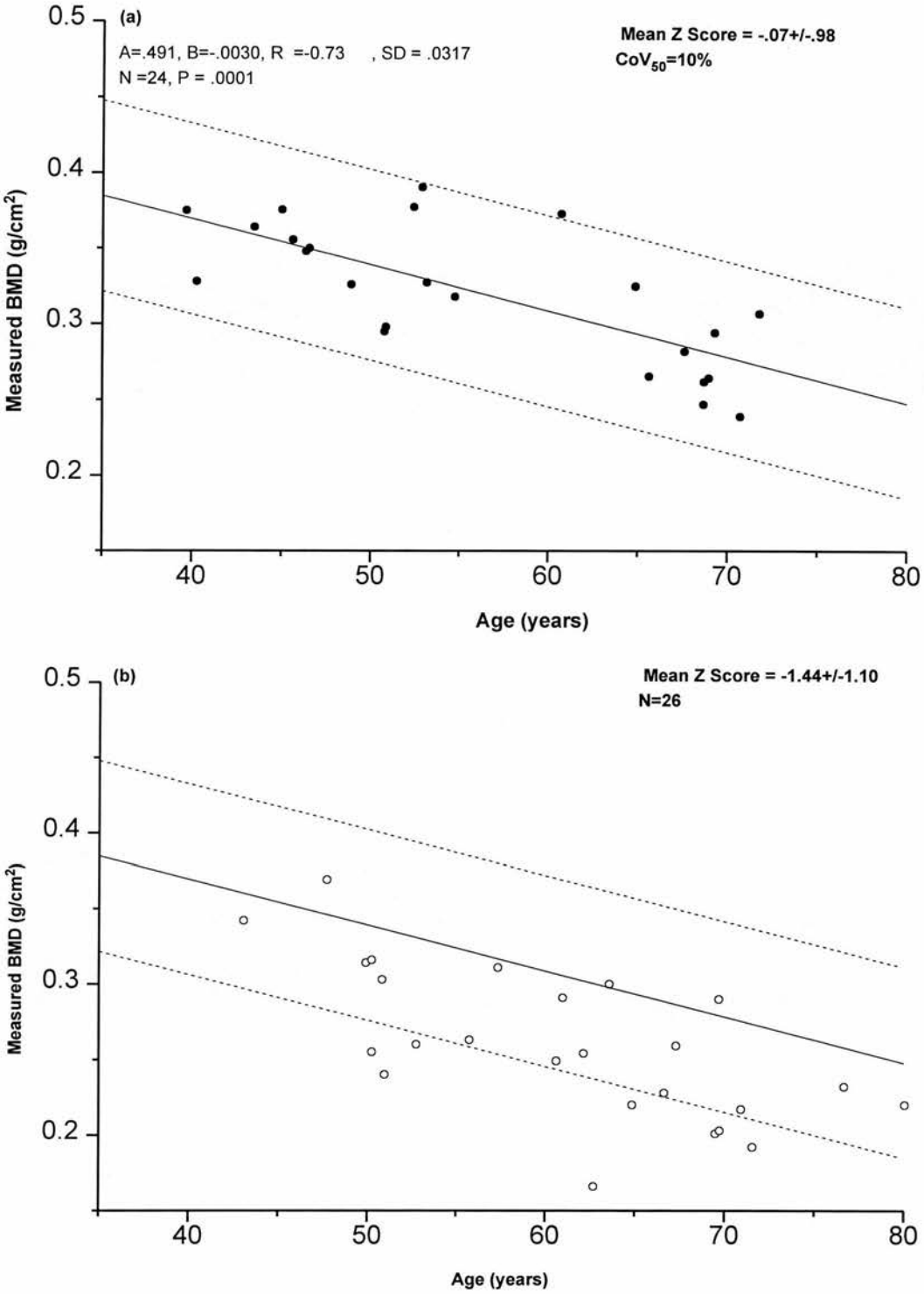

Figure 2.12 (a) Hand BMD as a function of age for the control females. (b) Comparison of the hand BMC of the RA with the normals. The solid line is the least square fit and the broken lines are the 95% confidence intervals for the normal females.

The CoVs were considerably lower for BMD compared to BMC. However, normalising BMC (denoted by *BMC in the Table) for females by height also improved the CoV significantly from 21% to 14%, separating the RA patients from controls ($Z = -1.2$, $P = 5x10^{-6}$).

2.3.13 Comparison of normal subjects and RA patients using two different methods

Figures 2.13 and 2.14 compare plots of males' and females' BMC and BMD for the two groups of controls and RA patients, respectively. The two groups were compared using Figures of merit, defined as:

$$F = (M_C - M_P)/(SD_C + SD_P)$$

M_C, M_P, SD_C and SD_P were the controls' and RA patients' mean hand bone mineral values and the standard deviations of the measurements for the same sex groups. A large difference between the mean of hand bone mineral variables and/or small standard deviations result in higher figures of merits, making a better separation between the normal and RA patients groups. Although higher mean hand bone mineral values were determined by the *P method, similar figures of merit for BMC and BMD for the same sex group were observed. For males' BMC and BMD figures of merit of ($F_{*P} = 39.4\%$, $F_{*HH} = 40.9\%$) and BMD ($F = 42\%$) were found. This demonstrates that the *P method had a similar ability (to *HH) to differentiate between the RA patients and the healthy control subjects. However, the figures of merit obtained for the females' BMC ($F_{*P} = 58.8\%$, $F_{*HH} = 56.4\%$) and BMD ($F = 63\%$) were considerably higher as compared to males' values for these variables (39% - 42%).

Figures of merit for BMC and BMD were used to assess which variable gives a better separation between the RA patients and the controls. For females a higher mean BMD figure of merit for both methods of measurements was found compared with the value

obtained for BMC (F_{BMD} = 62.9%, F_{BMC} = 57.6%).

Table 2.23 compares the RA patients with the healthy controls for BMC and BMD. Female RA patients had a significant ($P = 1x10^{-7}$) 25% loss of BMC and 22% loss ($P=1x10^{-8}$) in their BMD. Male RA had significant losses 17% (P = 0.007) and 12% (P=0.007) in BMC and BMD, respectively.

Table 2.23 Comparison of the RA with the normals for the hand bone mineral values. The results are expressed as the mean ± SD, the range and the number of measurements.

	Category	BMC (g)	BMD (gcm^{-2})
F	Controls	21.4 ± 5.4	0.320 ± 0.046
e	(n = 24)	12.3-35.9	0.230-0.399
m			
a	RA	16.1 ± 4.0	0.262 ± 0.046
l	(n = 26)	8.6-23.7	0.166-0.369
e	% diff in RA	-25 ($P = 1.07x10^{-7}$)	-22 ($P = 5.97x10^{-9}$)
M	Controls	29.7 ± 6.6	0.370 ± 0.053
a	(n = 15)	20.1-45.3	0.293-0.492
l			
e	RA	25.4 ± 3.9	0.331 ± 0.039
	(n = 12)	17.3-34.3	0.263-0.411
	% diff in RA	-17 (P = 0.007)	-12 (P = 0.007)

The mean values are for two hands.

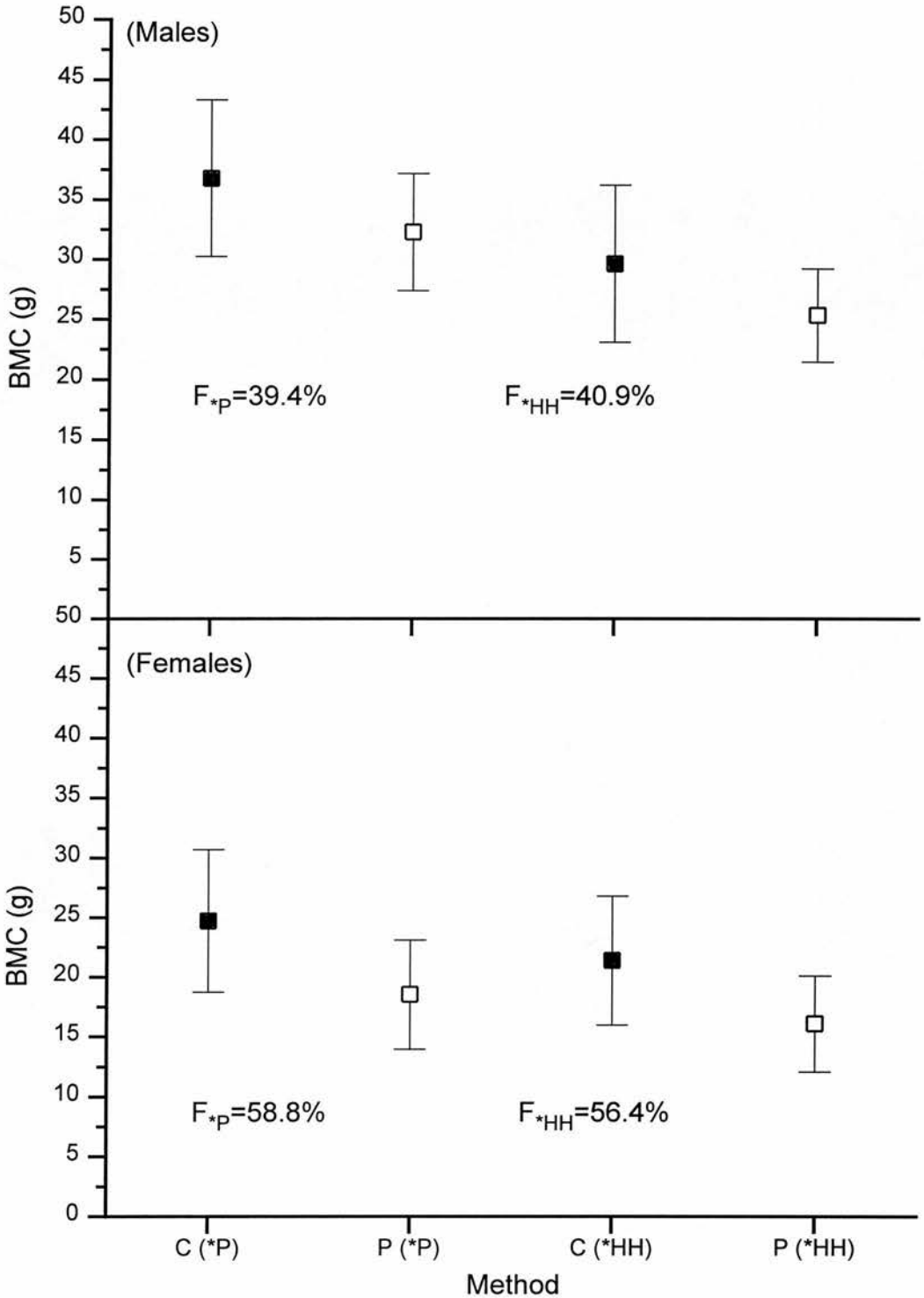

Figure 2.13 Comparison of males' and females' hand BMC (±SD) for two groups of controls (C) (M=15, F=24) and RA patients (P) (M=12, F=26). The values are shown for two different measurement methods of *P and *HH. The solid and open symbols show the mean BMCs of the control and RA patient groups. Figures of merit as explained in the text are shown.

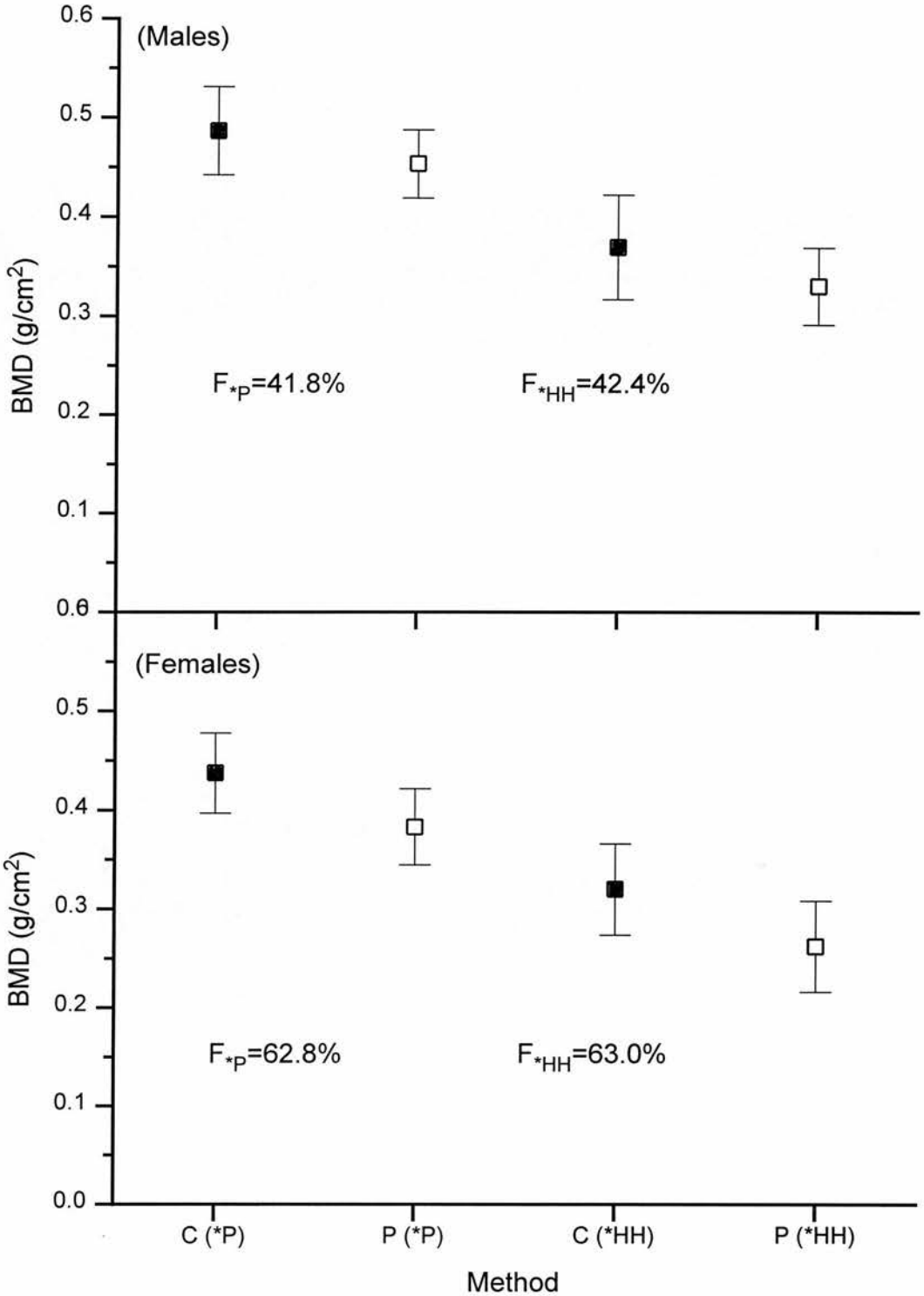

Figure 2.14 Comparison of males' and females' hand BMD (±SD) for two groups of controls (C) (M=15, F=24) and RA patients (P) (M=12, F=26). The values are shown for two different measurement methods of *P and *HH. The solid and open symbols show the mean BMDs of the control and RA patient groups. Figures of merit as explained in the text are shown.

2.3.14 Correlation of the *HH (P) with *HH (F) and FA protocols

To assess how significant the relations between the HH (P) and HH (F) protocols are, Figure 2.15 was plotted. The Figure illustrates in-vivo regression of hand bone mineral results using the *HH (F) protocol on the *HH (P) data. These measurements were acquired to determine if there were a high correlation between the two protocols so the fast mode (F) could be employed for future scan acquisition. The fast mode has the advantage of halving the scan time which would result in increased comfort for the patients and would save the time.

For the *HH (F) area versus *HH (P) area, there is a significant high correlation of $r > 0.96$, $p < 0.0001$ with a SD=0.763 cm^2, a slope of 0.961 ± 0.026 and a negligible offset. For the BMC plots, the *HH (F) versus *HH (P) protocols showed a strong significant relation of $r > 0.99$, $p < 0.0001$, SD = 0.329 g, a non-significant intercept and a gradient close to 1.0. Paired t-test showed that the *HH (F) mean was significantly lower ($t = 4.3$, $P = 0.0003$) than the *HH (P), because considerably lower areas were calculated by the *HH (F) protocol.

The *HH (F) BMD data, gave a non-significant intercept, a slope close to 1 and a high significant correlation of $r > 0.99$, $p < 0.0001$. A student t-test also revealed that there was no significant difference between the BMD means ($t = -1.30$, $P = 0.21$) measured by the two methods. Bland and Altman (1995) statistical method also assessed a good agreement between the *HH (P) and *HH (F) protocols over the entire BMD range. However, although there were high correlations between the *HH (P) and FA bone mineral variables, there were not good agreements between the two protocols in particular at the low BMD range.

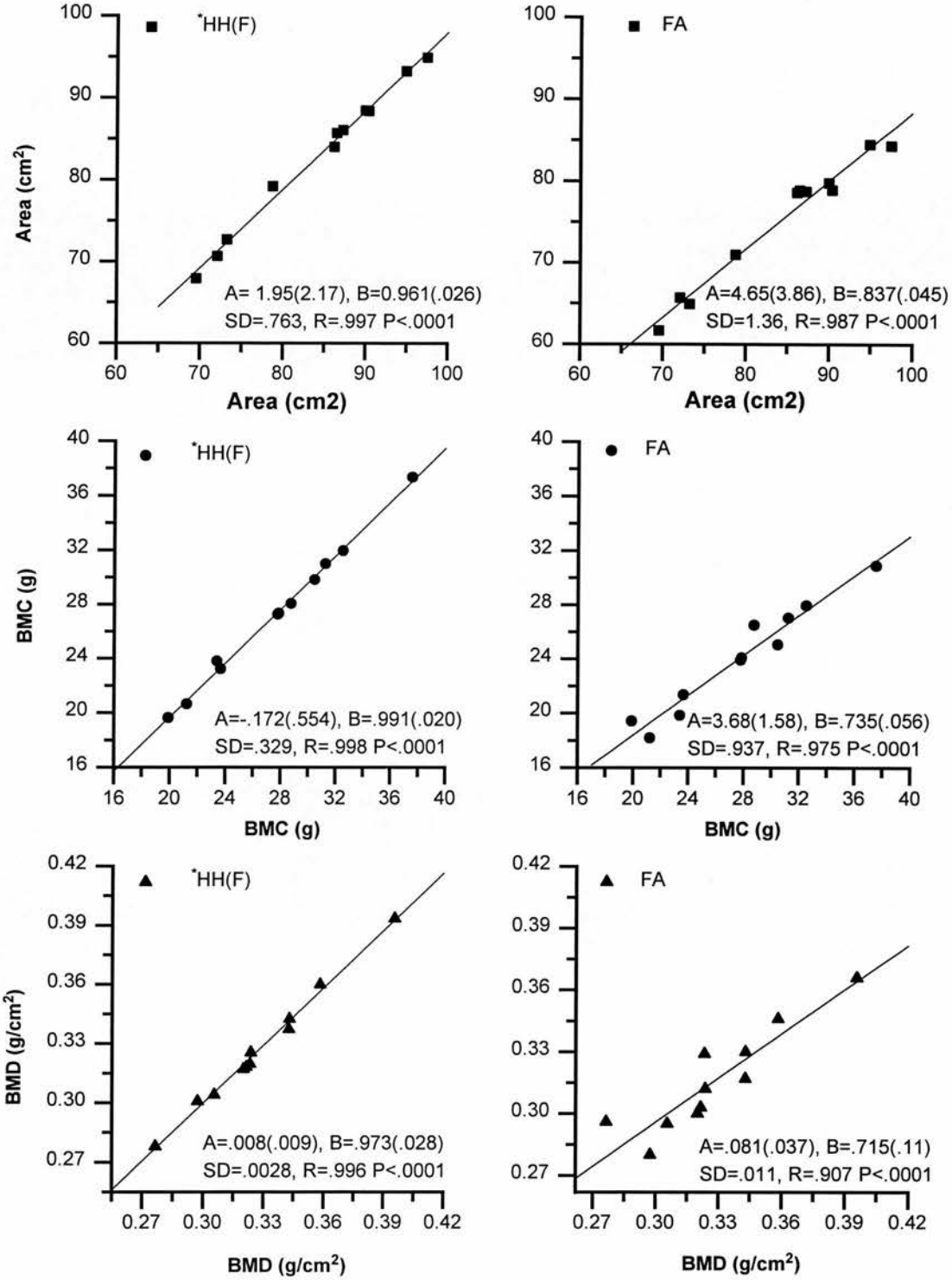

Figure 2.15 Correlation of the *HH (P) with *HH (F) and FA protocols for 11 control subjects. The solid lines are the least-square fits to the data (Y=AX+B) and the parameters of the fits are shown.

2.4 Discussion and conclusions

Hand bone mineral measurement by DXA is associated with very low exposure to ionising radiation. It has been shown that measurement of BMD by the standard Hologic Forearm and Spine protocols were non-linear in the hand BMD range and dependent on the soft tissue thickness. Moreover, the default Spine protocol in particular failed to detect the aluminium tubes or the first step of the aluminium step wedge. By making the necessary modifications to the standard protocols, linear relationships between the measured BMD and variations in the thickness of aluminium tube and step wedge were achieved. The modifications were verified by the assessment of the influence of the soft tissue thickness on the bone mineral. The effects of bone density threshold and hand posture on the bone mineral variables were evaluated using aluminium tubes embedded in perspex. The most appropriate threshold was established. The hand phantom was also used to examine the suitability of threshold selection by comparing the known hand phantom area with the values determined by different bone density thresholds. In-vivo effects of bone density threshold to minimise the variations in hand bone mineral with posture alterations were also examined. This approach was followed using the FA protocol. Significant reduction in the mean hand BMC variation between the two postures of relaxed-flat and loose-clenched was obtained.

Table 2.24 compares the various protocols for hand bone mineral measurement. For each of the factors considered the relative performance of each protocol was allocated a score between 1 and 6, where the lowest score corresponds to the best performance. Where the performances of different protocols were not significantly different, they were allocated the same score. In addition where a factor was considered particularly important, lower scores were allocated. For example, precision was considered to be particularly important but was not significantly different for any protocol and, therefore, all protocols were allocated 1 for this factor. The protocol with the lowest total score, therefore, represents the best overall performance. Although this scoring system is relatively arbitrary, it provides a useful indication of performance.

Table 2.24 Comparison of different protocols for hand BMD measurement.

Factor	Protocol						reference
	FA	*FA	P	*P	*HH (P)	*HH (F)	
Linearity	1	1	2	2	3	3	Tables 2.2
Soft tissue thickness	2	2	2	2	1	1	Table 2.8
Wall thickness	1	2	2	3	2	3	Figure 2.7
Height	1	1	1	1	1	1	Table 2.2
Inclined angle	6	2	3	2	5	6	Tables 2.9
Angle of deviation	1	1	1	1	1	1	Table 2.11
Precision	1	1	1	1	1	1	Tables 2.17 &2.18
Time	6	6	6	6	6	1	
Total points	19	16	18	18	20	17	

It can be seen from the Table that all the protocols except the *HH protocols were linear. However, the *HH protocols showed the smallest variation in BMD with variations with soft tissue thickness. The effect of wall thickness on tube area was the least for the FA protocol and the most for the *P and *HH (F) protocols. The effect of height above the couch on BMC and BMD was very small and so negligible. It is worth mentioning that the measurements were made using a hand support (transparent to x-ray). This hand support allows the hand to be positioned in a semi-clenched posture so that there is a minimum posture variation due to progression of RA disease or recovery from it. Therefore, with a maximum of a few centimetres hand height posture alteration, there would be negligible effect on BMC or BMD. The effect of angle of inclination on BMC or BMD was the least for the *P protocol. Moreover, there was no change in BMD between the two hand postures of intermediate and flat. The effect of angle of deviation was more critical on BMC and the most for the *HH and *P protocols. However, there was no BMD variation due to a deviation from the initial position, i.e. when the hand phantom

was aligned with the long axis of the couch. It was earlier shown that there were no significant differences between the various protocols for in-vitro or in-vivo precision and that they were all very precise.

Another important factor was the time required to acquire the scan. The time required to acquire a hand scan is approximately 12 minutes for any protocol, unless the scan is taken under the Fast mode of Spine acquisition protocol when it is reduced to 6 minutes. In the Table the best score for the time factor was given to *HH (F), i.e. the Fast mode taking half the time required for a performance mode scan, because the longer the scan time the more possibility of patient's hand movement while the scanning is in progress. This possibility of hand movement has a direct adverse effect on the precision. Use of the Fast mode also significantly saves the operator's and equipment time. Therefore, the total points for above protocols did not differ significantly. There were also excellent correlations between the *HH protocols for the hand bone mineral variables. Paired t-test on BMD measurements by *HH (P) and *HH (F) also revealed that there was no significant difference between the two means. It is, therefore, possible to perform scans in Fast mode. Bland and Altman statistical method also confirmed a good agreement between the *HH Performance and Fast protocols over the entire BMD range. However, there were not a good agreement between the *HH (P) and FA protocols in particular at the low BMD range.

In this study the control females had a mean BMC and a mean BMD of 21.4 ± 5.4 g and 0.320 ± 0.046 g/cm^2, respectively. The females with established RA had a mean BMC and a mean BMD of 16.1 ± 4.0 g and 0.262 ± 0.046 g/cm^2 with a 25% ($P = 1.1 \times 10^{-7}$) and a 22% ($P = 6.0 \times 10^{-9}$) reductions in BMC and BMD compared to the control females, respectively. The control males had a mean BMC and a mean BMD of 29.7 ± 6.6 g and 0.370 ± 0.053 g/cm^2, respectively. The males with established RA had a mean BMC and a mean BMD of 25.4 ± 3.9 g, 0.331 ± 0.039 g/cm^2 with a 17% ($P = 0.007$) and a 12% ($P = 0.007$) reductions in BMC and BMD compared to the control males, respectively.

Peel et al. (1994) studied 70 post-menopausal women with steroid treated RA and found a mean BMD of 0.396 ± 0.049 g/cm^2 for the control females and 0.306 ± 0.05 g/cm^2 for the RA patients, showing a 22.7% reduction in BMD. They measured hand BMD using the method of Pye and Law (1990), i.e. the subjects' hands were positioned palm-down on the build up plate on the scanner table with the fingers extended. The discrepancy between the BMD results is due to use of the Hologic hand protocol which was evaluated, because a mean hand BMD of 0.437 ± 0.040 g/cm^2 for the control females using the *P protocol was obtained.

Using a single photon imaging technique to assess the bone mass of the hand, Nicoll et al. (1987b) found the measurement precision of 1.9% for the BMC. They found 25.1 g and 18.0 g mean BMCs for normal men and normal women, respectively. The mean ages were 43(± 17) and 46 (± 16) years for men and women, respectively. For men they found hand BMC to correlate equally well with hand volume and arm span ($r_V = 0.81$ $P < 0.0001$, $r_S = 0.80$ $P < 0.0001$); however, the correlation with age alone was poor ($r = 0.25$ $P > 0.3$). For women both age ($r = 0.33$, $P < 0.02$) and years post-menopause ($r = 0.31$, $P < 0.02$) correlated with hand BMC, the positive correlation may be due to age range of 20 to over 70 years.

Using the method of Pye and Law (1990), Deodhar et al. (1994) studied 46 males and 49 female volunteers with means ages of 33(24 - 81) and 41(20 - 83) years, respectively. They found a total hand BMC in male volunteers of 90.9 g, compared to the 59.4 g that was obtained; and a total hand BMC in female volunteers of 62.2 g compared to the 42.7 g mean of control females we obtained, which is almost a 50% higher BMC than our results. Peel et al. (1994) found in practice that the projected hand area in women with established RA was the same as the value of 61 cm^2 in controls, i.e. a mean BMC of 24 g which, is much closer to what in this study was achieved.

Table 2.25 compares the present study and other reports for correlation of hand BMC and BMD with age and size and also the correlation of these variables with each other.

Table 2.25 Correlation (r) of hand bone mineral variables with each other and age, height and weight for the control subjects.

	Females			Male		
	Age	Ht	Wt	Age	Ht	Wt
BMC	*-0.46	***0.70	*0.52	0.34	0.34	*0.57
[N]BMC	*+*0.33*	*0.32*		*0.25*	****0.67*	
[D92]BMC	*NS*			*0.47*		
[D94]BMC	*NS*	****0.66*	**0.4*	*NS*	****0.57*	****0.58*
BMD	***-0.73	***0.63	0.38	0.17	0.30	0.49
[P]BMD_{RA}	*NS*	****0.31*	**0.38*			
	BMC	BMD		BMC	BMD	
Area	***0.90	***0.60		***0.82	*.58	
[P]$Area_{RA}$	**0.61*	*0 .07*				
BMC		***0.88			***0.94	

The figures *in italics* are other workers' results.
NS: not significant, *: P < 0.05, **: P < 0.01, ***: P < 0.001. *[N]: Nicoll et al., 1987 [D92]: Deodhar et al., 1992 [D94]: Deodhar et al., 1994 [P]: Peel et al., 1994*

Deodhar et al. (1994) found no correlation between hand BMC and age in both sexes. We found significant correlations between BMC and BMD with age for female controls. No significant correlations for male controls BMC and BMD with age were found. Deodhar et al. (1992) also found hand BMC did not change with age in women but increased with age in men (r = 0.47, the significance level was not quoted). Peel et al. (1994) found that the projected area in women with established RA was the same as that in the control (61 cm^2). We found a significant reduction of 8% for the female RA patients (60.3 ± 7.6cm^2 compared to 65.7 ± 9.1cm^2 t = -3.3 P = 0.001).

Indices of hand bone mineral using prediction equations for BMC and BMD were used to compare normal subjects and RA patients. The CoV for the control females slightly improved (from 21% to 20%) when BMC_I was plotted against age compared to the value for plot BMC versus age. The slight improvement in the CoV might be due to a low number of subjects or a narrow size variation. Therefore, there was also little improvement ($Z = -0.84$, $P = 0.005$ to $Z = -0.94$ $P = 2x10^{-22}$) in the Z-score. Normalising BMC by height improved the CoV quite significantly, resulting in a better separation between the control females and the RA subjects. Though body height could also be changed by disease related process, there was no difference in height between our control and RA patients. When BMD was plotted against age for the control females, a significantly better CoV (10%) compared to BMC versus age CoV of 21% was obtained. The BMD_I CoV did not change when BMD_I, was plotted versus age since there was a high correlation of ($r = -0.73$, $P < 0.0001$) between BMD and age. A Z_I-score difference of -1.3 ($P = 8 \times 10^{-7}$) and a $Z_I = -1.3$ ($P = 1x\ 10^{-6}$) between the control and RA were obtained. For males significant differences in mean BMC Z-score and BMD Z-score of -0.70 ($P = 0.002$) and -0.78 ($P = 0.01$) were calculated.

The normal subjects and RA patients were compared using the *HH (P) and *P methods. The assessment revealed that the *HH (P) protocol had no superiority over *P protocol to separate the RA from normals.

Provided the appropriate threshold and linearity factors were used, no protocol showed a marked overall advantage in terms of precision, linearity and posture dependency. However, the Hologic Hand protocol allows the scans to be acquired significantly faster and is now generally available to other centres using Hologic QDR systems. It is, therefore, recommended that this protocol should be used (Salamat, 1996).

To finalise the discussion, it can be concluded that there are still some inconsistent results when a comparison is made between the various published works, and there is still the need to study bigger populations of normal and RA patients. Normal ranges for

different sexes and different races should also be established. However, normalising by physical sizes is not satisfactory since body height or weight also could be affected by disease related process such as the presence of vertebral fractures or joint prostheses. Even normalising by forearm span, only men had a moderate correlation of 0.50, P = 0.0006 and a high correlation of r = 0.80 P < 0.0001 according to two different publications quoted on Table (2.25) which is still not significantly better for BMC and area correlation ($r_M = 0.82$, $P < 0.001$ present results). Normalising by hand volume (e.g. displacement technique) can also be altered by progression of joint deformities in RA and results in an increase in the hand volume and consequently a decrease in projected area which would produce an artifactual increase in areal BMD with progressive disease. Since DXA measurements of other skeletal sites are expressed as an area density (g/cm^2), it is more appropriate to apply the same approach to the hand, and normalise hand BMC for projected hand area ($r_F = 0.90$ $P < 0.0001$) giving an areal bone mineral density for the following reasons:

1. No difference between hand BMC and BMD precision.
2. No BMD variation with respect to the distance from the reference point (distal ulna radius junction).
3. Significantly lower CoV and consequently better separation between the RA and controls.
4. Use of normalised BMC by size such as body height or weight could also be influenced by disease related progression.

Concerning the accuracy of hand bone mineral measurement, several cadavers' hands of different sexes with a wide range of physical sizes would be required to be ashed since different hands have different biological structure and BMDs like other sites.

Chapter 3

Assessment of Bone Mineral of the Os Calcis

3.1 Introduction

The skeleton consists of 80% cortical (compact) bone, as found in the shafts of the limb bones, and 20% trabecular (cancellous) bone as in the ends of the long bones, the spine and the pelvis. Trabecular bone has a large surface to volume ratio, with a high turnover rate (about 8 times that of cortical bone) and is more responsive to metabolic stimuli (Evans, 1988).

Epidemiological studies confirm that the osteoporotic fractures are first seen in the vertebral body and the distal radius, both of which contain large fractions of trabecular bone (Genant et al., 1988). The fraction of trabecular bone at different sites of the body are in ultradistal radius (45%), neck of femur (up to 50%), vertebrae (65%) (Hosie et al., 1987) and os calcis (90-95%) (Vogel et al., 1988). The os calcis is not at risk of fracture itself, but because it is predominately a trabecular and load-bearing bone it might be a good predictor of hip/spine fracture.

In a prospective study for EPIDOS, Hans et al. (1996) assessed the value of os calcis measurements by ultrasound (US). They studied a large population of 5662 elderly women. Hans et al. (1996) measured the hip BMD by DXA. They reported that US measurements of the os calcis predicted the risk of hip fracture as accurately as the hip BMD measurements by DXA. It was also reported that for each SD reduction in US or BMD values, the risk of hip fracture was approximately doubled.

Glüer et al. (1996) studied 4698 post-menopausal women to assess the relationship of US variables and BMD in patients with and patients without recent fractures. They measured BMD of the proximal femur and lumbar spine with a DXA scanner; the BMD

of the os calcis was measured using a SXA device. Sensitivity and specificity with broadband ultrasound attenuation (BUA), velocity and BMD variables were reported to be comparable. Glüer et al. reported that both BUA and BMD were independently related to fractures. They also reported that for the prediction of hip fractures, BUA was not as strong as BMD of the femoral neck, and that BUA was comparable to BMD of the calcaneus, and it was better than BMD of the spine for the prediction of hip fractures. Many other studies have also shown the relevance and value of the US measurements of the os calcis for the prediction of hip/spine fractures (Funke et al., 1993; Stewart et al., 1994).

Jonson (1992) developed a method for determining BMC in the peripheral skeleton, e.g. calcaneus bone or radius and ulna, using a gamma camera measuring two different photon energies from two isotopes. For a measurement time of 15 minutes an effective dose of less than 10 μSv has been quoted. Drawbacks of the method are the errors caused by source decay and the short half life of the source. Another drawback is the handling of the flood source. This is specially true for an ^{125}I source, which needs careful handling because of the radiation hazard.

Using DXA, Cummings et al. (1993) assessed bone density at various sites for prediction of hip fractures. They studied a large population of 9704 post-menopausal women in a multi-centre trial. Cummings and his colleagues measured BMD and BMC of the calcaneus, mid and distal forearm with OsteoAnalyzer (Siemens-Osteon, Wahiawa, Hawaii). They measured the spine and proximal femur with Hologic QDR 1000 scanners. Cummings et al reported that low hip bone density was a stronger predictor of hip fracture than bone density at other sites. The os calcis was the next best site for measuring bone density to predict hip fractures. The radius and the spine were the least predictive values.

Pye et al. (1994) looked at the performance, patient acceptability and precision of software developed for the measurement of calcaneal BMD. The developed software

was based on Forearm protocol of their Lunar DPX-L whole body scanner. Although the precision was acceptable, the overall analysis time was quite long (~30 min). More details of the study are given in the discussion and conclusion section.

Many comparisons between bone mass measurements at different skeletal sites have been reported. In general, better correlations are obtained between sites with similar proportions of trabecular and cortical bone. Using SPA, Christiansen (1982) found that the measurement of the BMC of the radial shaft (95% cortical bone) was well correlated ($r = 0.86$) with the total weight of the skeleton (80% cortical). The os calcis which is predominantly trabecular bone showed only a moderate correlation ($r = 0.59$) with the total skeletal mass but was found to be well correlated ($r = 0.77$) with dual photon measurements of the lumbar spine (65% trabecular) (Wasnich et al., 1985).

There is continuing uncertainty about the relative merits of bone mineral measurements at different skeletal sites in the diagnosis and management of osteoporosis. Some reports suggest that spinal compression is more closely associated with spinal than with forearm bone mass or bone density (Sogaard et al., 1994) and that appendicular measurements are of limited value in clinical practice (Wark, 1993 and Van Berkum et al., 1989). Other reports suggest that peripheral and central measurements are of comparable value both in diagnosis and fracture prediction (Black et al., 1992 and Melton et al., 1993). It is also not always possible to measure bone density of spine and hip due to existing spine fractures or hip replacement. Therefore, to address these issues the focus of this study was to detect the usefulness of the os calcis as a site for BMD measurement with DXA.

DXA for bone assessment of the axial skeleton for a variety of reasons is a universal and established technique. The equipment is widely available and has the capacity of multi-site measurements mainly of the spine, hip and forearm. Furthermore, these scanners allow precise and rapid measurement of the sites prone to osteoporosis. The effective dose for the measurement of the os calcis is very small and is less than 1 μSv (Genant

et al., 1996). However, there were a number of problems with the measurement of the os calcis that had to be dealt with. One of the problems was the limitation of the detector arm movement and therefore a feasible and appropriate way of patient positioning had to be achieved. It was, therefore, vital for patient comfort that the most appropriate positioning technique was achieved. Another problem is that os calcis is a bone with non-uniform density. This non-uniformity considerably affects precision so the appropriate regions had to be established for measurement and analysis.

It has been reported that wrist and vertebral fractures occur predominantly from trabecular bone loss, whereas hip fractures are due to cortical bone loss (Riggs, Melton 1983). For these reasons, two different regions were defined, one of purely trabecular bone with less BMD variation for better precision and one with mixed (trabecular and cortical) bone using a group of normal subjects. It was also vital to find a feasible way to position the osteoporotic patient, who might already suffer a chronic back pain, in a comfortable position while the scanning was in progress. Other factors that had to be considered were to assess the effect of soft tissue and the total time required for the examination (set-up, scanning and analysis). The effect of size of ROI due to counting statistics on precision was also investigated.

Three DXA protocols were modified and assessed to establish the most appropriate protocol for measuring the os calcis in patients with severe established osteoporosis i.e., osteoporotic patients having hip replacement, vertebral wedges or fractures with consequent height alterations. The current methods for the measurement of the conventional sites differ in terms of resolution, pixel size, line spacing, scan speed, linearity correction coefficients and bone density thresholds. The linearity coefficients are used for beam hardening effects and the coefficients used by the manufacturer are appropriate for particular ranges of soft tissue and bone density. Therefore, the linearity coefficients for bone density appropriate to the os calcis were established. An os calcis phantom was constructed and used to assess the precision and the effect of size of region of interest on precision. The phantom was also used to assess the effects of clothing and

soft tissue thickness. In-vivo suitability of the patient positioning in two different positions of sitting relaxed or lying towards one side for the measurement of the site was examined in a group of normal volunteers. An appropriate ROI with uniform density (trabecular) for better precision was established. This ROI is in the centre and flat part of the os calcis. Another ROI was also established. This ROI covered the entire posterior portion of the os calcis, with one of the borders of the ROI placed on a perpendicular line along the fibula to the base line of the bone. A group of normal subjects were measured to establish the ROI and also develop the ROI size for the measurement and analysis. The mean values for young sex matched normals of the os calcis, hip and spine were used to compare the osteopenic/osteoporotic women with the normal values according to the WHO criteria (Kanis et al., 1994).

3.2 Methods and materials

3.2.1 Derivation of linearity correction coefficients

In order to compensate for the low soft tissue and bone equivalent of os calcis compared with spine and forearm sites, it was necessary to establish appropriate linearisation values for the methods of Spine and Forearm. The linearisation values for the Spine method, with and without the use of a build-up plate, and for the Forearm method, without the use of a build-up plate, were obtained.

To derive linearisation values for the Spine and Forearm methods without the use of the build-up plate, a 20 mm thick poly methyl methacrylate (perspex) plate was used to simulate soft tissue. The reason for using the perspex plate was that the software does not recognise any bone without enough soft tissue around it. The build-up plate consisted of 4.5 mm aluminum alloy (EH30) and 20 mm perspex. To investigate the linearity for the os calcis bone mineral measurement with the established linearity correction coefficients and also to compare the linearity using the default software, 8 aluminium slabs were used. The aluminum slabs had square shapes with equal areas of

25 cm^2. The slab thickness varied from 1.6 mm - 7.8 mm with CaHA equivalent of 0.19 - 0.93 g/cm^2.

3.2.2 Subject positioning

Figure 3.1a shows a subject lying on her right side to have her right heel scanned. For this position the foot was held against a material transparent to x-ray and supported by a device at the bottom edge of the couch while the scanning was in progress. Figure 3.1b shows the same subject sitting relaxed for her heel measurement.

3.2.3 Region of interest selection

Selection of ROI has a crucial effect on precision, because the os calcis is a bone with non-uniform density. 5 (2M/3F) normal subjects aged 25 - 75 years with a wide range of BMD (0.35 - 0.77 g/cm^2) were used to find the bone density distribution along the x- and y-axis. To improve the precision and to choose a purely trabecular bone site, appropriate ROIs with less BMD variation were defined. Figure 3.2a shows the various regions of interest defined for the study. To assess whether trabecular or a combination of trabecular and cortical bone predicts hip fracture more accurately, a region of interest containing both types of bones was selected. This region (R5) was enclosed between a line drawn along the fibula and perpendicular to the x-axis of os calcis in such a way that the os calcis was surrounded between the ends of the heel and the fibula. The trabecular regions included a rectangle (R4) with a 4.0 cm^2 (2.2 cm x 1.8 cm) area, having a position in which its centre is a point about 3 cm from the heel end and 4 cm from the sole of the foot. R3 is an octagon having an area of 2.5 cm^2 surrounded by R4. R2 is another octagon with the same area as R3 but adjacent to the left side of the Figure (Figure 3.2a), and finally R1 which is a rectangle with an area of 2.0 cm^2 (1.24 cm x 1.6 cm) enclosed by R2.

Figure 3.1 DXA bone mineral assessment of a volunteer's heel. (a), (above), subject was lying on her right side. (b), (below), subject was sitting relaxed.

Medical Physics, WGH. Edinburgh.

U1014940B Fri 14.Oct.1994 14:58
Name: [redacted]
Comment:
I.D.: CTL112 Sex: F
S.S.#: - - Ethnic: W
ZIPCode: Height: cm
Scan Code: CM Weight: kg
BirthDate: 27.Nov.73 Age: 20
Physician:
Image not for diagnostic use

k = 1.369 d0 = 162.9(1.000)[4]

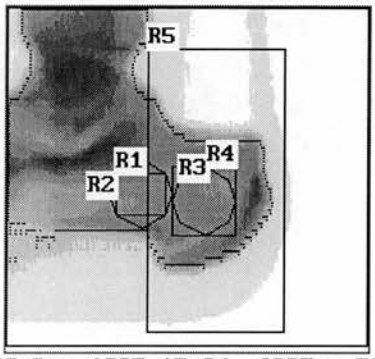

·03.Dec.1997 17:24 [207 x 50]
Hologic QDR-1000/W (S/N 967 P)
Subregion Forearm V5.55Q

	C.F.	1.017	1.108	1.000
Region		Area (cm2)	BMC (grams)	BMD (gms/cm2)
GLOBAL		36.09	25.51	0.707
R1		1.98	1.03	0.520
R2		2.53	1.34	0.531
R3		2.53	1.19	0.471
R4		3.97	1.97	0.495
R5		12.15	6.42	0.528
NETAVG		13.72	7.24	0.528

HOLOGIC

Figure 3.2a A volunteer's DXA image of the os calcis with different ROI for the assessment of bone mineral and precision.

Medical Physics, WGH. Edinburgh.

U1017940A Mon 17.Oct.1994 17:02
Name: Os calcis Phantom QC
Comment:
I.D.: 17.10.94 Sex: F
S.S.#: - - Ethnic:
ZIPCode: Height: cm
Scan Code: Weight: kg
BirthDate: / / Age:
Physician:
Image not for diagnostic use

k = 1.376 d0 = 168.6(1.000)[4]

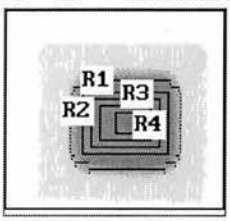

·03.Dec.1997 17:41 [126 x 30]
Hologic QDR-1000/W (S/N 967 P)
Right Forearm V5.55Q

	C.F.	1.017	1.108	1.000
Region		Area (cm2)	BMC (grams)	BMD (gms/cm2)
GLOBAL		8.32	4.50	0.541
R1		4.88	2.87	0.588
R2		3.12	1.84	0.589
R3		1.76	1.03	0.589
R4		0.47	0.28	0.588
NETAVG		4.88	2.87	0.588

HOLOGIC

Figure 3.2b DXA image of the os calcis phantom with different ROI for performing various experiments and the assessment of long term precision.

In-vivo precision was estimated for the 5 ROIs from repeat lateral scans of the right heel of 10 (6M/4F) subjects. Precision was defined as the mean coefficient of variation in percentage terms (%CV) for duplicate measurements with re-positioning between the scans. The volunteers had a mean age of 37 ± 15 (20 - 72) years, a mean weight of 68.9 ± 10.6 (51.2 - 85.0) kg, a mean height of 1.70 ± 0.09 (1.58 - 1.81) m.

3.2.4 Phantom measurements

An os calcis phantom was used to assess precision and perform various experiments. The os calcis phantom, with dimensions of 4.7 mm thickness (Al), equivalent to 0.53 g/cm^2 CaHA, and equal length and width of 3 cm was used. Area, BMC and BMD precisions were obtained using 10 repeat scans. To assess the equipment stability 30 daily phantom measurements were also taken. The precision expressed as the percentage coefficient of variation (%CV), is defined as:

$$[(\text{standard deviation}) \div (\text{mean})] \times 100$$

The effect on the precision of the size of the region of interest was also investigated using the os calcis phantom (Figure 3.2b). The effect of soft tissue was investigated using the phantom in water. The effect of clothing was also investigated using the phantom covered with different layers of stockings. For a phantom measurement 3 minutes was required.

3.2.5 Subject measurements

The BMD of the os calcis was measured in a group of normal subjects (n = 21) and also in patients (n = 31) who were diagnosed as osteopenic/osteoporotic based on the spine and/or femur BMD. The os calcis measurements were performed in the Forearm mode. An os calcis image took only 2 minutes. Table 3.1 shows the details of the normal and osteopenic/osteoporotic female subjects.

Table 3.1 Details of studied females. The results are expressed as the mean ± SD (range).

Subjects/Variables	Age (y)	Height (cm)	Weight (kg)
Normals	27.9 ± 3.7	165.1 ± 6.9	68.3 ± 14.2
(n = 21)	22 - 36	155 - 183	46.9 - 96.8
Osteopenic/Osteoporotic	59.6 ± 12.9	157.4 ± 7.2	63.9 ± 13.9
patients (n = 31)	20.0 - 81.0	143.0 - 171.5	43.9 - 99.6

3.2.6 Statistics

Linear regression analysis was used to investigate the linearity and the effect on os calcis bone mineral of soft tissue and clothing. Linear regression analysis was also used to assess the relationship between the spine, total femur and neck of femur T-score with the total os calcis and trabecular os calcis T-score. T-score is calculated as the difference between the patient bone mineral value (P) and the mean value for young sex matched normals (M_Y), divided by the standard deviation of the mean value for young normals (SD_Y):

$$\text{T-score} = (P - M_Y)/SD_Y$$

In order to assess if the measurements of different regions of the os calcis are reproducible, the scans were analysed by two different operators.

3.3 Results

3.3.1 Derivation of linearisation values for calcaneal bone

Figure 3.3 reveals the significance of the use of the appropriate linearity correction coefficients for the os calcis measurement, when the conventional methods of measurement are used. For the measurement of the os calcis the Forearm and Spine acquisition methods with and without the use of the build-up plate were developed. As can be seen, the Spine protocols failed to detect the aluminium slab with BMD of less than 0.3 g/cm^2. The Spine method plots without the use of the build up plate (c and d) showed significant intercepts and different slopes for BMC and BMD. The default Forearm protocol showed significant intercepts and significantly higher slopes compared to the modified Forearm method. The modified Forearm protocol (graphs e and f) was significantly improved yielding insignificant intercepts and the same slope for aluminium (g/cm^2) versus BMD (g/cm^2) and A1(g) versus BMC (g) plots.

The Spine method (with the use of the build up plate) showed the same slopes for both plots (a and b). However, to appreciate the difference more easily, assuming an initial aluminium mass area = 0.7 g/cm^2 and aluminium mass = 3.0 g being increased by 10% the Forearm protocol increased by 9.9% in both BMD and BMC. The Spine protocol (without the use of the build up plate) increased by 9.0% and 10.1% in BMC and BMD respectively. Regarding the linearity, there was no significant difference between the Spine (with the use of the build up plate) and Forearm methods. The acquired linearisation correction coefficients for the os calcis for the Forearm and Spine methods with and without the use of the build up plate are shown below. These coefficients were used in place of the current software correction coefficients. Q1, Q2 and Q3 are the software environment variables which correct for non-linearity with BMD.

(Q1 = 0.3193, 0.451; Q2 = 0.6386, 0.801; Q3 = 1.117, 1.219)
(Q1 = 0.3200, 0.456; Q2 = 0.6399, 0.796; Q3 = 1.120, 1.203)
(Q1 = 0.3281, 0.391; Q2 = 0.6563, 0.743; Q3 = 1.149, 1.216)

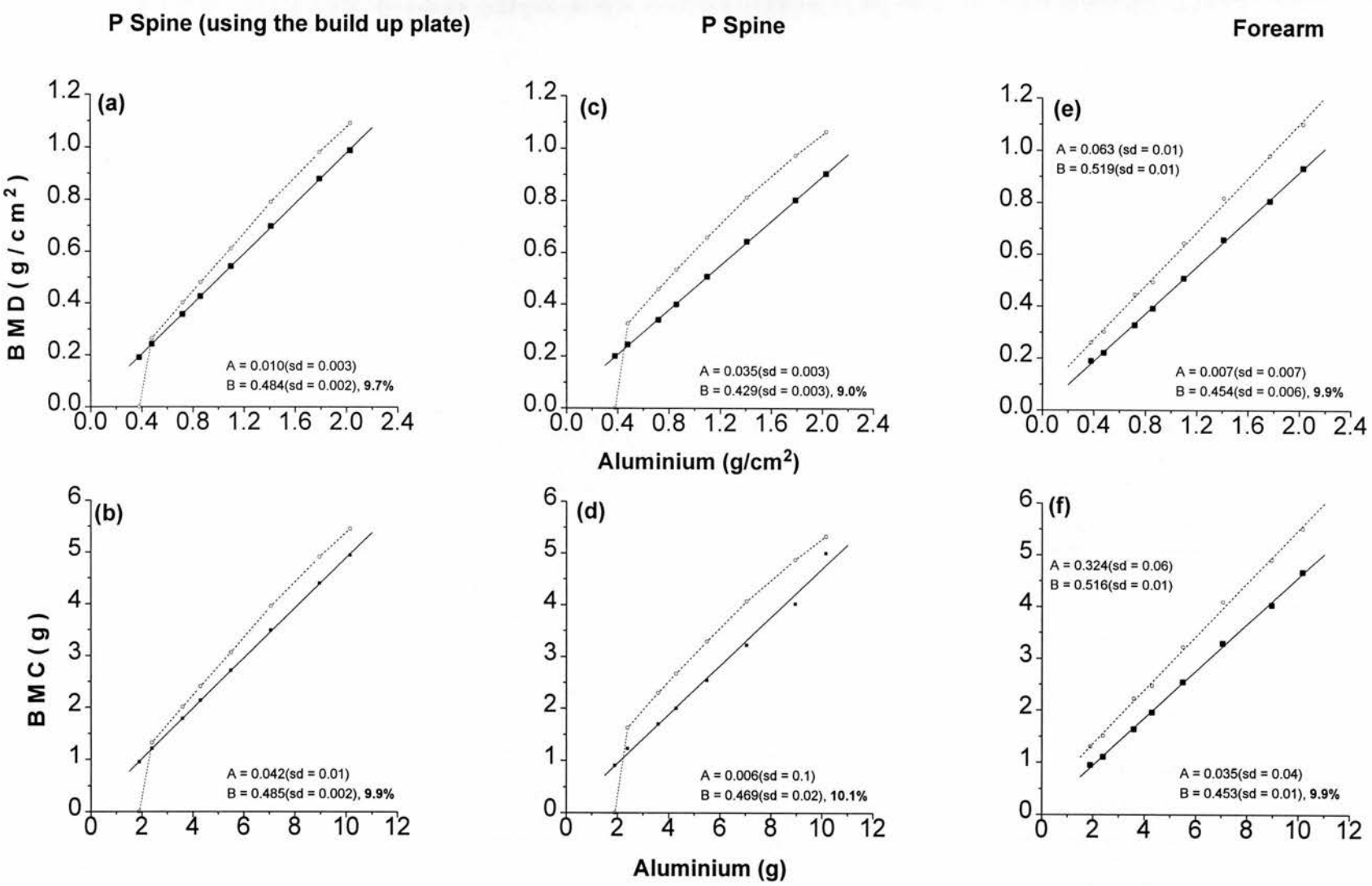

Figure 3.3 Linearity between measured BMD (g/cm^2) and actual Al (g/cm^2), measured BMC (g) and actual Al (g) for different protocols. Slabs of different thickness of Al (simulating os calcis) covered with perspex (simulating soft tissue) having a thickness of 5 cm were measured. In all cases R>0.999 and P<0.0001. The solid lines show the least square fits to the data when the acquired linearity correction coefficients were used. The dashed lines show the trends when the default linearity coefficients were used.

3.3.2 Development of os calcis phantom and in-vitro precision

For the evaluation of in-vitro precision and other experiments an os calcis phantom was required. To find a typical value for BMD, a normal female's heel was scanned. Figure 3.2a shows a volunteer's DXA image of the os calcis with different ROIs, having a net average BMD of 0.53 gcm^{-2}. The os calcis phantom, constructed of 4.7mm aluminium equivalent to 0.54 g/cm^2 CaHA, had a 9.0 cm^2 (3x3) area and was embedded in 4 cm thick perspex sheet. The perspex area was 25 cm^2 (5x5). 10 repeat measurements were taken and a CV of 0.3% (for all bone mineral variables) was achieved. Table 3.2 shows the details of the phantom and the repeat and medium-term precision. For the medium-term precision, 30 daily measurements were performed and a CV of 0.6% was found for both BMC and BMD. Figure 3.2b shows the phantom DXA image.

Table 3.2 Os calcis phantom bone variables, repeat and medium term precision.

	Variable	Mean ± SD	CV%
10 repeat measurements	Area (cm^2)	8.43 ± 0.029	0.3
	BMC (g)	4.51 ± 0.013	0.3
	BMD (g/cm^2)	0.535 ± 0.0016	0.3
30 medium-term measurements	Area (cm^2)	8.39 ± 0.057	0.7
	BMC (g)	4.45 ± 0.027	0.6
	BMD (g/cm^2)	0.530 ± 0.0033	0.6

3.3.3 The effect of size of region of interest on precision

The os calcis phantom image was used, to assess if the size of region of interest affects the precision due to photon counting statistics. Figure 3.2b shows the details of different regions. Figure 3.4 shows the plots of the os calcis phantom BMD and precision against

Area. Figure 3.4a shows that, except for the smallest ROI (A = 0.5 cm^2) which had the highest SD, the other regions with area between 1.8 - 4.9 cm^2 showed similar precision of around 0.4% (Figure 3.4b).

3.3.4 The effect of soft tissue thickness

In following the course of bone mineral measurements in a patient over time, the patient might undergo weight alterations. Such weight alterations could affect the thickness of soft tissue overlying the os calcis. To assess if soft tissue variations affect the apparent bone density and to verify the results of application of the established linearity correction values, the os calcis phantom was scanned with different perspex thicknesses. The perspex thickness varied from 1.0 - 4.5 cm in increments of 0.5 cm. Figure 3.5a shows the measured bone density (g/cm^2) changes against perspex thickness (cm). A significant ($P < 0.001$) relation of ($r = - 0.94$) was found. However, a negligible slope of - 0.004 g/cm^2 per cm soft tissue was obtained.

3.3.5 The influence of clothing

It is difficult for the patients with established osteoporosis to take-off their foot coverings (e.g. socks, stockings/tights), and it is also time consuming for the patient, operator and the equipment. It was therefore, important to assess if covered feet affected the os calcis bone mineral measurements. The influence of clothing on os calcis was investigated using the os calcis phantom covered with different clothing layers (0.0 mm -2.0 mm). The graphs of BMD (g/cm^2) and BMC (g) versus clothing thickness (mm) were plotted in Figures 3.5b and 3.5c. There was no significant ($P > 0.05$) correlation between BMC, BMD and clothing thickness. Slopes of - 0.003 (g/cm^2) per mm clothing thickness for BMD and - 0.009 (g) per mm clothing thickness for BMC were found. The changes in BMD and BMC per mm clothing thickness were negligible, showing that there was no need to remove their foot coverings.

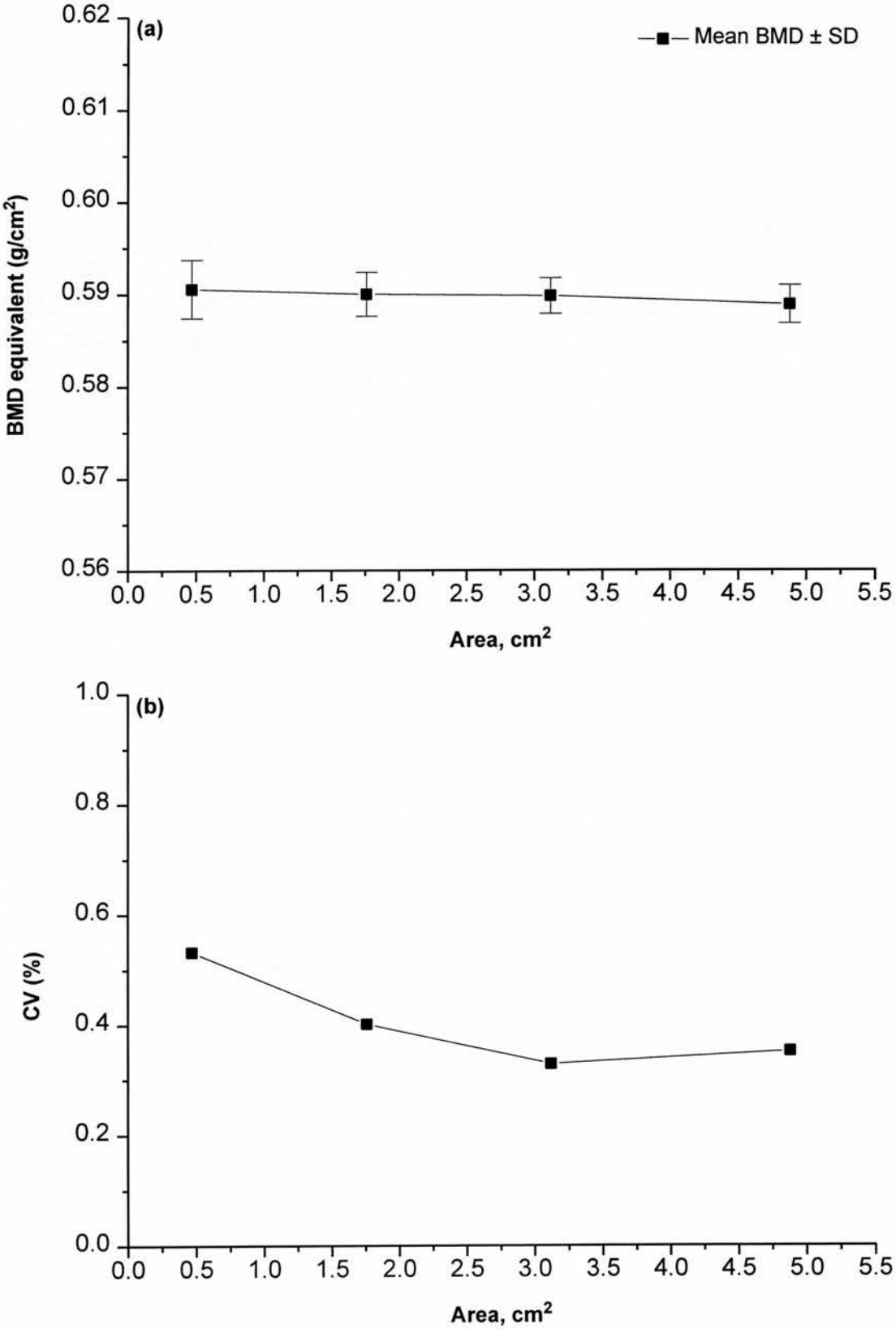

Figure 3.4 Investigation of effect of size of region of interest on os calcis phantom bone density (a) and precision (b).

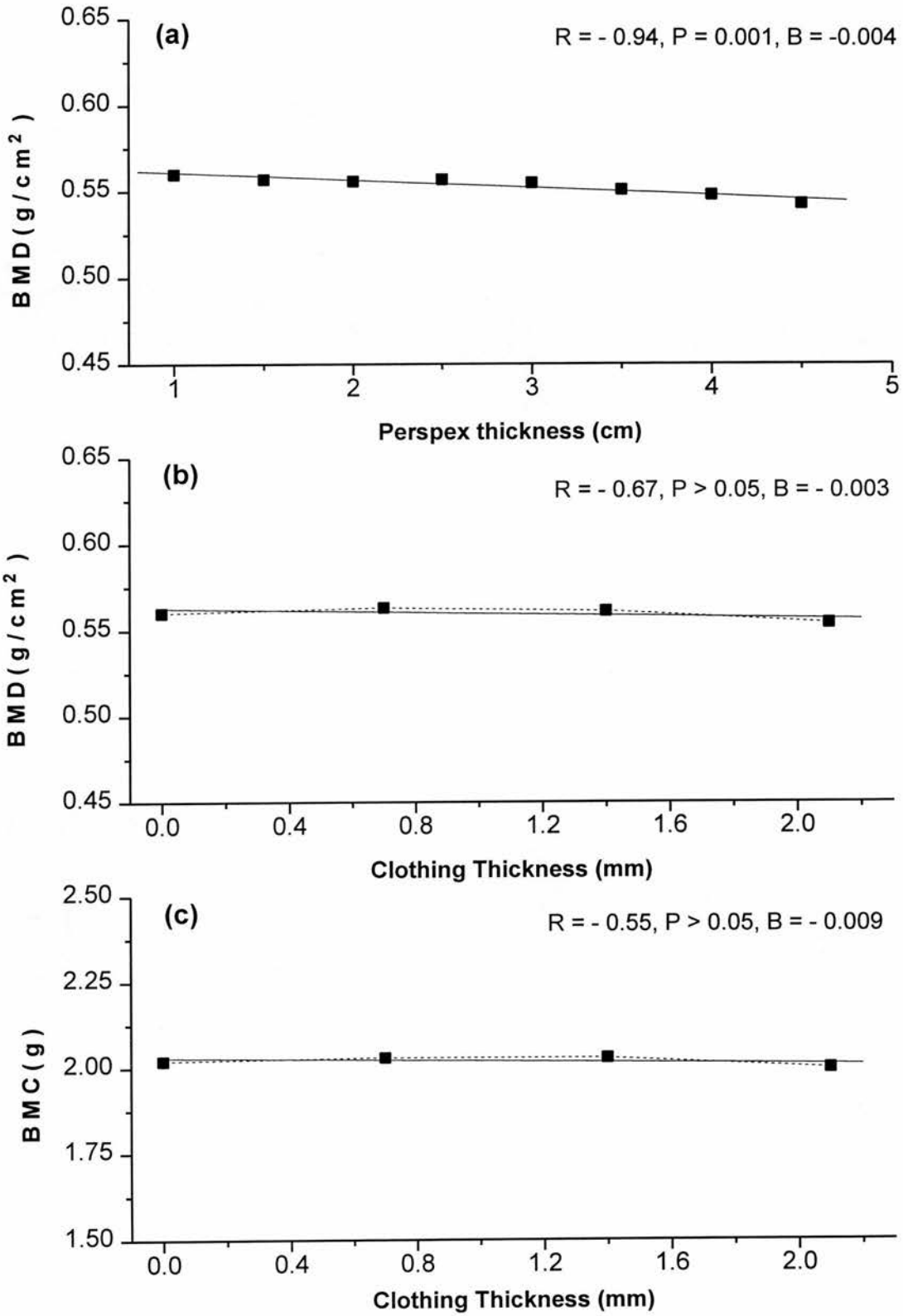

Figure 3.5 The influence of soft tissue thickness on BMD (a). The influence of clothing (stockings and tights) on BMD (b) and BMC (c) respectively. The os calcis phantom was used for the above investigations.

3.3.6 Os calcis bone mineral heterogeneity

Figure 3.6 shows that the os calcis is a heterogeneous bone, i.e. a bone with non-uniform density. This non-uniform density can substantially affect the precision. It was therefore crucial to select regions of interest with less BMD variation. Table 3.3 and Figure 3.6a show variation in BMD with distance from the sole of the foot for five healthy volunteers. It can be observed that the density distribution varies considerably from the compact part of the site to less dense (purely cancellous) regions. Here from about 3 cm to 5 cm there is less change in BMD (~ 6.6%) giving a mean length of approximately 2 cm and a measurement point of approximately 4 cm from the sole of the foot. Table 3.4 and Figure 3.6b show the density distribution with increasing the distance from the heel end; the average change is about 6% for a mean length of 1.5 cm and a measurement point of 3 cm from the heel end. The criteria to establish the plateau region are shown in Tables 3.3 and 3.4. The plateau region had less than 10% variation in BMD with a measurable length in order to get precise measurements. Therefore, to reduce the scan time and increase comfort of the patient a measurement point of 3 cm from the heel end and 4 cm from the sole of the foot would be measured. The os calcis region of interest measurement size would have equal length and width of 8 cm.

3.3.7 In-vivo reproducibility

Table 3.5 shows the os calcis BMC and BMD precision for the various ROIs for each subject. Table 3.5 shows that in-vivo BMC precision ranges from 0.0% - 9.4% and the BMD ranges from 0.0 - 4.5%. Table 3.6 shows the mean BMC and BMD precision ranges obtained by two different operators. Each operator found similar BMC and BMD precision for all the regions. Figure 3.2a shows the details of the various regions. Both operators found similar BMC and BMD precision for all the regions except R1 (for both variables) and R5 (for BMC). A low BMC precision was found for R5. However, the BMD measurement was as precise as the R3 and R4 regions. R5 bone density measurement was precise, because the bone density is uniform around the line aligned with the right side of the fibula (left side of R5 box). R5 is referred to as the 'total' os calcis and R4 as the 'trabecular' os calcis in the chapter.

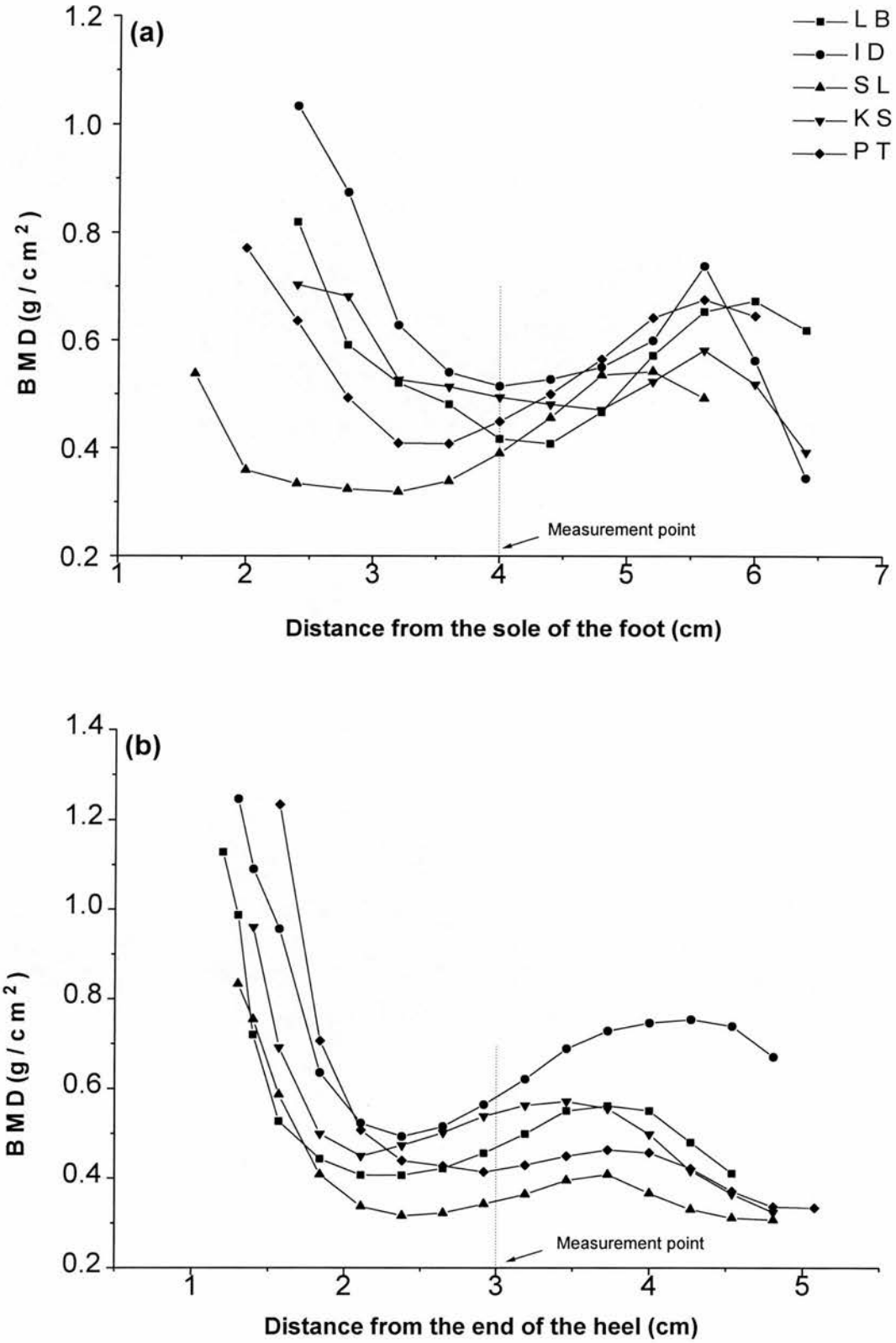

Figure 3.6 Variation of BMD (g/cm^2) with the distance (cm) from the sole of the foot (a) and from the end of the heel (b).

Table 3.3 Variation of heel BMD with distance from sole of foot for five healthy subjects.

Distance from foot sole (cm)	LB F	ID M	SL F	KS F	PT M
1.6	-	-	.537	-	-
2.0	-	-	.359	-	.771
2.4	.820	1.03	.334	.703	.636
2.8	.591	.875	.324	.681	.493
3.2	.520	.628	.319	.526	.409
3.6	.481	.540	.339	.513	.408
4.0	.417	.514	.390	.494	.449
4.4	.408	.527	.456	.481	.500
4.8	.467	.550	.535	.471	.565
5.2	.572	.600	.542	.523	.642
5.6	.654	.739	.493	.582	.676
6.0	.674	.563	.519	.646	-
6.4	.620	.345	.393	-	-
change in BMD	8.1%	6.0%	4.6%	4.5%	9.8%

The underlined numbers show less variations in heel BMD (i.e. between a certain distance from sole of foot).
Average BMD change for the underlined ranges = 6.6% Average plateau length ~ 2cm
Measurement point ~ 4cm from foot sole F and M denote female and male

Table 3.4 Variation of heel BMD with distance from heel end for five healthy subjects.

Distance from heel end (cm)	LB F	ID M	SL F	KS M	PT M
1.3	1.13	-	-	-	-
1.4	.720	1.25	.833	.960	-
1.6	.527	.956	.586	.691	1.23
1.8	.443	.635	.408	.499	.706
2.1	.407	.523	.337	.449	.507
2.4	.406	.493	.316	.473	.439
2.6	.422	.515	.322	.501	.427
2.9	.456	.564	.342	.538	.414
3.2	.499	.621	.364	.562	.429
3.5	.550	.689	.395	.571	.449
3.7	.561	.728	.408	.555	.463
4.0	.550	.746	.366	.498	.457
4.3	.480	.754	.330	.417	.422
4.5	.411	.739	.311	.365	.371
4.8	-	.671	.307	.324	.336
5.1	-	-	-	-	.334
change in BMD	8.1%	5.9%	5.6%	7.8%	4.0%

The underlined numbers show less variations in heel BMD (i.e. between a certain distance from heel end).
Average BMD change for the underlined ranges = 6.3%

Average plateau length ~ 1.5cm

Measurement point = 3cm from heel end F and M denote female and male

Table 3.5 In-vivo precision for various regions of the os calcis. CV% is (100 x SD/Mean) for duplicate measurement.

Subject	ROI	Mean BMC ± SD (g)	CV (%)	Mean BMD ± SD (g/cm^2)	CV (%)
	R5	8.54 ± .24	2.8	0.607 ± .001	0.2
	R4	2.20 ± .035	1.6	.562 ± .008	1.5
MA	R3	1.35 ± .035	2.6	.535 ± .013	2.4
	R2	1.41 ± .007	0.5	.559 ± .007	0.4
	R1	1.11 ± .000	0.0	.559 ± .002	0.4
	R5	10.0 ± .32	3.2	.621 ±.004	0.6
	R4	2.10 ± .014	0.7	.528 ± .003	0.7
LB	R3	1.28 ± .028	2.2	.507 ± .013	2.5
	R2	1.37 ± .007	0.5	.542 ± .002	0.4
	R1	1.07 ± .007	0.7	.541 ± .002	0.4
	R5	11.1 ± .58	5.2	.727 ± .009	1.2
	R4	2.45 ± .007	0.3	.617 ± .002	0.3
ID	R3	1.48 ± .014	0.9	.585 ± .003	0.6
	R2	1.96 ± .000	0.0	.774 ± .002	0.3
	R1	1.52 ± .007	0.5	.769 ± .001	0.2
	R5	6.81 ± .16	2.3	.532 ± .005	0.9
	R4	1.79 ± .000	0.0	.496 ± .001	0.3
FF	R3	1.19 ± .007	0.6	.473 ± .003	0.7
	R2	1.36 ± .007	0.5	.524 ± .004	0.8
	R1	1.05 ± .020	2.0	.532 ± .011	2.0
	R5	5.63 ± .53	9.4	.478 ± .008	1.7
	R4	1.88 ± .060	3.5	.456 ± .015	3.4
JH	R3	1.07 ± .030	3.3	.426 ± .013	3.1
	R2	0.99 ± .070	0.7	.395 ± .003	0.7
	R1	0.75 ± .007	0.9	.380 ± .003	0.9

Table 3.5 Continued

Subject	ROI	Mean BMC ± SD	CV%	Mean BMD ± SD	CV%
	R5	5.00 ± .092	1.8	.451 ± .007	1.5
	R4	1.58 ± .007	0.5	.399 ± .001	0.3
	R3	0.94 ± .007	0.7	.374 ± .002	0.6
SL	R2	0.88 ± .020	2.4	.350 ± .006	1.8
	R1	0.69 ± .014	2.0	.347 ± .006	1.6
	R5	8.31 ± .12	1.4	.547 ± .004	0.7
	R4	2.03 ± .030	1.7	.509 ± .011	2.1
SP	R3	1.24 ± .030	2.2	.490 ± .011	2.2
	R2	1.16 ± .090	0.6	.433 ± .004	1.0
	R1	0.83 ± .007	0.8	.421 ± .005	1.2
	R5	6.34 ± .035	0.5	.563 ± .003	0.5
	R4	2.12 ± .000	0.0	.534 ± .001	0.3
	R3	1.29 ± .000	0.0	.511 ± .000	0.0
KS	R2	1.26 ± .021	1.7	.499 ± .009	1.8
	R1	0.96 ± .007	0.7	.486 ± .006	1.3
	R5	6.2 ± .014	0.3	.538 ± .008	1.5
	R4	1.60 ± .060	3.5	.469 ± .016	3.5
	R3	0.92 ± .040	4.6	.443 ± .020	4.5
RS	R2	0.91 ± .007	0.8	.580 ± .007	1.2
	R1	1.20 ± .000	0.0	.580 ± .003	0.5
	R5	7.58 ± 0.57	0.7	.595 ± .003	0.5
	R4	2.08 ± .000	0.0	.523 ± .007	0.1
	R3	1.28 ± .014	1.1	.507 ± .006	1.1
PT	R2	1.12 ± .028	2.5	.444 ±. 011	2.5
	R1	0.86 ± .021	2.4	.438 ± .011	2.4

Table 3.6 In-vivo precision (mean CV ± SD) for heel bone mineral measurements, calculated from the data shown in Table 3.5.

	Operator I.		Operator II.	
ROI	CV_{BMC} (%)	CV_{BMD} (%)	CV_{BMC} (%)	CV_{BMD} (%)
R5	1.2 ± 1.4	1.2 ± 1.3	1.8 ± 1.1	1.8 ± 1.2
R4	1.8 ± 1.4	1.8 ± 1.4	1.9 ± 1.2	2.0 ± 1.1
R3	1.0 ± 0.9	1.1 ± 0.7	0.9 ± 0.9	0.9 ± 0.6
R2	1.0 ± 0.8	1.1 ± 0.7	0.9 ± 0.8	1.1 ± 0.6
R1	2.8 ± 2.8	0.9 ± 0.5	3.8 ± 3.1	0.8 ± 0.6

3.3.8 Subject results

The os calcis BMD of the normal females and females with osteopenia/osteoporosis are compared in Table 3.7. The student t-test reveals that there is a significant difference between the normals and the patients.

Table 3.7 Comparison of os calcis bone density of normal females with osteopenic/osteoporotic females.

Subjects/Variables		BMD ± SD	Range	t-value	p-value
Normals	Trabecular	0.543 ± 0.058	0.418 - 0.651		
(n = 21)	Total	0.560 ± 0.057	0.454 - 0.664		
Osteopenic/Osteoporotic	Trabecular	0.423 ± 0.104	0.256 - 0.658	- 4.7	0.0002
patients (n = 31)	Total	0.457 ± 0.103	0.297 - 0.689	- 4.1	0.0001

Figure 3.7 shows regression of normal female trabecular os calcis and total os calcis BMD on age. The graphs show that there were no significant slopes ($P \geq 0.13$) over the age range of 22 - 36 years. This age range is similar to other site age ranges that the manufacturer used to establish the young normal BMDs. The age ranges for spine and total femur are 20 - 35 years and 22 - 34 years, respectively. Coefficients of variation (SD/mean) obtained for trabecular and total os calcis were found to be 10.7% and 10.1%, respectively. These values are also comparable to the values that have been found for other sites by the manufacturer. However, to appreciate more easily if there were any significant changes from the mean BMD values for a decade, the regression equations were used. For an age range of 23 -33 years as examples, there was less than 1 SD change in BMD for the trabecular and total os calcis.

Figure 3.8 reveals the relationships between BMD T-scores for spine, total femur, neck of femur and those for the total os calcis and trabecular os calcis for the female subjects who were referred for spine/femur bone assessment. The Figure compares the T-score values obtained for each site and shows how many women were identified as normal, osteopenic or osteoporotic by each site according to the WHO criteria. The relations between each of the above sites and total os calcis and trabecular os calcis are also compared with each other. High correlations were found between spine, total femur and neck of femur and trabecular os calcis. Similar correlations between these sites and the total os calcis were obtained. However, higher correlation for the spine compared to the correlation of the sites with the trabecular os calcis was found.

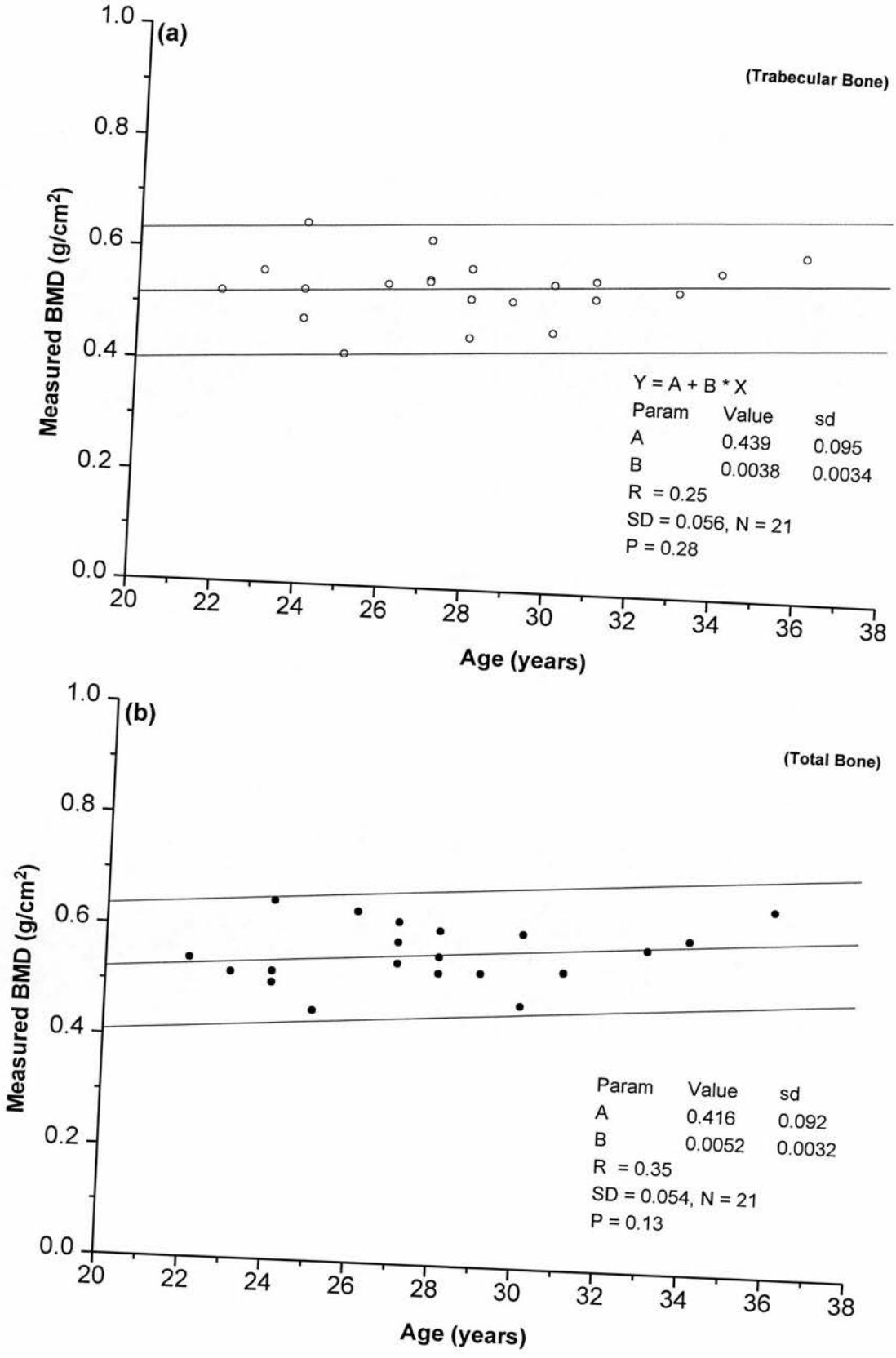

Figure 3.7 BMD of different regions of the os calcis as functions of age for the normal females (n=21). (a) and (b) show the data for the trabecular and total regions respectively. The solid lines are the least square (±2SD) fit to the data.

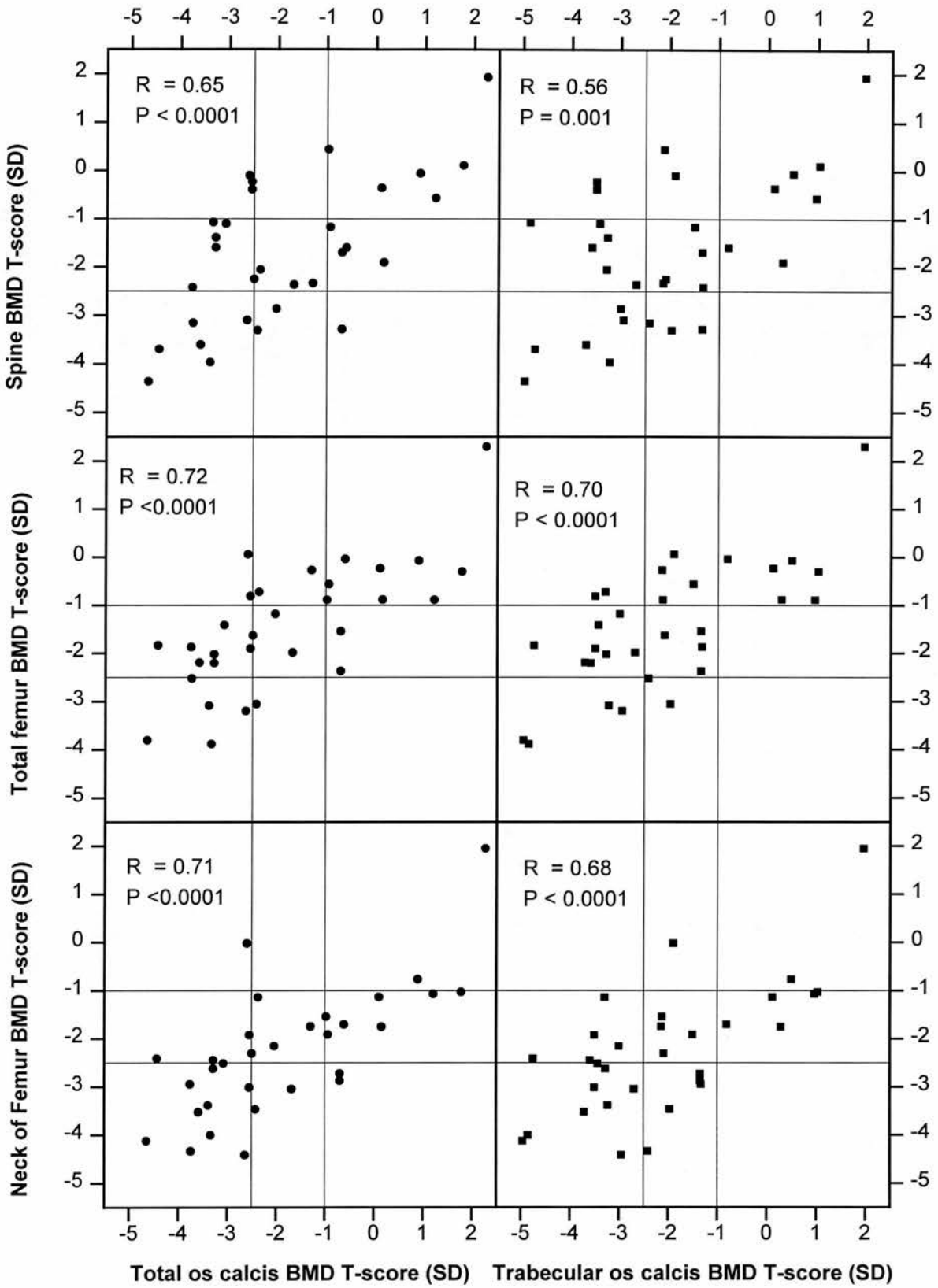

Figure 3.8 Relationship of spine, total femur and neck of femur with the total os calcis and trabecular os calcis. The symbols show the patients bone density values (N=31). The boxes correspond to the WHO criteria for normal, osteopenic and osteoporotic patients.

The predictive equations for the spine, total femur and neck of femur from the total/trabecular os calcis are shown in Table 3.8. The table also shows the correlation (r), standard deviation (SD) and the significance value (p) for the equations.

Table 3.8 Prediction of spine, hip and neck of femur BMD T-score from the total os calcis and the trabecular os calcis in women (n = 31).

Predictive equation Y = A + B * X	r	SD	p
Spine = - 0.754 + 0.532 * total os calcis	0.65	1.15	< 0.0001
Spine = - 0.759 + 0.462 * trabecular os calcis	0.56	1.26	0.001
Total femur = - 0.224 + 0.510 * total os calcis	0.72	0.902	< 0.0001
Total femur = - 0.099 + 0.506 * trabecular os calcis	0.70	0.926	< 0.0001
Neck of femur = - 0.757 +0.474 * total os calcis	0.71	0.865	< 0.0001
Neck of femur = - 0.662 + 0.459 * trabecular os calcis	0.68	0.905	< 0.0001

SD = standard deviation of prediction, r = linear correlation and p = significance value.

Table 3.9 shows the number of female subjects measured by each site identified as normal, osteopenic and osteoporotic. The table reveals that 9/31 = 29% had a normal spine, 13/31 = 42% were osteopenic and 9/31 = 29% were osteoporotic. A higher number of subjects were assessed as normal and fewer as osteopenic or osteoporotic patients based on the total femur measurement. Femur neck measurements identified many more subjects as patients with osteopenia or osteoporosis and only 3 (10%) subjects as normal. The very high number of patients apparently identified as osteopenic/osteoporotic is due to an artifact in the measurement of the neck of femur by QDR DXA scanners (Lunar News July 1996 and December 1996). The reasons for this artefact will be given in more detail in the discussion and conclusion section.

Table 3.9 The T-score values for the female subjects who were referred for a bone density assessment.

	Normal	Osteopenic	Osteoporotic
Spine	9 (29%)	13 (42%)	9 (29%)
Total femur	13 (42%)	12 (39%)	6 (19%)
Neck of femur	3 (10%)	14 (45%)	14 (45%)
Total os calcis	11 (36%)	6 (19%)	14 (45%)
Trabecular os calcis	7 (23%)	10 (32%)	14 (45%)
Spine + total femur	8 (26%)	13 (42%)	10 (32%)
Spine + total femur + total os calcis	6 (19%)	8 (26%)	17 (55%)

Normal: A value of BMD that is not more than 1 SD below the young adult mean value.
Osteopenic: A low BMD that lies between 1 and 2.5 SD below the young adult mean value.
Osteoporotic: A value of BMD that is more than 2.5 SD below the young adult mean value.
NB the above definitions are the WHO criteria for normal subjects, osteopenic and osteoporotic patients.

3.4 Discussion and conclusions

This study established a feasible technique for the os calcis measurement that is linear, soft tissue thickness independent and precise. Os calcis bone mineral measurement by DXA is associated with very low exposure to ionising radiation. The time required for an os calcis measurement is one-third of the time required for spine/femur measurement. A point of measurement that has a uniform distribution of trabecular bone tissue was established. This measurement point is situated in the centre and at the flat part of the calcaneus. Two ROIs were developed for future measurements. These ROIs are (a) a square box, having an area = 4 cm^2, positioned away from the os calcis cortical layers in a site with the least non uniformity in density. (b) A region positioned so its area includes the whole posterior part of the os calcis, with one of the sides of ROI placed on a perpendicular line along the fibula to the baseline of the os calcis. These ROIs can easily be created for any subject by comparing her/his image with a pre-analysed

reference scan. The created ROI can be located in the most appropriate position just like other conventional measurement sites. The region with the minimum BMD can clearly be observed on the monitor screen to locate the created ROI.

In the present study high correlations between spine, neck of femur and total femur with trabecular and total os calcis were found and in particular better correlation between spine/total os calcis was found compared to spine/trabecular os calcis. Despite, moderate correlation between US parameters and femoral neck (Korczyk et al., 1993 and Lees et al., 1993), US measurements at os calcis predict hip fracture as accurately as do femoral neck BMD (Hans et al,. 1996). The reason is that both BUA and BMD are independently related to fractures (Glüer et al., 1996). Excellent correlations between the os calcis BMD (using SXA) and US parameters have been reported (Glüer et al., 1992; Waud et al., 1992; Salmone et al., 1994). It has also been reported in a large epidemiological study that os calcis BMD was better than BMD of spine for the prediction of hip fractures (Glüer et al., 1996). Therefore, it seems that the os calcis DXA measurement has a significant value for the prediction of fractures and response to therapy.

In this study the patients with osteopenia/osteoporosis were compared with normals using the T-score. Spine, neck of femur and total femur were compared with trabecular os calcis and total os calcis. Using the WHO criteria spine, total femur and total os calcis found a different number of subjects as normal, osteopenic or osteoporotic patients. A higher number of the referred subjects were diagnosed as osteopenic/osteoporotic for the neck of the femur than either spine/total femur or even spine plus total femur. The reason is that the reference values for neck of femur BMD provided with the QDR scanner differed significantly from that observed in the National Health and Nutrition Examination Survey (NHANES) (Looker et al., 1995). There is a particular problem with the values for young normal subjects which are used to calculate the T-score. The disparity between the QDR neck of the femur and NHANES values are due to higher young normal BMD and lower SD established by the QDR

compared to NHANES, leading to a + 6.5% difference from NHANES values. Combination of spine and total femur diagnosed a higher number of patients at fracture risk. Adding the total os calcis to spine/total femur measurements, a further number of subjects at risk of fracture were identified. ANOVA also confirmed that there was no significant difference (P = 0.23) between the osteopenic/osteoporotic patients and the normal group for the T-scores of the spine, the various regions of the os calcis and the femur. Therefore, assessment of os calcis can predict the risk of fracture at other sites at an earlier stage so that appropriate measures can be taken to slow or stop the progression of the diseases.

Wasnich et al. (1987a) used identical ROI to Vogel et al (1979) who used a modified rectilinear SPA technique. Using DPA the anatomic location of os calcis scanning site encompassed a 2.5mm section through the central portion corresponding to the area of least mineral content. They obtained a CV of 1.16% and a total time of 10 minutes for each scan. However, DPA scanners are no longer manufactured due to them having some disadvantages.

Kotzki et al. (1993) measured the BMD of the os calcis by DXA (Sophos LXRA osteodensitometer). The outline of the calcaneus was automatically defined, except for the line beginning in the location of the trigon bone and perpendicular to the main axis of the calcaneus. The in-vivo precision of the method was 1.28%. They showed the superiority of the os calcis as a measurement site over the lumbar spine, in relation with the existing fractures in the presence of osteoarthritis.

Yamada et al. (1993) performed absorptiometry with a QDR-1000 bone densitometer. They measured the lumbar spine and calcaneal bone laterally using a group of pre- and post-menopausal women. In-vivo os calcis precision was 3.1%. In our study we found significantly better precision (1.1%). They found a correlation of 0.76 between the os calcis and spine, which is similar to the present results (0.65).

Suleiman et al. (1994) studied 124 normal post-menopausal women aged 57 ± 2 years. They used a Norland XR-26 DXA scanner. In-vivo precision was 1.2%. They obtained an os calcis mean value of 0.547 ± 0.083 g/cm^2, which is comparable with our results (0.543 ± 0.058). However, the total os calcis measurement time was not quoted.

Pye et al. (1994) performed DXA of the calcaneus using a Lunar DPX-L bone densitometer with a modified version of the manufacture's forearm protocol. They examined 4 ROIs placed in positions comparable to the regions examined by two different US bone scanners. A BMD precision range of 1.6% - 4.9% was reported. However, the disadvantage of their technique was the long time (~ 30 min) required for the analysis.

In summary, it can be concluded that the main drawbacks of the above methods are either the long total measurement time, poor reproducibility, the requirement of a waterbath when the SPA technique is used or the technique is no longer used. Later generations of DXA bone densitometers offer the possibility of supine lateral scanning. These fan beam bone scanners take high quality lateral images of the entire spine in a few seconds with even better resolution. These two advantages, i.e. lateral scanning and a short scanning time, can further assure the osteopenic patients comfort who usually suffer chronic back pain and who cannot sit comfortably on the scanner table without support. This short screening time allows several images to be taken each time to compare the means of BMDs, giving improved diagnostic sensitivity and therapy response.

Because os calcis bone assessment has a significant value in the management of osteoporosis, different methods for assessment of this site have been developed. The Lunar bone scanner manufacturer has recently introduced a new generation of peripheral DXA bone densitometer. The equipment is portable and it is called Peripheral Instantaneous X-ray Imager (PIXI) which measures the os calcis in less than a minute. PIXI employs the DXA technique, eliminating the need for a waterbath.

There is still some controversy over the significance of BMD determination at different skeletal sites as indicators of skeletal integrity. Measurements of hip and spine are generally considered as the most reliable predictors, since these are the sites most prone to osteoporotic fracture. Measurements of such sites may not be the most appropriate method of screening a large proportion of the population, for a variety of reasons. BMD measurements of os calcis, though it is not at risk of osteoporosis fracture, may provide valid alternatives for initial bone mineral assessment, and a complementary bone evaluation in addition to DXA imaging of the femur and spine.

In summary, due to the following facts, it can be concluded that although it might have seemed that os calcis measurement had limited value, it warrants the prediction of osteoporosis at an early stage and seems a useful site for bone quality assessment at other sites.

1. Short measurement time required.
2. With appropriate linearity correction factors the measurement is linear, precise and independent of soft tissue thickness.
3. Measurement of os calcis can be a complementary to spine/femur measurements.
4. There was no significant difference between the patients' T-scores for the spine, os calcis and the femur.
5. Modern DXA systems with faster scanning speeds and/or lateral supine imaging would offer significant advantages.

Chapter 4

Bone Mineral Assessment of Different Regions of the Lower Leg

4.1 Introduction

There is substantial evidence suggesting that presence of compact or cortical bone is a major factor contributing to bone strength and fracture resistance (Rockoff et al., 1969; Mazess et al., 1990 and Vesterby et al., 1991). Thompson (1980) in his study of a group of white cadavers, measured the anterior mid-shaft section of right femurs and cortical thickness was measured using callipers. The cortical thickness decreased by 18% in men and by 30% in women, in non-osteoporotic femurs between the sixth and ninth decades. Similar results were described by Laval-Jeantet et al. (1983) in non-osteoporotic humeri. Ruff et al. (1988) found, in tibiae and femurs of men and women, gradual medullar expansion with age. In addition, they found a greater reduction with age in the cortical area of the tibial shaft (between 5.6% and 11.0% per decade) than in the femoral neck (5.5% per decade) in women.

The measurement of ultrasound velocity and ultrasound attenuation provides information on skeletal status and has recently received attention (Langton et al., 1984 and Miller et al., 1993). In cross-sectional studies, ultrasound measurements have been shown to differ significantly between osteoporotic and normal individuals (Miller et al., 1993 and Herd et al., 1992). The technique discriminates between individuals with and without spinal fractures as well as absorptiometey (Heany et al., 1989). The sites most widely evaluated by ultrasound scanners have been the os calcis and patella. Most information is available for the heel, which is predominantly trabecular bone. However, loss of cortical bone is also important in determining the risk of fracture, even at sites of predominantly cancellous bone such as the spine (Vesterby et al., 1991 and Spardo et al., 1992). Therefore, an ultrasound scanner has recently been developed for the diagnosis and monitoring of osteoporosis (SoundScan 2000, 1994). The instrument

measures the speed of propagation of ultrasound waves along a fixed length of the cortical layer at the tibial shaft.

Using DXA, Mottet et al. (1996) studied thirty four patients on hemodialysis (HD), twenty five patients on continuous ambulatory peritoneal dialysis (CAPD) and 125 normal subjects. BMD was measured at the lumbar spine (trabecular bone), the femoral neck (mixed cortical and trabecular bone), the distal tibial diaphysis (cortical bone) and the epiphysis (trabecular bone) in all subjects. At the lumbar spine, no significant difference in BMD was observed between the three groups. At the femoral neck and the tibial epiphysis, HD patients had lower BMD ($P < 0.001$) than normal controls. They reported that at the tibial diaphysis, patients on HD had a lower BMD ($P < 0.001$) than the patients on CAPD and the normal controls.

Accurate determination of BMD of the spine and femur is not always possible in patients with scoliosis, vertebral fractures, wedging or apophyseal osteophytosis and femoral fractures (Wahner et al., 1984). Furthermore, bone mineral measurements of the forearm or wrist are inadequate predictors of the lumbar spine and the proximal femur and neither can be used to predict the femur nor the femur to predict the spine with sufficient accuracy on an individual basis (Krolner et al., 1980). Therefore, the purpose of this chapter was to assess the usefulness of the lower leg as a site for bone density measurements with DXA.

Excellent correlations between measurements of trabecular bone in the distal radius and in the spine ($r = 0.92$) and tibia ($r = 0.88$) have been reported (Rüegsegger et al., 1984). Using dual photon absorptiometry (DPA) with ^{153}Gd as a source, Checovich et al. (1989) measured proximal tibia BMC and BMD of a group of women, aged from 23 to 87 years. They found that BMD was significantly correlated with the lumbar spine ($r = 0.70$), femoral neck ($r = 0.73$) and femoral trochanter ($r = 0.74$). In conclusion, the majority of evidence points to the considerable contribution of the compact layer of bone to fracture resistance. Therefore, assessing different tibial ROIs which contain different proportions of cortical and trabecular bone by DXA may be useful to identify fracture risk among post-menopausal women and the elderly population at large.

The two most important criteria in the selection of a technique for the assessment of bone quality are its ability to discriminate between normal and osteopenic patients prior to the appearance of a compression fracture, referred to as diagnostic sensitivity, and its effectiveness in monitoring changes with time, e.g. response to therapy, for which precision is the crucial factor. The precision was, therefore, assessed. The objective of this study was to develop a DXA technique for the measurement of bone density along the tibia and lower leg bones (tibia/fibula).

For accuracy, precision, stability, cost, subject dose and compliance DXA is the most appropriate choice. DXA also has the advantages of freedom to select skeletal site, speed and ease of scanning. However, the available protocols differ in terms of pixel size, line spacing and consequently scan speed, linearity correction factors and bone density thresholds. Therefore, the three acquisition methods of Forearm, Spine and Whole body were evaluated to assess linearity and the effect of soft tissue thickness. The agreements for leg bone mineral measurements between the Forearm/Whole Body and the Spine/Whole Body acquisition protocols were also assessed.

In order to assess the bone loss caused by the osteoporosis in different regions of the lower legs, four ROIs along the lower leg were defined. The ROIs included the predominantly trabecular bones (combined tibia/fibula) of the distal and proximal leg, a mixed region (trabecular and cortical bone) between the proximal ROI and the middle of the lower leg and a cortical region along the middle of the leg.

Thirty five pre-menopausal normal female subjects' images of the spine and total body were analysed. The total body scans were then re-analysed using the sub-region analysis facility. The required ROIs were created. The effect of rotation of the lower leg on bone mineral measurements of different ROIs of the combined tibia/fibula was investigated. Precision was assessed for each ROI using 32 subjects of the normal group who had repeat measurements in 6 months. The young normal subject ranges for different ROIs were established. The correlations between the various ROIs of the leg with physical

size and the vertebral body were established. Thirty seven female subjects referred, on the suspicion of suffering from osteoporosis /osteopenia, were used. The subjects had scans of the whole body, femur and spine. The two groups were compared using the T-score of the various ROIs of the lower leg, femur neck, total femur, spine and the whole body. The T-scores for the various regions of the lower leg were derived using the normal group. The T-score for the spine was calculated using the Hologic young normal data. There was a particular problem with the manufacturer values used for young normal subjects to calculate the T-score for the femur neck and the total femur (Lunar News, July 1996 and Lunar News, December 1996). Therefore, the National Health and Nutrition Examination Survey (NHANES) (Looker et al., 1995) young normal data were used to derive the femur neck and the total femur T-scores. The manufacturer has also recently converted their data for the femur to NHANES normal data. The effect of the osteoporosis on the dominant and non-dominant leg was also investigated. The World Health Organisation (WHO) classification of normal, osteopenia and osteoporosis (Kanis et al., 1994) was used to compare the two groups.

4.2 Methods and materials

4.2.1 In-vitro measurements

X-ray beam hardening may result in a non-linearity between the measured and true BMD. For each protocol the manufacturer incorporates correction factors into the analysis program to compensate for this effect but these are dependent on the actual density and the thickness of the tissue. To investigate the linearity aluminium strips were used to simulate the tibia and hardboard sheets were used to simulate the overlying soft tissue. The aluminium strips had equal length, width and thickness of 40 cm, 4.5 cm and 1.78 mm, respectively. The linearity was investigated over a range of 0.75 - 1.8 g/cm^2 equivalent of calcium hydroxyapatite (CaHA) by increasing the thickness (5.3 - 12.5 mm) of the aluminium strips. The same aluminium strips were used to determine the effect of the soft tissue on the tibial bone mineral measurements. Hardboard sheets

having 3 mm thicknesses were used over a wide thickness range of 4 - 13.8 cm.

A whole body phantom was used to make the in-vitro investigations. The detailed construction of the whole body phantom is explained in chapter 5. In-vitro tibial bone mineral measurements were performed in the three acquisition methods of Forearm, Spine and Whole Body. The relationships between the measured tibial bone mineral parameters of the methods of Forearm and Spine with the total body acquisition method were assessed.

4.2.2 In-vivo measurements

To study the feasibility of DXA imaging of the tibia in the Forearm acquisition mode, five healthy volunteers of both sexes (25 - 73 years) were scanned. An example of the type of image obtained is shown in Figure 4.1a. The subjects turned the right leg to one side to have the images of tibia/fibula taken separately. However, most of the subjects felt uncomfortable because they had to hold the leg in this posture for about 15 minutes while the scanning was in progress. The other disadvantage was that the Forearm mode did not allow a measurement length exceeding 23 cm. It was not, therefore, possible to scan the entire lower leg even in a normal posture. Therefore, previously acquired whole body and lumbar spine scans of 35 normal females were re-analysed. The spine scans were used in order to assess the correlations between the various ROIs of the lower leg with the spine BMD. In order to assess the effect of osteoporosis on the neck of the femur, total femur, spine, total body and the various regions of the lower legs, scans of 37 osteopenic/osteoporotic females based on the spine/ or femur BMD were re-analysed. The analysis of the scans of the lower legs included both the tibia and fibula. Table 4.1 shows the characteristics of the subjects. Precision was calculated as the mean coefficient of variation (CV) of repeat measurements on 32 normal subjects where the measurements were approximately 6 months apart.

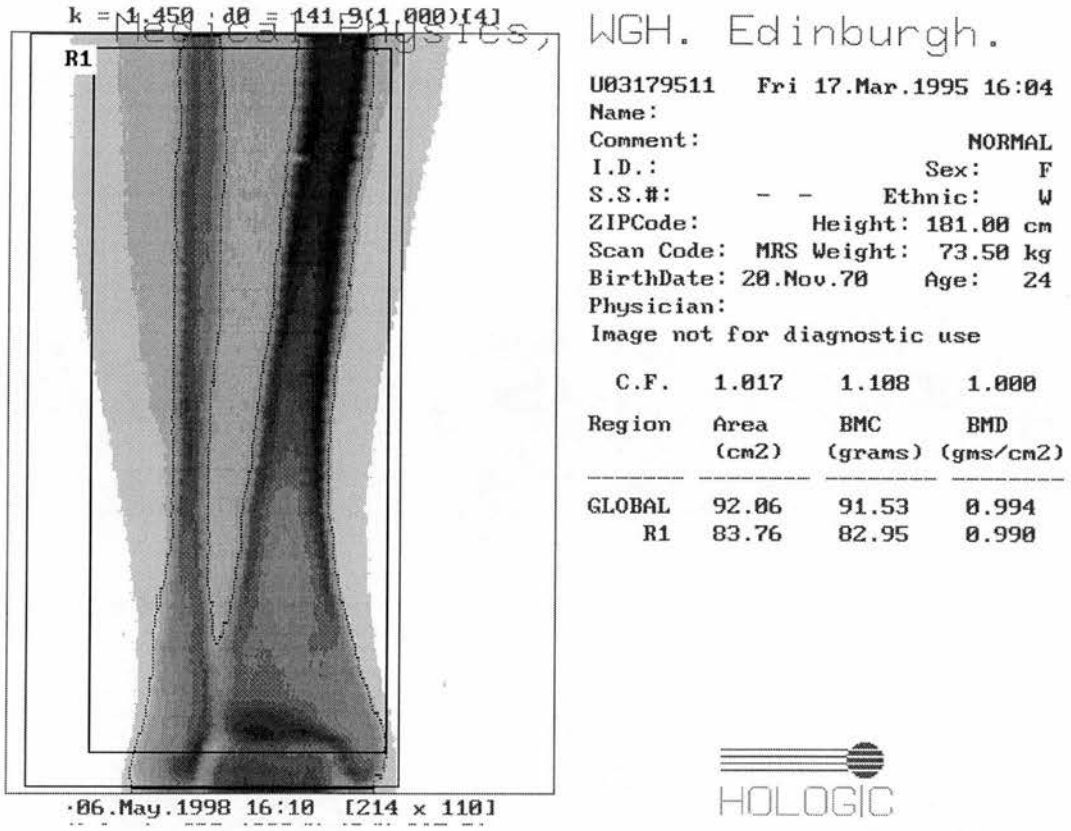

Figure 4.1a A lower leg DXA scan, using the Forearm acquisition protocol.

Table 4.1 Details of females studied. The results are expressed as the mean ± SD and range.

Subjects/Variables	Age (years)	Height (cm)	Weight (kg)
Normals (n = 35)	34.4 ± 9.1 23.0 - 52.0	163.2 ± 6.6 150.0 - 181.5	68.9 ± 14.8 42.0 - 112.6
Osteopenic/Osteoporotic patients (n = 37)	57.5 ± 15.2 19.0 - 76.0	158.4 ± 8.1 136.0 - 176.5	61.1 ± 11.8 37.7 - 104.6

4.2.3 Region of interest selection

Using the regional body composition analysis facility of the scanner, the lower-right leg

selected from total body images was divided into 4 ROI (R1 - 4). The proximal tibia, R1 (spongy bone) was created having a height of 4 - 5 line intervals (1 line interval = 1.3 cm) depending on the subject height and consequently the leg size. The difference between the two kinds of bones (i.e. trabecular and cortical) could be differentiated on the monitor screen. R2 (compact bone) was chosen having 8-10 line intervals, below R1 (Figure 4.1b). R3 (cortical bone) was created with the same size as R1 and below R2. Finally, R4 (trabecular bone) was selected to have the same length as R2. The bottom of R4 ROI box just touched the widest part of the tibia, which can usually be easily seen visually on the monitor screen. R4 was positioned in such a way that prevented over-lapping of the more dense part of the foot (the talus) with the tibia/fibula. There was one line interval space between each ROI box so that the areas of the ROI boxes do not over-lap giving an over-estimate of the total lower leg. The width of the ROIs had no influence on the BMD.

Selecting different sub-regions of the lower-right leg, with different proportions of cortical and trabecular bone, allowed the regions which correlated best with the BMD of the spine and femur to be determined. In addition, this provides an indication of which sub-region gave the best separation between the control subjects and the patients referred because they were considered to have a high risk of osteopenia/osteoporosis. The total regions corresponding to the right and left lower legs are shown as regions R5 and R6, respectively, in Figure 4.1b.

4.2.4 The effect of rotation of the legs

In order to investigate the effect of rotation of the leg on the bone mineral measurements of the different ROIs of the lower leg due to changes in bone projected area, 3 subjects (1 male/2 females) were measured. The subjects rotated their legs inwards and held their feet against a device provided by the manufacturer for holding the legs in a proper posture for hip bone density measurements.

Medical Physics, WGH. Edinburgh.

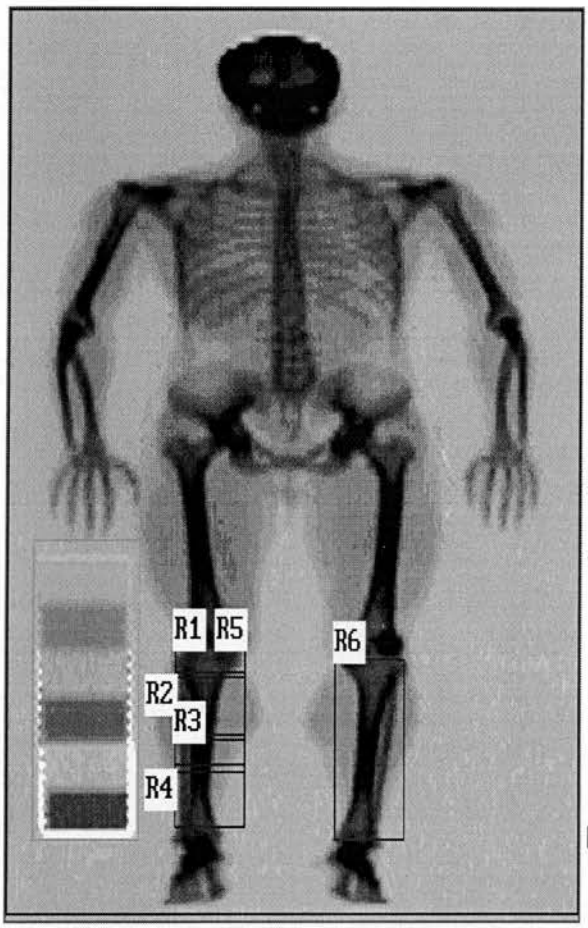

·02.Sep.1996 11:04 [330 x 146]
Hologic QDR-1000/W (S/N 967 P)
Enhanced Whole Body V5.55

U0823960B Fri 23.Aug.1996 12:21
Name:
Comment: Normal
I.D.: R01A016 Sex:
S.S.#: - - Ethnic: W
ZIPCode: Height:
Scan Code: MRS Weight:
BirthDate: 09.Sep.58 Age:
Physician:
Image not for diagnostic use

	C.F.	1.014	1.090	1.000
Region		Area (cm2)	BMC (grams)	BMD (gms/cm2)
R1		44.62	50.38	1.129
R2		64.09	74.72	1.166
R3		26.77	38.00	1.419
R4		54.76	64.39	1.176
R5		190.25	227.48	1.196
R6		188.22	229.40	1.219
NETAVG		378.48	456.88	1.207

HOLOGIC

Figure 4.1b Lower leg regions selected from a whole body DXA scan.

In order to investigate the effect of an extreme change in leg orientation on the bone mineral measurement of the various ROIs of the combined tibia/fibula, the 6 legs were rotated inwards. This resulted in an angular rotation of 26° ± 9° (14° - 35°). The subjects were measured twice; first the legs were kept in a normal posture and then rotated inwards. The subjects had different leg rotation angles from the initial normal posture and even for the same subject the rotation angle was different between the two legs. The percentage changes in the bone mineral parameters from the initial values were calculated for the various ROIs and the values were compared with each other.

4.2.5 Data analysis

Linear regression analysis was used to investigate the linearity and the effect of soft tissue thickness on the tibial bone mineral measurements. Linear regression analysis was also used to assess the relationships between the different protocols of Forearm and Spine with the Whole Body protocol for tibial bone mineral measurements. The correlations between the bone density of the various ROIs of the lower leg with the lumbar spine for the normal subjects were investigated using regression analysis. T-score is defined as the deviation from the sex-matched young normals and is calculated as:

$$\text{T-score} = (P - M_Y) \div SD_Y$$

P is the patient bone mineral value and M_Y is the mean value for young sex matched normals and SD_Y is the standard deviation of the mean value for young normals.

The T-score for the various regions of the lower legs were derived using our normal group. The manufacturer's normal data were used to calculated the T-score for the spine and the whole body. However, the reference values for the neck of femur and total femur BMD provided by the manufacturer differed significantly from that reported in NHANES (Looker et al., 1995). Therefore, NHANES (Looker et al., 1995) young normal data were used to calculate the T-score for the femur neck and the total femur.

Analysis of variance (ANOVA) was used to find if there were any significant difference between the T-score means of the femur neck, total femur and proximal and distal leg. A student t-test was used to find if there were any significant difference between the T-score of the dominant and non-dominant leg. Using linear regression analysis, the correlations between the T-scores of the spine, femur neck and total femur with the various ROIs of the lower leg were found. The correlations between the T-score of the femur neck and the total femur and the various ROIs of the lower leg with each other were also assessed.

4.3 Results

4.3.1 Linearity

Figure 4.2 shows the variation of measured bone mineral parameters with respect to aluminium strip thickness. The apparent variation in area for an aluminium thickness range of 5.3 - 12.5 mm was measured. The Whole Body method under-estimated the area quite considerably for an aluminium thickness of less than 7 mm; for higher aluminium strip thicknesses, closer results to the true value were found, but still with almost a 6% under-estimation. The Forearm technique over-estimated the area by approximately 10%. The BMC and BMD results were linear for all the protocols. The maximum difference in BMC was 123% over the range measured but the maximum difference in BMD was 95%. Because of the non-zero intercepts the apparent percentage change for any particular true change in BMC or BMD depends on the initial value. The measured changes corresponding to 10% increases from a reasonably typical bone thickness corresponding to 10 mm aluminum were calculated. For BMC the measured changes were 10.1, 8.8 and 9.5% for the Whole Body, Spine and Forearm protocols, respectively. The corresponding changes for BMD were 9.6%, 9.3% and 8.3%, respectively.

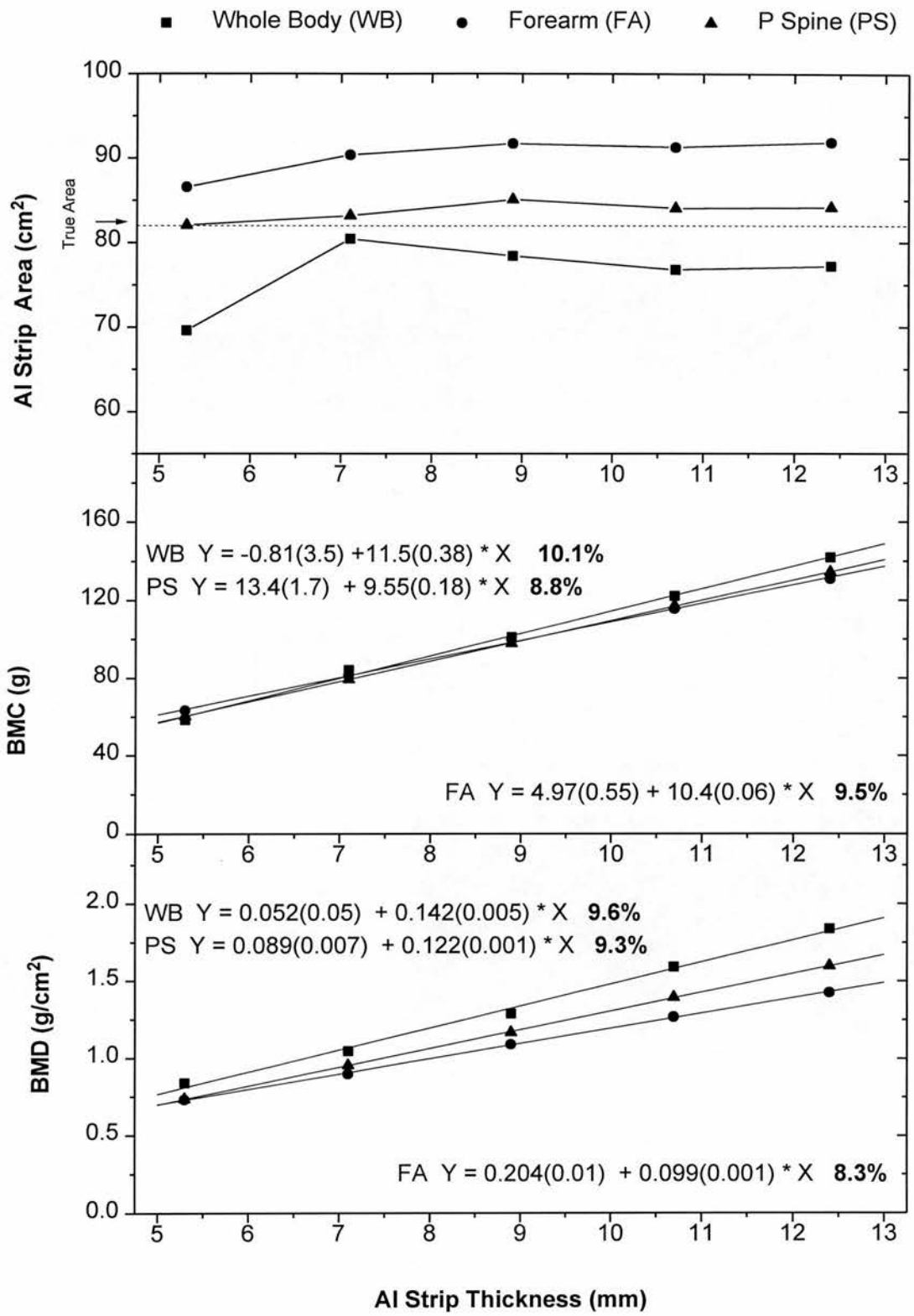

Figure 4.2 Investigation of the linearity of bone mineral measurements with Al strip (simulating tibia) thickness. The regression equations are shown for the various protocols. In all cases $r > 0.999$ and $p < 0.00001$. The figures in bold show the percentage increase in the measured bone mineral parameter for a 10% increase in an initial Al thickness of 10 mm.

4.3.2 The influence of soft tissue thickness

Figure 4.3 illustrates the effect of soft tissue thickness on area, BMC and BMD measurements. Significant linear correlations were found between area, BMC and BMD with the soft tissue thickness for the Forearm and Spine acquisition methods. The Whole Body acquisition method did not show linear correlations for area and BMC with soft tissue thickness variations. In fact there were large under-estimations in area and BMC for a soft tissue thickness of over 11 cm. Because the effects on BMC and area for soft tissue thickness greater than 11 cm were similar there was no corresponding effect on BMD. Therefore, the effect of soft tissue thickness variation was similar for all methods for BMD measurements. The effect of soft tissue on BMD measurements was minor (less than precision) and the change in BMD per centimetre soft tissue thickness variation was $\leq$ 0.41%. However, to appreciate the changes in BMD for an increase of 25% in soft tissue thickness from an initial thickness of 10 cm, the Whole Body, Spine and Forearm methods estimated changes of 0.71%, - 0.71% and - 1.1%, respectively.

4.3.3 In-vitro correlation of the Forearm and Spine methods with the Whole Body method

Figure 4.4 shows the in-vitro correlation of the Forearm and Spine acquisition methods with the Whole Body acquisition method for the tibial bone mineral measurements. Aluminium strips were used to simulate the tibia. The data obtained from the Forearm and Spine methods were regressed on the data acquired by the Whole Body acquisition method. Significant linear relationships for BMC and BMD, but different intercepts (A) and slopes (B) were found. In order to appreciate more easily the percentage difference obtained for a 10% increase in BMC and BMD from initial values of 100 g and 1.0 g/cm^2 for the Whole Body acquisition method, the Spine and the Forearm methods showed 10.1%, 9.9% increase in BMC and 9.4%, 9.1% increase in BMD, respectively.

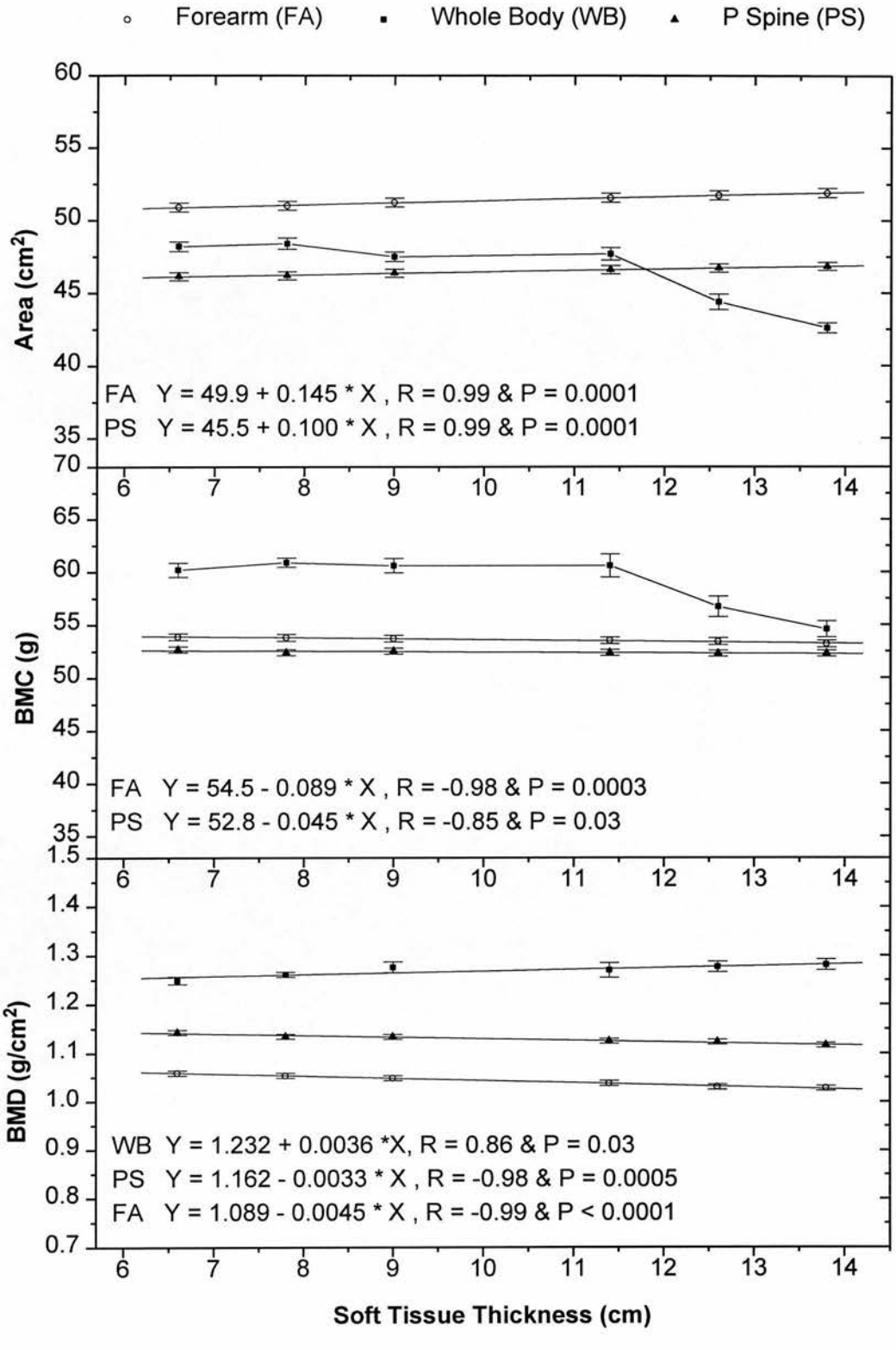

Figure 4.3 The effect of soft tissue thickness on tibial bone mineral measurements for the various protocols. For this investigation AI strips were used to simulate the bone. Error bars show the SD of the data.

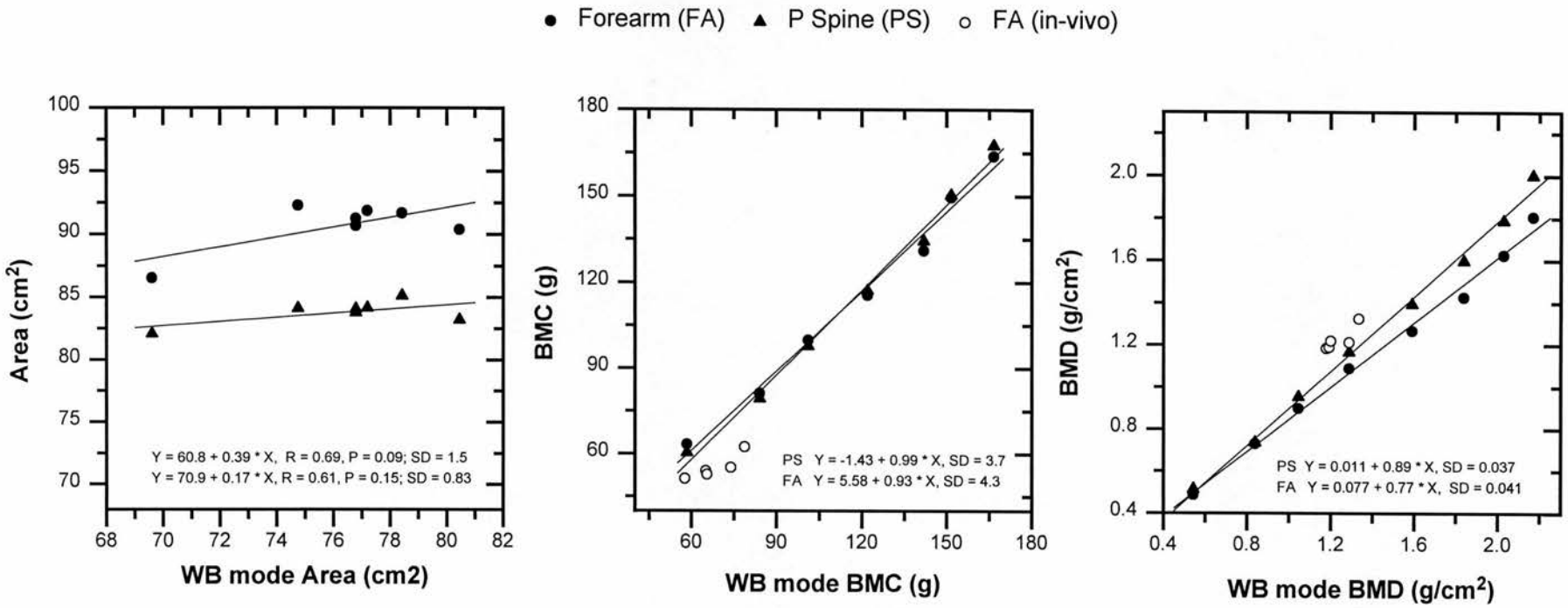

Figure 4.4 Correlation of the Forearm and Spine acquisition methods with the Whole body (WB) acquisition method for tibial bone mineral measurement. In all cases the correlation and the significance level were $R > 0.995$ and $P < 0.0001$, except where noted. Al strips were used to mimic the bone.

The data for the five normal subjects agrees reasonably well with the in-vitro data, considering the limitations of the semi-anthropometric Whole Body phantom.

4.3.4 The effect of rotation of the legs on the various ROIs of the lower leg

Figure 4.5 shows the effect of rotation of the legs on the various ROIs of the combined tibia/fibula bone mineral measurements. Figure 4.5a shows that when the legs were rotated inwards the projected areas were decreased (except R1) from their initial normal orientation values. However, due to the anatomical structure of the tibia/fibula orientation, the projected area increased for the proximal leg (R1) when the legs rotated inwards. The maximum percentage change in bone area in the two different leg postures was found for the distal leg (R4). The maximum percentage change in BMC due to the leg rotation was found for the proximal and distal leg and the minimum for the entire leg (Figure 4.5b). However, due to an apparent increase in the proximal leg (R1) bone area, caused by rotation of the legs and a decrease in the mean BMC for the same ROI, there was a minimal and insignificant change in BMD of the proximal leg ROI (1.5% $\pm$ 6.0%) (Figure 4.5c). The maximum increase in BMD ($P < 0.05$) due to rotation of the legs was found for the distal leg (R4). This large BMD change (10% $\pm$ 3.6%) was caused by an under-estimation in bone area and over-estimation in BMC.

4.3.5 In-vivo bone mineral and precision values for the different ROIs of the lower leg

Table 4.2 shows the details and precision of bone mineral parameters of each ROI of the lower legs selected from the whole body scans of 32/35 normal female subjects. ANOVA between the precision of different ROIs of the lower-right leg was performed. The BMD precision was not significantly different for any region ($F = 2.6$, $P = 0.06$).

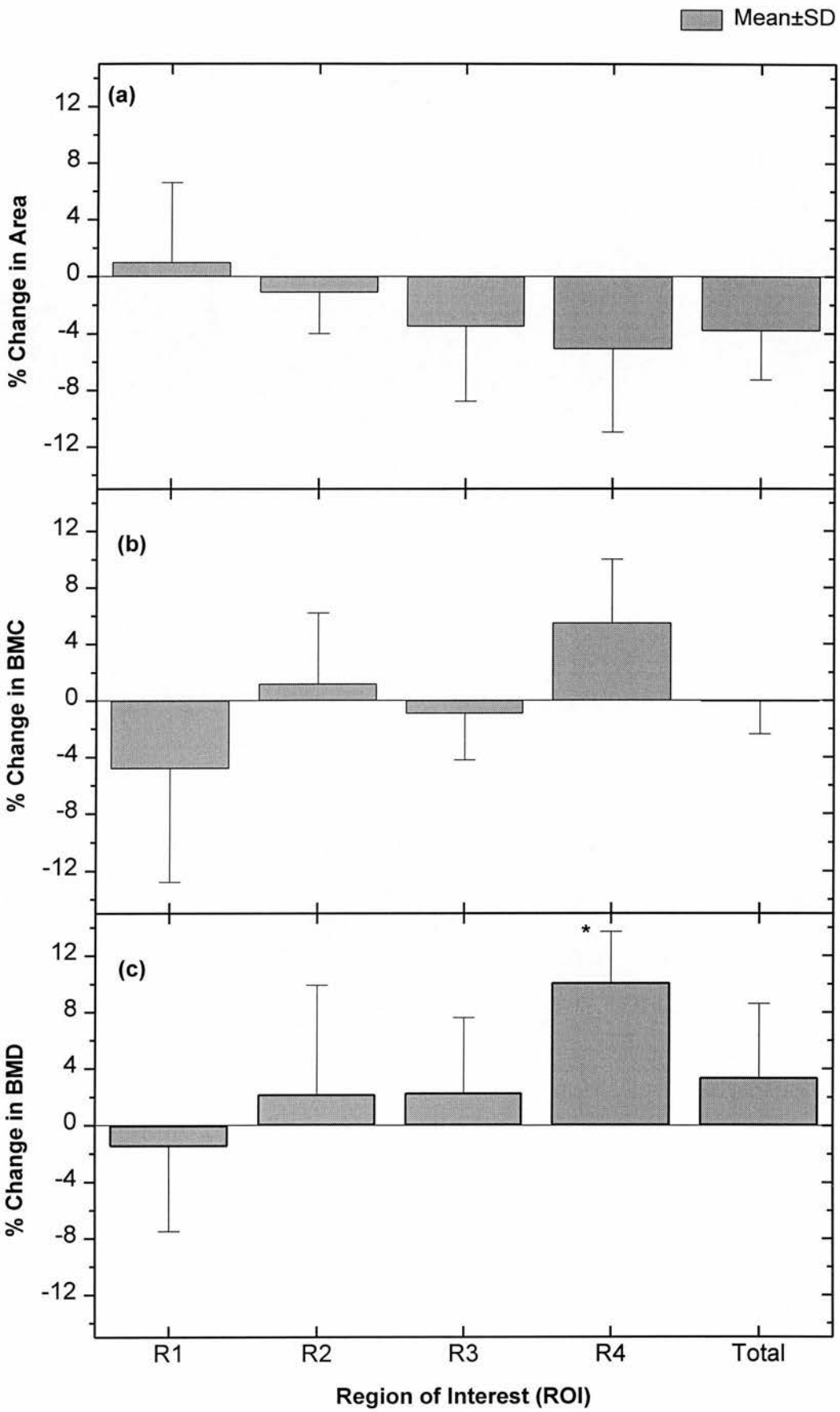

Figure 4.5 The effect of extreme rotation (26 ± 9 degrees) of the lower legs on the various ROIs of the combined tibia/fibula bone mineral measurements.
* $P < 0.05$

Table 4.2 Mean (±SD), range, and precision (CV) for bone mineral parameters of the various ROIs of the lower legs selected from the whole body scans of 32 normal females.

	Area (cm^2)			BMC (g)			BMD (g/cm^2)		
	Mean (SD)	Range	CV% (SD)	Mean (SD)	Range	CV% (SD)	Mean (SD)	Range	CV% (SD)
R1	32.9 (5.2)	24.7-46.8	2.8 (3.2)	35.7 (7.6)	19.2-60.5	2.9 (3.4)	1.08 (0.13)	0.696-1.35	1.2 (0.95)
R2	51.4 (7.1)	35.3-74.8	3.2 (2.9)	60.0 (10.9)	29.3-91.7	2.6 (5.8)	1.18 (0.14)	0.901-1.44	2.1 (2.3)
R3	21.4 (4.3)	13.8-33.4	3.7 (3.6)	27.3 (5.9)	15.6-47.7	2.4 (2.8)	1.28 (0.18)	0.969-1.64	2.4 (1.7)
R4	45.1 (5.3)	31.6-56.8	2.7 (2.4)	51 (8.8)	30.0-74.6	3.7 (3.4)	1.12 (0.12)	0.786-1.39	1.9 (1.9)
R Leg	151 (19.8)	112-209	2.3 (2.5)	177 (32.4)	107-272	3.4 (6.1)	1.15 (0.12)	0.916-1.39	1.3 (1.1)
L Leg	150 (20.2)	108-212	2.7 (2.6)	173 (30.5)	106-271	3.7 (7.2)	1.16 (0.11)	0.919-1.40	1.4 (1.1)

R: right, L: left

However, the CV was consistently lower for BMD than BMC. ANOVA also revealed that there was no significant ($F = 1.8$, $P = 0.12$) difference between the means of the lower-right leg both lower legs and distal lower-right leg (R4) BMD.

4.3.6 Correlation of BMD of the various ROIs of the lower leg with body stature

Figure 4.6 demonstrates BMD of the various regions of the lower-right leg, total lower-left leg and both legs as a function of age. As can be seen, despite a wide age range there was no significant correlation between BMD of any region and age. BMD correlation of each ROI of the lower-right leg, total lower-right leg and both lower legs with age, height and weight are tabulated in Table 4.3. There were no significant ($P > 0.05$) associations between BMD of R1, R2, R4 and height. Good correlations were found between the proximal (R1) and distal (R4) lower leg BMD's and weight. Higher correlations were found between the BMD of the predominantly trabecular regions of the lower leg (R1, R4) than the predominantly cortical regions (R2, R3) with weight. Moderate correlations between the lower-right, lower-left and both lower legs and weight were found.

Table 4.3 Correlation (r) of BMD of the various ROI of the lower-right leg, both lower-right and left leg and both lower legs with age, height and weight.

Variable		R1	R2	R3	R4	right leg	left leg	both legs
Age	r	0.12	0.16	0.19	0.24	0.19	0.18	0.19
	P	NS	NS	NS	NS	NS	NS	NS
Height	r	0.16	0.21	0.22	0.20	0.23	0.22	0.23
	P	NS	NS	0.04	NS	0.04	0.04	0.03
Weight	r	0.70	0.40	0.47	0.71	0.62	0.60	0.63
	P	In all cases $P < 0.0001$.						

NS = non significant.

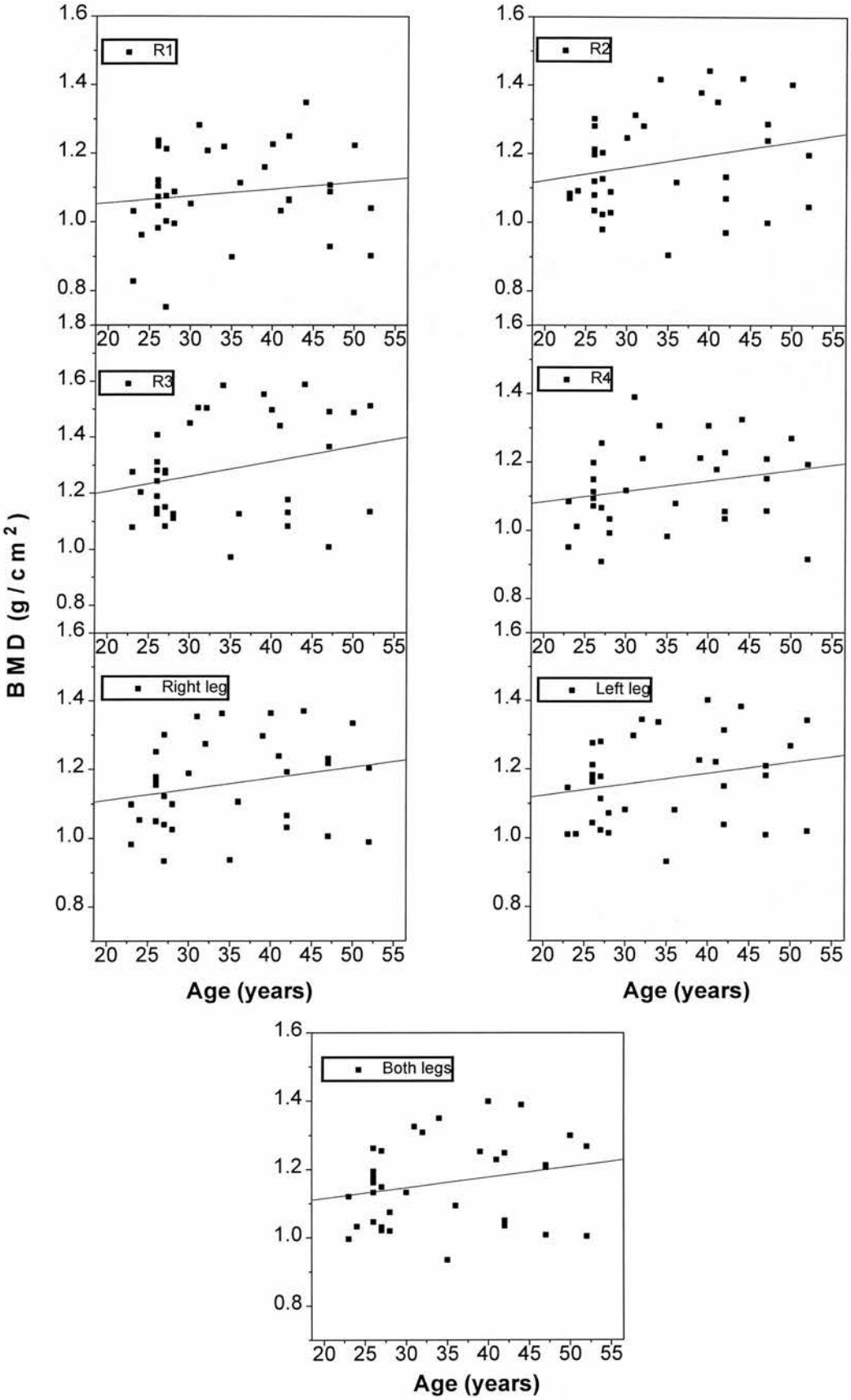

Figure 4.6 The correlation of lower-right leg and its different ROIs (R1- R4), lower-left leg and both legs with age (35 normals). For all $P > 0.1$.

4.3.7 Correlation of BMD of the various ROIs of the lower leg with the spine BMD

Figure 4.7 illustrates the relationship between BMD of the various regions of the lower-right leg selected from the whole body images, and the lumbar spine BMD for the 35 normal females. The relationships for the lower-right leg and both lower legs with the lumbar spine are also shown. The relations varied from an r value of 0.40 ($P = 0.02$) to an r value of 0.68 ($P = 0.0001$), with the lowest for the compact ROIs (i.e. R2 and R3) and the highest for the distal lower-right leg. The lower legs were highly correlated ($r = 0.88$, $P < 0.0002$), having an intercept = 0.089, a slope of = 0.91 and a SD = 0.061 gcm^{-2}. The correlations of the lower right/left leg or both lower legs BMD with lumbar spine BMD was moderate ($r = 0.58$, $P < 0.0002$).

4.3.8 Correlation between T-score at different sites of the body and regions of the legs

Figure 4.6 showed that there was no significant correlation between any region of the lower leg and age. It was, therefore, possible to derive the T-scores for the various regions of the lower leg using the normal group. Table 4.4 compares the linear correlation coefficients (r) between BMD T-score at different sites of the body in patients with osteopenia/osteoporosis. The Table also compares the correlation between the different ROIs of the right-leg as well as the right and left leg. The Table reveals that the proximal leg (R1) highly correlates with the spine and femur neck. The correlation of the R1 with the spine was stronger than the correlation between the spine and femur neck. Excellent correlation ($r = 0.92$, $P < 0.0001$) was found between the R1 and total femur, i.e. as good as the correlations between the femur neck and total femur or proximal (R1) or distal (R2) leg. Moderate correlation was found between the cortical region of interest of the leg (R3) and the spine, but better with the total femur. A correlation coefficient of $r = 1$ was observed between the right and left leg. This very high correlation was double checked with another statistical package.

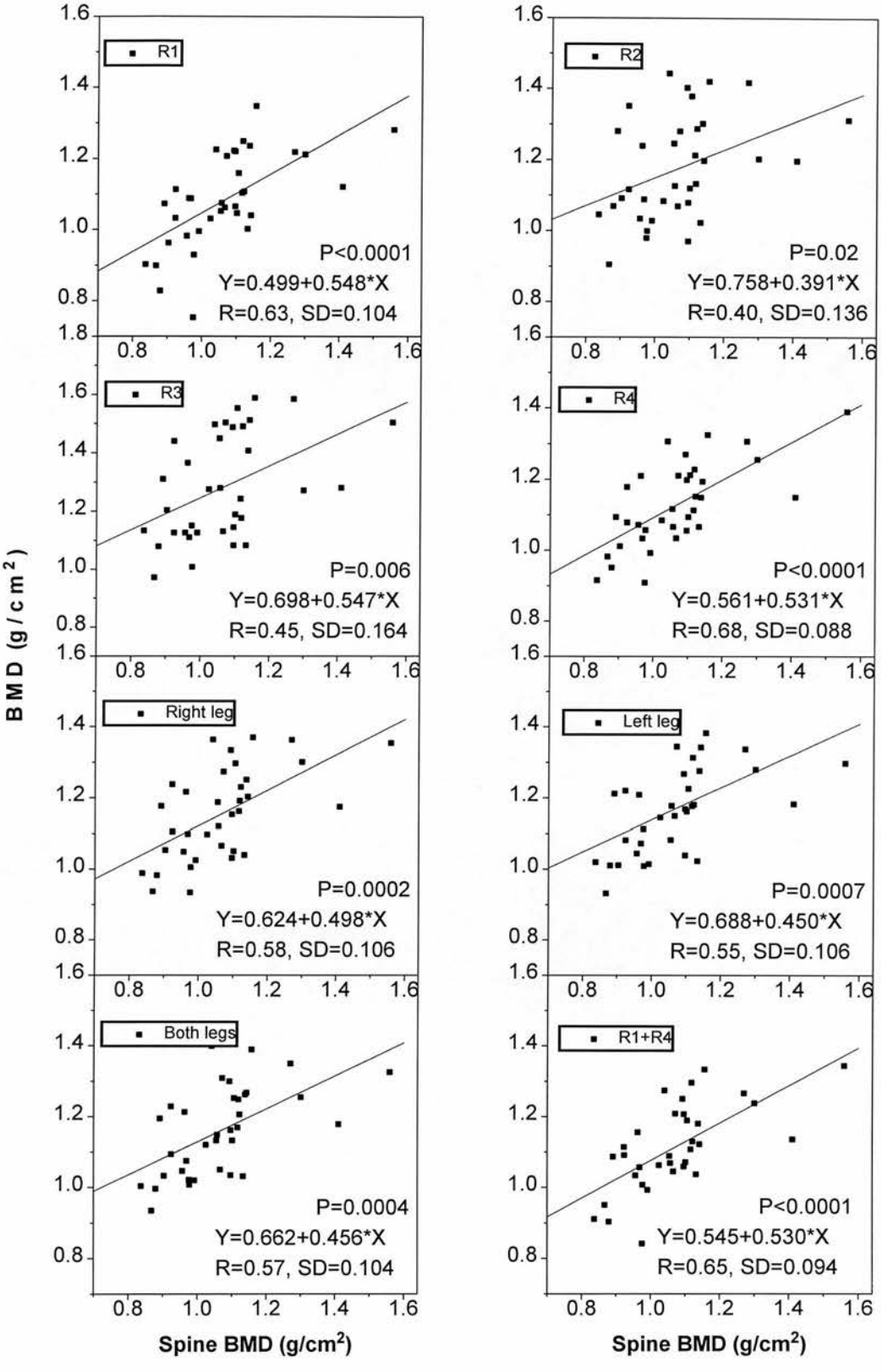

Figure 4.7 The correlation of lower-right leg and its different ROIs (R1 - R4) and lower-left leg with total lumbar spine (35 normals).

Table 4.4 Coefficient of correlation between BMD T-score at different sites of the body and regions of the legs in 37 patients with osteopenia/osteoporosis.

	FN	TF	R1	R2	R3	R4	RL	LL
Spine	0.77	0.83	0.81	0.67	0.66	0.72	0.75	0.75
FN		0.91	0.79	0.72	0.71	0.73	0.77	0.77
TF			0.92	0.79	0.78	0.85	0.87	0.87
R1				0.85	0.84	0.92	0.94	0.94
R2					0.94	0.88	0.96	0.96
R3						0.92	0.96	0.96
R4							0.96	0.96
RL								1

FN: Femur neck, TF: Total femur, R1 - R4 show the different ROIs of the Right leg
RL: Right leg and LL: Left leg. All $p < 0.0001$.

4.3.9 Comparison between the osteopenic/osteoporotic patients and normal subjects for the various sites of the body

Figure 4.8 compares the BMD T-score for the spine, femur, different ROIs of both the right and left legs for the female subjects who had been referred for the femur, spine and total body bone quality assessment. The Figure shows that the BMD T-score for the proximal (R1) and distal (R4) leg separate the osteopenic/osteoporotic patients from the normals as well as the neck of the femur and total femur. ANOVA also revealed that the means of the T-score for the neck of femur, total femur, proximal and distal leg were not significantly different ($F = 0.098$, $p = 0.961$). The student t-test also revealed that there was no significant difference between the means of the right/left leg T-score ($t = 0.475$, $p = 0.636$), i.e. the dominant and non-dominant leg were equally affected due to the disease.

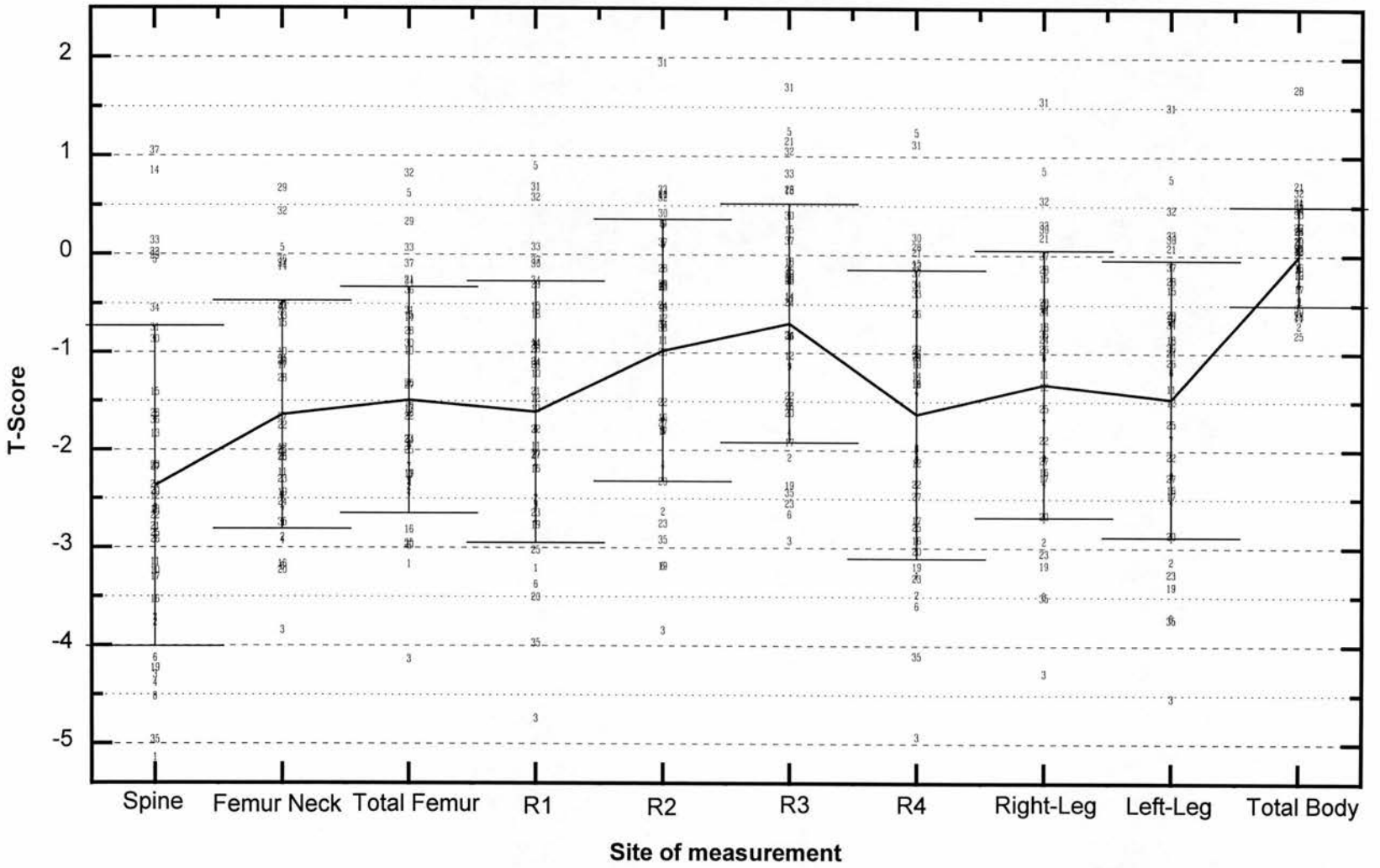

Figure 4.8 BMD T-scores for the spine, femur neck, total femur, different regions of interest of right leg (R1 - 4) and left leg for 37 female patients. The corresponding T-scores for whole body BMC, normalised for weight and height (see chapter 5) is shown for comparison. The error bars show the SDs from the mean values.

Figure 4.8 shows the BMD T-score of each of the referred subjects with a number. As an example subject number 37 had a spine BMD T-score of +1 with the T-score values of 0 for the total femur, R1 and R4; or subject number 1 had the lowest T-score of -5 for the spine, having T-score values of -3 for the total femur, R1 and R4. The Figure shows that the least differences between the young normal subjects and the osteopenic/osteoporotic patients were observed in the cortical region of interest of the leg (R3) and the total body normalised for weight and age. The full details of the whole body normalisation are discussed in chapter 5.

4.4 Discussion and conclusions

The present study of bone densitometry at different sections of the lower legs provides valuable information on bone quality assessment of the spine, femur neck and in particular, total femur. The measurements were precise for all the different sections of the leg containing different proportions of trabecular and cortical bone. Linear measurements for BMC and BMD using the various acquisition protocols of Forearm, Spine and Whole Body were obtained. However, the Whole Body acquisition protocol showed closer change in BMC and BMD than the other methods for a change in aluminium (simulating the bone) thickness. No method showed any significant change in the measured BMD with a realistic soft tissue thickness variation. The effect of rotation of the legs on BMD due to changes in the projected area of the various regions of the leg showed the least change in the proximal leg BMD. There were no good agreements between the various protocols for the lower leg bone mineral measurements, because of obtaining slopes of less than unity and non-zero intercepts. However, significant correlations between the Forearm/Whole Body and Spine/Whole Body acquisition methods for the lower leg bone mineral measurements were obtained. The Spine acquisition protocol showed closer slopes to 1 for BMC and BMD measurements. The regression equations for BMC and BMD measurements using the Spine method also had considerably lower intercepts compared to the Forearm protocol.

Attempts were made to scan the tibia by the Forearm acquisition protocol. Five healthy subjects of both genders participated. However, most of the subjects felt uncomfortable, since they had to hold their legs turned towards one side for approximately 15 minutes while the scanning was in progress. Therefore, it was found impractical to scan patients, in particular the elderly using the Forearm protocol. Therefore, approaches were made to make use of the whole body images and appropriate RIOs of the lower legs were defined and assessed.

Despite a higher bone image quality of the Forearm protocol (Figure 4.1a) as compared to the Whole Body protocol (Figure 4.1b), it was not possible to scan the tibia/fibula separately or the entire length of the lower leg. Now that an appropriate region of the lower leg for the assessment of bone quality of the femur and spine has been established, it is worth pursuing the study using a fan beam DXA scanner and scan the proximal lower leg laterally. Scanning the proximal lower leg laterally with an image quality similar to the Forearm images might improve the precision even further. The improvement in the precision might be achieved with a much smaller line spacing between the scan path and smaller pixel size. It is, therefore, useful that the DXA manufacturers develop a protocol that measures the lower leg laterally.

Table 4.5a compares BMD and the precision of the various ROIs of the lower leg/ tibia with other studies. Our findings of proximal tibia/fibula BMD were similar to those reported by Sievänen et al. (1992). The bone mineral values of the proximal tibia reported by Checovich et al. (1989) were considerably lower. Those were probably due to different scanning apparatus (DPA) or different populations studied (44 women aged 23 -87 years). Casez et al. (1995) measured BMC and BMD using DXA at lumbar spine and tibial diaphysis in 151 military men, 30 of the subjects were signalmen whose BMD is shown in Table 4.5a. That is why they had considerably higher tibia diaphysis BMD and a very low SD, which is due to a narrow variance in physical variables.

Table 4.5a Comparison of BMD and CV of the various ROIs of the lower leg/tibia with other studies.

Skeletal site	BMD (g/cm^2)			Technique Publisher
	Mean (SD)	Range	CV%	
Proximal lower leg	1.08 (0.13)	0.696-1.35	1.2	DXA (Hologic QDR 1000/W)
Proximal tibia	*1.14 (0.20)*	*0.862-1.46*	*0.7*	*DXA (Norland XR-26), Sievänen*
	0.78 (0.17)	*0.380-1.18*		*DPA (Lunar DP3), Checovich*
Diaphysis lower leg	1.28 (0.18)	0.969-1.64	2.4	DXA (Hologic QDR 1000/W)
Diaphysis tibia	*1.74 (0.029)*			*DXA (Hologic QDR 1000) , Casez*
Distal lower leg	1.12 (0.12)	0.786-1.39	1.9	DXA (Hologic QDR 1000/W)

The figures in *italics* are other publishers' findings.

Table 4.5b compares the correlation coefficients obtained in this study and other studies between the BMD of the proximal, diaphysis and distal lower leg/tibia and spine with anthropometric parameters. No significant correlation was found for BMD's of the spine and the proximal part and the diaphysis of the lower leg/tibia with age. No significant correlation between the above parameters with age was found due to a limited age range of 23 -52 years (i.e. before the onset of menopause). However, a weak but significant correlation with age was found for the distal lower leg. No significant correlation between proximal tibia/fibula and height was calculated, while using DPA Checovich et al. (1989) found a moderate positive correlation. However, weak, but significant correlation between the diaphysis tibia/fibula and height was observed ($r = 0.22$ cf. $r = 0.28$ Casez et al., 1995). A correlation of $r = 0.70$, $P < 0.0001$ was found for proximal tibia/fibula BMD with weight, while, Checovich et al. (1989), reported a correlation of $r = 0.25$, $P < 0.05$. The correlation between the diaphysis lower leg/tibia with weight found in this study was consistent with Casez et al. (1995) report. They also reported a weak correlation between the lumbar spine and weight. In contrast, a high correlation between those parameters was obtained in the present study.

Table 4.5b Comparison of correlations (r) between different ROIs of tibia/fibula BMD, lumbar spine BMD and anthropometric parameters obtained by different studies.

Variable	Publisher	Proximal tibia	diaphysis tibia	distal tibia	spine
Age		NS	NS	0.24*	NS
	Checovich	*-0.700***			
Height		NS	0.22*	NS	0.30**
	Checovich	*+0.48***			
	Casez		*0.28**		*0.14 NS*
Weight		0.70***	0.47***	0.71***	0.71***
	Checovich	*+0.25**			
	Casez		*0.43****		*0.34****

The figures in *italics* are other authors findings.
NS = not significant *: $p < 0.05$ **: $p \leq 0.001$ ***: $p \leq 0.0005$.

Checovich et al. (1989) found correlations of 0.70 and 0.73 between the tibial BMD and lumbar spine and the femur neck, respectively. In this study correlation coefficients of 0.63 and 0.81 between the proximal tibia/fibula and spine for the normals and patients with osteopenia/osteoporosis, respectively, were found. A correlation coefficient of 0.79 between the proximal tibia/fibula and femur neck for the patients with osteopenia/osteoporosis was found in the present study.

In this study, excellent correlation ($r = 0.92$, $p < 0.0001$) was found between the proximal lower leg T-score and the total femur T-score. This correlation was as strong as the correlation between the femur neck/total femur and the proximal/distal lower leg BMD T-score. The correlation of the proximal lower leg T-score with the spine or femur neck was very high and as close as the correlation between the spine and femur neck. The

diaphysis lower leg, which is predominantly cortical bone, showed a moderate correlation with the spine, but a good correlation with the femur neck and a very good correlation with the total femur. Correlation of the total lower legs with the spine and femoral neck was similar and consistent with Nordin et al. (1996) report. The correlation between the dominant and non-dominant legs was 1, and they also showed similar difference between the normals and patients.

The difference between the normals and osteopenic/osteoporotic patients was more significant at the spine. However, the bone loss at the proximal/distal lower leg was as significant as the bone loss at the femur neck/total femur. The least difference between the two groups was observed at the predominantly cortical section of the lower leg and the total body normalised for age and weight.

In conclusion, in order to assess the risk of fracture due to reduced bone mass accurately, it is necessary to ideally measure the actual site of interest. However, bone quality assessment of the proximal regions of the legs by DXA, which showed the closest correlation with the spine, total femur and femur neck as well as showing the least change in BMD due to the rotation of leg, might be a useful measurement. DXA of the lower legs might be useful where measurement of lumbar spine or femur is not possible. Further investigation of a much larger population yielding normative information of the lower legs is required.

Chapter 5

DXA Assessment of Total Body Bone Mineral

5.1 Introduction

The high precision of DXA measurements combined with the stability of calibration of the instrumentation make DXA an ideally sensitive technique for studying the outcome of new therapeutic regimes to protect the skeleton (Blake et al., 1991). Until recently, most clinical DXA studies have been limited to antero-posterior projection scans of the lumbar spine and studies of the femur. However, recent developments in DXA scanning now provide additional sites that will enable more complete data to be obtained (Uebelhart et al., 1990; Slosman et al., 1990 and Ryan et al., 1992). Herd et al. (1993) described DXA scanning of the total skeleton and its regional parts which offers a comprehensive view of bone content in the whole skeleton.

There is a growing interest in studying bone in all regions of the body, since the various therapeutic regimes available may affect parts of the skeleton differently. Sodium fluoride therapy has been shown to increase BMD in the spine but has little effect on the peripheral skeleton (Hodsman and Drost, 1989 and Pouilles et al., 1991). There is evidence that bisphophonates may behave similarly (Fromm et al., 1991 and Miller et al., 1991). In contrast, oestrogen-based therapies can preserve both trabecular and cortical bone (Gallagher et al., 1991). There is also substantial interest in looking at tissue changes induced by growth hormones (Hansen et al., 1995; Beshyah et al., 1995a and Beshyah et al., 1995b). Therefore, DXA assessment of the total body may offer valuable information on bone quality of the total body as well as the appendicular and axial sites.

One of the first applications of total body DXA was to evaluate bone and tissue compositions in large samples of normal adults, something that could not be done easily and reliably with older composition methods (Wellens et al., 1994 and Gasperino et al., 1995). Moreover, DXA can be used readily in both young children and the elderly

(Baumgartner et al., 1995; Ogle et al., 1995 and Gutin et al., 1996). This makes it possible to monitor the effects of dietary restrictions and/or exercise on regional and total body composition (Svendsen et al., 1995a). An obvious use of composition methods has been to assess changes occurring after weight loss; gross changes can be monitored with a balance, but DXA allows the clinicians to assess changes in bone and lean tissue (Svendsen et al., 1995b).

There is particular interest in the pattern of growth of the skeleton, so there have been a number of investigations of whole body bone mineral in infants, children and adolescents (Bachrach, 1990; Venkataraman and Ahluwalia, 1992; Rice 1993). Venkataraman and Ahluwalia (1992) measured new born infants and found that the values for bone mineral agreed with the values reported by chemical analysis of cadavers. Bachrach et al. (1990) measured young patients with anorexia nervosa and found that whole body bone mineral was more sensitive than mid-radius BMD as a measure of cortical bone loss.

DXA has become widely accepted for the measurement of body composition because of: (a) its ease of use, (b) its high precision, (c) the ability to measure bone mass as well as lean and soft tissue and (d) the ability to use regional as well as total composition. However, the technique has some limitations (Hannan et al., 1993; Hannan et al., 1995; Tothill et al., 1994 and Tothill et al., 1997). For measurements of the lumbar spine the simple assumption that the thickness of fat over the vertebrae is the same as that in the adjacent soft tissue background is usually made. However, it has been demonstrated that the non-uniform distribution of adipose tissue in the abdomen leads to small, but variable and unpredictable errors in the determination of BMD in the lumbar spine (Tothill and Pye, 1992). For whole body scanning more complex assumptions are necessary. The DXA measurements allow the determination of the proportions of fat and lean soft tissue in non-bone areas. These assessments are used to extrapolate or interpolate over bone. These assumptions cannot be valid for all subjects. Therefore, absolute accurate bone mineral measurement is not possible.

In summary, total body bone mineral measurement for the examination of skeletal integrity is essential for the following reasons:

1. The need to study the outcome of new therapeutic regimes to preserve the skeleton.
2. The need to investigate how various therapeutic regimes may affect different parts of the skeleton.
3. The need to monitor the effects of exercise and/or dietary restrictions on regional and total body bone mineral.
4. The need to monitor the pattern of growth of the skeleton in children.

There is usually a need to normalise bone mineral measurements for the size of the subject. It has become customary to divide the measured bone mass by the area, which is determined from the number of bone-containing pixels, to give an areal bone mineral density. This is convenient and works reasonably well for spine and femur measurements, although the normalisation does not fully allow for size. There is also substantial information for spine and femur BMDs in normal subjects, providing reference ranges for a given population. Results from patients can, therefore, be expressed in relation to age-matched normal (Z-score) or young normal (T-score).

In an eating disorder study carried out over a period of one year, Tothill et al. (1997), however, measured total body bone mineral values, using a Hologic QDR 1000W in a group of subjects and observed anomalies that called into question the accuracy of such measurements. A change in total body bone mineral content (TBBMC) was related to a change in weight, but a loss of weight appeared to be correlated with an increase in total body bone mineral density (TBBMD). There is also some controversy that bone mineral density is not appropriate for use in total body measurements, because there are over-lapping bones and orientation effects. Moreover, normalising by bone area is not complete due to variations of bone mineral density with size, such as shoulder width or weight.

Therefore, the objective of this study was to overcome the anomaly observed in TBBMD measurements and to assess the limitations of the method. In order to find an explanation for the reported artifact in the subjects whose weight changed, the following experiments were conducted. Firstly, the in-vitro measurements were made to investigate the effect of soft tissue on the part body and total body bone mineral measurements. For this investigation a whole body phantom representing different TBBMDs and variable lean and fat content was used. In order to explore and to find the reason(s) for the observed artifact, a whole body sub-region analysis was used to detect the bone threshold for each region, and the effect of soft tissue variations on regional parts and as a whole, using the whole body phantom. Secondly, the in-vivo effect of weight change, using a group of subjects with different genders and a wide range of BMD was assessed. Thirdly, the effect of rotation of the legs on total body bone mineral measurements was also investigated. In order to normalise TBBMC for body size, and therefore to overcome the observed anomaly, predictive equations based on body habitus were derived. Two female groups of anorexic patients and normal subjects were compared for the whole body and spinal body bone mineral, using total body indices (TBIs) and spine BMD , respectively. TBIs were calculated using predictive equations based on stature. Precision in bone mineral measurement is important for characterisation of a technique's ability to detect the long term skeletal changes. Therefore, the precisions of TBBMC/TBBMD and TBI were assessed.

5.2 Methods and materials

In an eating disorder study carried out over a period of one year by Tothill et al. (1997), an anomaly was reported. Figure 5.1 shows the observed anomaly; where, despite a positive correlation between TBBMC and weight, a negative correlation between TBBMD and weight was found. The Figure shows that a +10% change in weight was associated with a +2.5% change in TBBMC and a -1% change in TBBMD. Therefore, to find the reason(s) and possibly overcome the artefact, in-vitro and in-vivo studies were conducted.

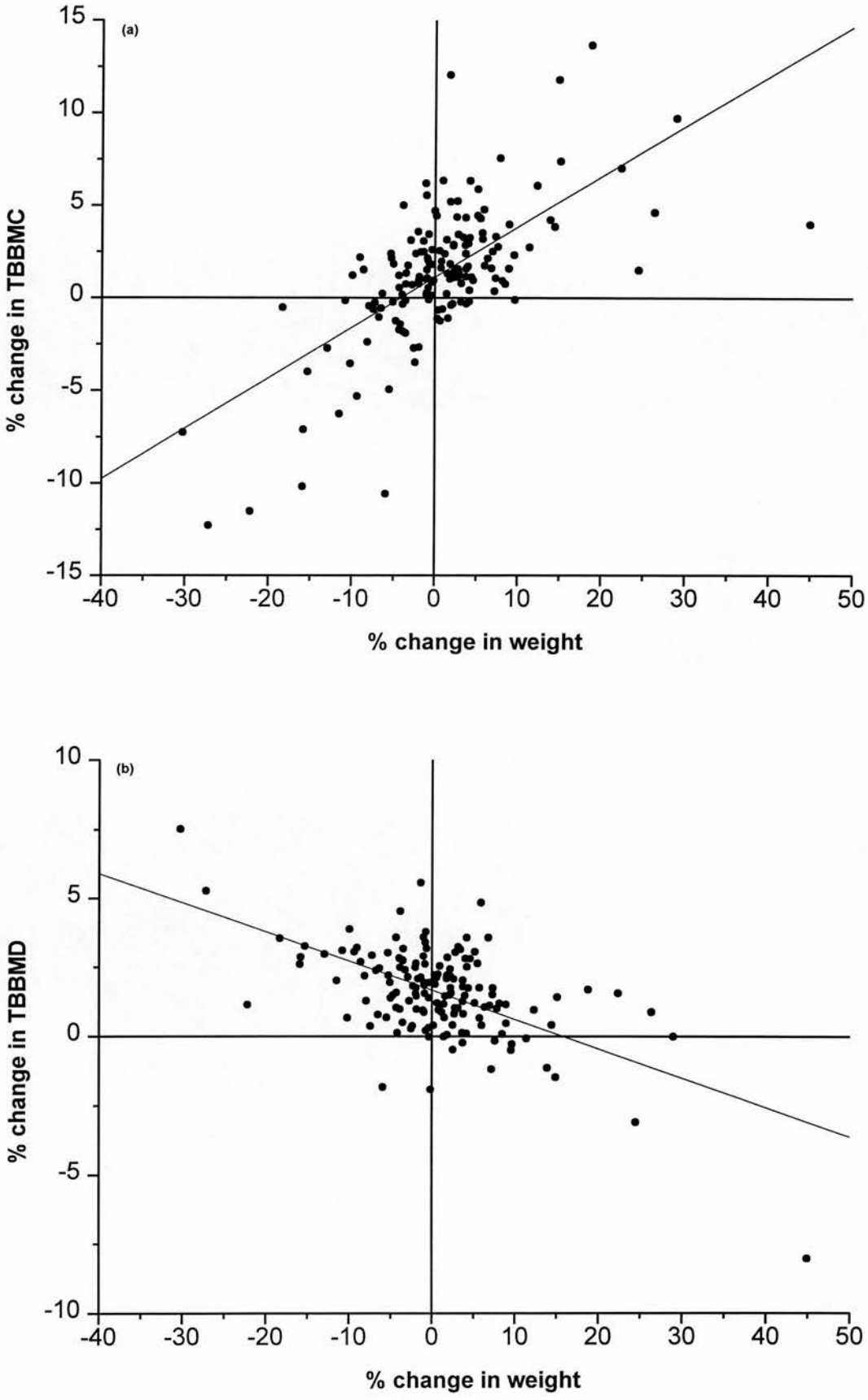

Figure 5.1 Plots of changes in (a) total body BMC and (b) BMD against change in weight (Tothill et al. 1997).

5.2.1 In-vitro measurements

5.2.1.1 Whole body phantom

A whole body phantom was used to perform various experiments. The phantom was constructed from aluminium sheets (simulating different bones) and hardboard sheet (simulating soft tissue). The hardboard sheets consisted largely of cellulose, which is reasonably equivalent to soft tissue in its x-ray attenuation characteristics. The fat content equivalent of the hardboard based on DXA measurement was 40% and its density close to 1 g/cm^3. The hardboard sheet thickness was 3 mm. The hardboard sheets had rectangular shapes with different widths and stacked to form circular cylinders corresponding to the neck, arms and legs, and nearly elliptical cylinders were used for the head, chest and pelvis. The dimensions of the cylinder approximated those of a standard man. Antero-posterior thickness ranged from 10 to 20 cm. The weight and the height of the phantom was 70 kg and 1.72 m, respectively. The full skeleton had area, BMC and BMD of each component similar to those found in-vivo.

The number of aluminium sheets could be varied to simulate a change in bone density. The aluminium sheet thickness was 1.7 mm. The aluminium width in the arms was 25 mm and in the legs and spine 45 mm. To perform various experiments the phantom was set-up in different configurations to simulate normal or low skeleton bone densities. The normal bone density (1.14 g/cm^2) phantom consisted of 10 aluminium sheets for the head, 5 for the pelvis, 4 for the legs, thoracic spine, lumbar spine and the arms, and 2 for the ribs. For the low bone density (0.988 g/cm^2) phantom the number of aluminium sheets in the head and ribs was kept constant and 1 aluminium sheet was removed from the pelvis, legs, thoracic vertebrae, lumbar vertebrae and arms. Figure 5.2a shows an example of a whole body DXA image. The Figure shows bone mineral values of the various sites of the normal density phantom and compares it with the values obtained by the sub-region analysis values.

(a)

Medical Physics, WGH. Edinburgh.

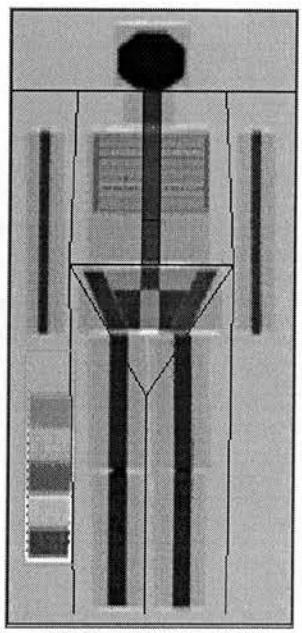

·25.Apr.1996 15:38 [330 x 138]
Hologic QDR-1000/W (S/N 967 P)
Enhanced Whole Body V5.55

U04109615 Wed 10.Apr.1996 16:39
Name: Whole Body Phantom
Comment: Scan Number 4
I.D.: Sex: M
S.S.#: - - Ethnic: W
ZIPCode: Height: 1.72 cm
Scan Code: MRS Weight: 69 kg
BirthDate: Age.
Physician:
Image not for diagnostic use

TOTAL BMC and BMD CV is < 1.0%

	C.F.	1.014	1.090	1.000
Region		Area (cm2)	BMC (grams)	BMD (gms/cm2)
L Arm		161.86	150.06	0.927
R Arm		163.48	146.04	0.893
L Ribs		83.56	36.72	0.439
R Ribs		105.88	46.25	0.437
T Spine		152.93	163.03	1.066
L Spine		47.46	52.61	1.108
Pelvis		316.41	353.16	1.116
L Leg		343.59	446.19	1.299
R Leg		337.91	447.31	1.324
SubTot		1713.08	1841.36	1.075
Head		247.04	388.57	1.573
TOTAL		1960.12	2229.93	1.138

HOLOGIC

Medical Physics, WGH. Edinburgh.

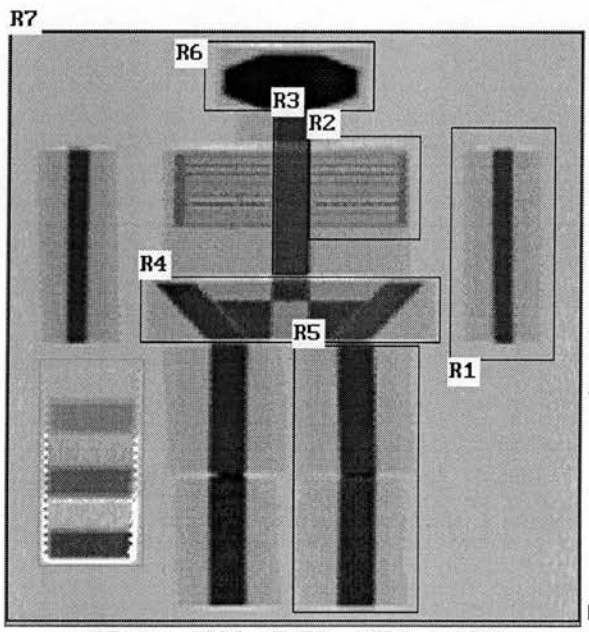

·25.Apr.1996 15:59 [330 x 138]
Hologic QDR-1000/W (S/N 967 P)
Enhanced Whole Body V5.55

U04109615 Wed 10.Apr.1996 16:39
Name: Whole Body Phantom
Comment: Scan Number 4
I.D.: Sex: M
S.S.#: - - Ethnic: W
ZIPCode: Height: 1.72 cm
Scan Code: MRS Weight: 69.90 kg
BirthDate: Age:
Physician:
Image not for diagnostic use

	C.F.	1.014	1.090	1.000
Region		Area (cm2)	BMC (grams)	BMD (gms/cm2)
R1		161.86	150.06	0.927
R2		76.67	32.94	0.430
R3		208.51	218.25	1.047
R4		294.10	321.68	1.094
R5		354.14	459.82	1.298
R6		247.04	388.57	1.573
R7		1960.12	2229.91	1.138
NETAVG		1960.12	2229.91	1.138

HOLOGIC

(b)

Figure 5.2 Comparison of (a) whole body bone mineral results with (b) whole body sub-region analysis.

5.2.1.2 Auto-scan and sub-regional body composition analysis

The scanner has an auto-scan facility that allows repeat measurements without the intervention of the operator. The auto-scan facility was used to take repeat measurements.

In the analysis of whole body scans the operator, guided by the computer protocol, divides the body into regions including head, upper and lower trunk, arms and legs. However, the scanner also has a sub-regional body composition analysis facility that allows the measurement of the regional body composition. The final image appears expanded horizontally with a small square in the centre. The shape of the box can be adjusted and a maximum of seven boxes can be created (Figure 5.2b). This sub-regional body composition analysis allows assessment of the effect of therapy/weight change on the part/total body bone mineral measurements.

5.2.1.3 Bone threshold and position dependency

In order to find a possible explanation for the reported artifact, the density of the various body parts of the phantom was reduced to find the bone detection threshold for a particular site. The measured areas were compared with the true areas, and it was , therefore, possible to identify the site(s) which were not completely detected. Bone threshold position dependency was also investigated, by comparing the measured bone density for particular thicknesses of aluminium positioned in different regions of the body.

5.2.1.4 Effects of changes in weight and soft tissue composition

The effect of soft tissue thickness and composition was investigated, using the whole body phantom with different bone densities of normal and low for the following procedures:

A. Placing lard over the whole body phantom.

B. Reducing the antero-posterior thickness by 30% (18.4 kg).

C. Replacing the same thickness of the hardboard with lard.

Experiment A was undertaken by placing lard (simulating fat) over the whole body phantom in amounts of 4, 8 and 16 kg. These amounts of lard were equal to 6%, 11% and 23% of the phantom's weight, which were similar to the weight gain range observed in the subjects whose weight changed. 3 kg of the 4 kg lard was placed on the trunk and 1 kg on the thighs; 5 kg of the 8 kg lard was placed on the trunk, 2 kg on the thighs and 1 kg on the upper arms. When 16 kg of lard was used, 11 kg of the lard was placed over the trunk and 5 kg over the thighs.

Experiment B was performed by reducing the antero-posterior thickness by 30% in decrements of 15%, keeping the head contents constant.

Experiment C was performed because of the difference in the fat content of the hardboard and the lard. In order to detect if there were similar patterns with the soft tissue thickness variations on the part body/total body bone mineral measurements, the above investigations were undertaken with the use of the phantom with the normal and low skeleton bone densities. For this purpose 8 kg of lard with a thickness of 6 cm was used to replace the same thickness of hardboard over the trunk. The difference in the skeleton bone thickness/density or over-lying soft tissue might have a possible beam hardening effect.

A total body phantom scan took 16 minutes and an assembly time of approximately 45 minutes if a change of phantom thickness was required. The mean of 3 measurements for each investigation was calculated. Where a paired t-test was required, 5 measurements were taken.

5.2.2 In-vivo measurements

5.2.2.1 In-vivo effect of weight change

It was possible that the anomaly reported by Tothill et al. (1997) was caused by an artifact in the DXA analysis related to the differences in subjects thickness or fat content. To examine this possibility lard was used to simulate changes in weight and fat content.

In order to investigate the in-vivo effect of soft tissue thickness or weight change on bone mineral measurements, a group of subjects were measured. The group consisted of 6 volunteers including 2 females, one of which was a teenager with a low TBBMD. The subjects had a wide range of BMI (18 - 30 kg/m^2) and TBBMD (0.90 - 1.2 g/cm^2). In order to simulate a weight change each subject had two measurements, with and without the distribution of lard over the body.

Over 95% of the subjects in the above report had a weight change of less than 25%. Therefore, 12 to 20 kg of lard, equivalent to 22% to 25% of the subject's weight was distributed anteriorly over the trunk and thighs. 1/3 of the lard was placed equally over the thighs and 2/3 over the trunk. A single scan took approximately 15 minutes. Figure 5.3 shows an example of a total body bone density image of a subject. Bone mineral values for the various regions of the body are also shown. The sex matched T- and Z-scores are also calculated.

5.2.2.2 The effect of rotation of the legs

The same method and material described in section 4.2.4 of chapter 4 were used and the effect of the rotation of legs on TBBMC and TBBMD measurements was investigated.

(a)

Medical Physics, WGH. Edinburgh.

U04139405 Wed 13.Apr.1994 13:38
Name:
Comment:
I.D.: DRLD551 Sex: F
S.S.#: - - Ethnic: W
ZIPCode: Height: 151.50 cm
Scan Code: SC Weight: 34.20 kg
BirthDate: 21.Jan.64 Age: 30
Physician:
Image not for diagnostic use

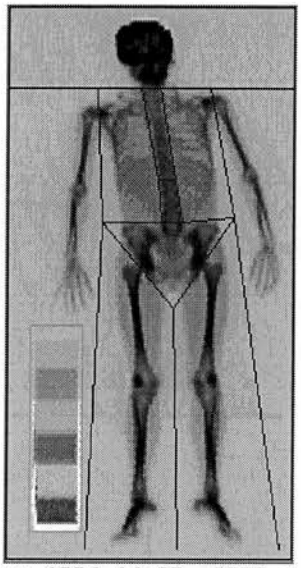

·13.Apr.1994 14:20 [330 x 129]
Hologic QDR-1000/W (S/N 967 P)
Enhanced Whole Body V5.51

TOTAL BMC and BMD CV is < 1.0%

	C.F. 1.015	1.091	1.000
Region	Area (cm2)	BMC (grams)	BMD (gms/cm2)
L Arm	88.89	50.50	0.568
R Arm	90.92	54.09	0.595
L Ribs	84.42	38.04	0.451
R Ribs	81.99	36.84	0.449
T Spine	106.34	65.68	0.618
L Spine	49.92	31.52	0.631
Pelvis	145.31	102.30	0.704
L Leg	230.14	206.21	0.896
R Leg	235.01	211.94	0.902
SubTot	1112.95	797.11	0.716
Head	226.08	367.13	1.624
TOTAL	1339.03	1164.24	0.869

HOLOGIC

Medical Physics, WGH. Edinburgh.

U04139405 Wed 13.Apr.1994 13:38
Name:
Comment:
I.D.: DRLD551 Sex: F
S.S.#: - - Ethnic: W
ZIPCode: Height: 151.50 cm
Scan Code: SC Weight: 34.20 kg
BirthDate: 21.Jan.64 Age: 30
Physician:

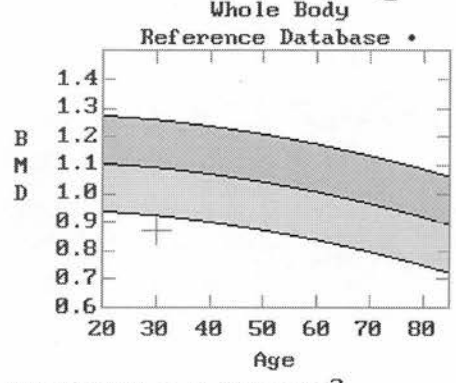

BMD(WHOLE) = 0.869 g/cm^2

T(20.0)		Z	
-2.67	79%	-2.50	80%

• Age and sex matched
T = peak bone mass
Z = age matched PS 25 Oct 91

HOLOGIC

(b)

Figure 5.3 (a) Total body DXA scan of an anorexic patient showing the bone mineral values for the various regions and the total body. (b) Plot of TBBMD as a function of age.

5.2.2.3 Subjects

This study consisted of 39 normal female subjects and 34 age-matched female patients with anorexia. The normal subjects were those who had no history of any disease or being on any drug that might affect the bone metabolism. The subjects had their total body and spine measured. Table 5.1 shows the details of the anorexic patients and normal subjects.

Table 5.1 Details of the female anorexic patients and normal subjects.

	Patients (n = 34)	Normals (n = 39)
Age (years)	30.4 ± 8.2 (20.0-47.8)	34.7 ± 9.1 (23.0-52.4)
Height (cm)	161.6 ± 5.8 (150.0-177.5)	163.5 ± 7.0 (150.0-181.5)
Weight (kg)	40.4 ± 5.1 (27.8-53.8)	68.6 ± 15.3(44.9-112.6)
BMI (kg/m^2)	15.5 ± 1.8 (11.5-20.3)	25.6 ± 5.1 (18.5-39.2)
Shoulder width (cm)	35.0 ± 1.4 (33.0-38.5)	37.5 ± 2.1 (33.5-43.0)
Antero-posterior thickness (cm)	15.3 ± 1.3 (13.0-19.0)	18.5 ± 2.1 (14.0-22.0)

Results are expressed as mean ± SD (range).
BMI, body mass index, calculated as weight/$height^2$.

Height was measured using a wall stadiometer (precision 5 mm) with the patient standing upright and without shoes. Weight was measured on digital scales with a precision of 0.1 kg. Subjects wore a light gown. The antero-posterior thickness was measured using callipers and was taken as the maximum thickness along the full length of the sternum. Enhanced whole body software version 5.51 and spine software version 4.47P were used for the analysis.

5.2.3 Statistical methods

Paired t-tests were performed to find the significance of the differences between bone mineral values obtained for body parts/whole body with and without the use of lard for in-vitro and in-vivo measurements. In order to reduce the biological variance in bone mineral measurements, DXA manufacturers supply the normal data as BMD for the

various sites of the body for different age and sex groups. However, in normal subjects TBBMD is still correlated with weight and body size. Therefore, alternative means of normalising TBBMC for body stature were investigated. Prediction equations for TBBMC in normal subjects were derived using body habitus as independent variables in multiple stepwise regressions. Weight was included as an independent variable but for patients with eating disorder this was not appropriate and alternative prediction equations which did not include weight were derived. Variables were only included in the prediction equations if they resulted in a significant reduction in the standard error of prediction. Total body bone indexes (TBI) were calculated as the ratio of the measured TBBMC to the predicted one. The CoV of TBI was compared with the CoVs of TBBMC, TBBMD and spine BMD.

Linear regression analysis was used to assess the effect of age on bone mineral values. Unpaired t-tests were performed to assess the differences in the T-scores between the patients with anorexia and the normal subjects for the TBI and spine BMD. The T-score is calculated as the difference between the patient's value (P) and the mean value (M_Y) for young sex-matched normals, divided by the standard deviation (SD_Y) of the mean value for young normals as:

$$\text{T-score} = (P-M_Y)/SD_Y$$

The precisions of TBBMC, TBBMD and TBI were assessed as the mean coefficient of variation (CV) of duplicate measurements on 11 normal subjects. The measurements were carried out within a few days on each subject.

5.3 Results

5.3.1 The in-vitro effects of changes in soft tissue thickness and composition

Table 5.2 shows the effect of distribution of lard over the trunk and thighs on total/part body bone mineral measurements, using the phantom. The Table also reveals the effect of the removal of soft tissue or replacement of lard with the same thickness of soft tissue on bone mineral measurements.

When 15% of soft tissue thickness was removed, there were no significant changes on the part-body bone areas except the trunk and therefore the total. No significant change was observed for BMC of any region, but since there was a significant increase in total body bone area and no significant change in TBBMC, a significant reduction in TBBMD was found. The head BMD was unchanged.

When lard was placed on the trunk and thighs in any amount (4 to 16 kg), significant changes in trunk area (except for 4 kg) and BMC were observed. However, no significant change in BMD was found because the changes in area and BMC were in proportion. For legs, all measured bone mineral parameters were significantly altered. For the head there were significant reductions in area and BMC when 4 kg of lard was used, but a significant increase in BMD was found. When 8 kg or 16 kg of lard was added, no changes in BMCs or BMDs were found.

The Table shows that there were no variations in the bone mineral parameters of the arms when 4 kg of lard was used on the trunk and thighs, but when 8 kg of lard was used (1 kg on the arms) significant changes in area, BMC and BMD were found. When 16 kg of lard was distributed on the trunk and thighs, significant increases in BMC and BMD of the arms were found.

For total body area, TBBMC and TBBMD significant changes were observed when any amount of lard was added, except for total body area when 4 kg of lard was used. Figure 5.4 illustrates the changes in total and part-body bone mineral measurements with the soft tissue alterations.

To determine if there were any changes in bone mineral measurements due to the replacement of lard with the same thickness of the hardboard, 8 kg of lard was replaced with the same thickness of hardboard, using the normal bone density phantom. Significant changes for BMD and bone area were found, respectively.

Table 5.2 Unpaired t-test results when lard was added to the phantom or some soft tissue was removed or lard was replaced by the same thickness of hardboard.

		Trunk	Legs	Head	Arms	Total
Area	-	*742, 3.60, .02S*	*695,1.64, 0.17NS*	*249, 0, 1NS*	*346, 2.3, 0.08NS*	*2032, 4.2, 0.01S*
	Initial value	*715*	*686*	*249*	*338*	*1988*
	+	694, -2.41,0.05NS	704, 6.93, 0.0004S	238 -13.2, 0.00001S	340, 1.0, 0.35NS	1976, -1.38, 0.22NS
	++	679,-9.31, 0.0001S	701, 4.24, 0.005S	241, -10.5, 0.0004S	353, 10.2, 0.0001S	1973, -3.25, 0.02S
	+++	827, 8.40, 0.0002S	711, 7.71, 0.0002S	248, -1.70, 0.14NS	336, -1.24, 0.26NS	2121, 8.27, 0.0002S
	◦					*1965*
	⊙					*2005,9.59, 0.001S*
BMC	-	*649, -2.75,0.05NS*	*878, -1.50, 0.21NS*	*397, 0.25, 0.82NS*	*315.7, -0.08, 0.94NS*	*2240, -1.3, 0.25NS*
	Initial value	*659*	*888*	*395*	*316*	*2258*
	+	636, -4.27, 0.005S	876, -2.85, 0.03S	385, -2.88, 0.03S	314, -0.89, 0.41NS	2210, -7.09, 0.0004S
	++	618, -13.1, 0.00001S	874, -2.74, 0.03S	388, -1.92, 0.10NS	318, 0.84, 0.43NS	2198, -12.6, 0.0002S
	+++	733, 2.65, 0.04S	908, 3.60, 0.01S	400, 0.92, 0.39NS	325, 3.02, 0.02S	2368, 3.64, 0.01S
	◦					*1941*
	⊙					*2237, 0.81, 0.44NS*
BMD	-	*0.875, -5.80, 0.00S*	*1.263, -8.27, 0.001S*	*1.594, 0.43, 0.69NS*	*0.912, -3.34, 0.03S*	*1.102, -8.4, 0.001S*
	Initial value	*0.921*	*1.298*	*1.585*	*0.935*	*1.136*
	+	0.916, -0.68, 0.52NS	1.245, -21.0, E-7S	1.612, 2.60, 0.04S	0.924, -2.13, 0.08NS	1.118, -6.89, 0.0005S
	++	0.913, -1.05, 0.33NS	1.246, -18.3, 1.7E-6S	1.612, 2.32, 0.06NS	0.903, -5.11, 0.002S	1.114, -9.88, 0.0001S
	+++	0.888, -1.47, 0.19NS	1.277, -2.58, 0.04S	1.616, 1.79, 0.12NS	0.968, 6.39, 0.0007S	1.116, -8.41, 0.001S
	◦					*0.988*
	⊙					*1.116, 6.80, 0.0001S*

Key -: 15% off soft tissue thickness +: 4 kg lard added ++: 8 kg lard added +++: 16 kg lard added

The results are expressed as Mean, t-value and P-value obtained from unpaired student t-test. S and NS denote significance and non significance. Figures in *italics* are the results for the same day measurements. ◦ and ⊙ show the results for the low BMD phantom with normal soft tissue thickness and when 8 kg of lard was replaced the same soft tissue thickness (hardboard) , respectively.

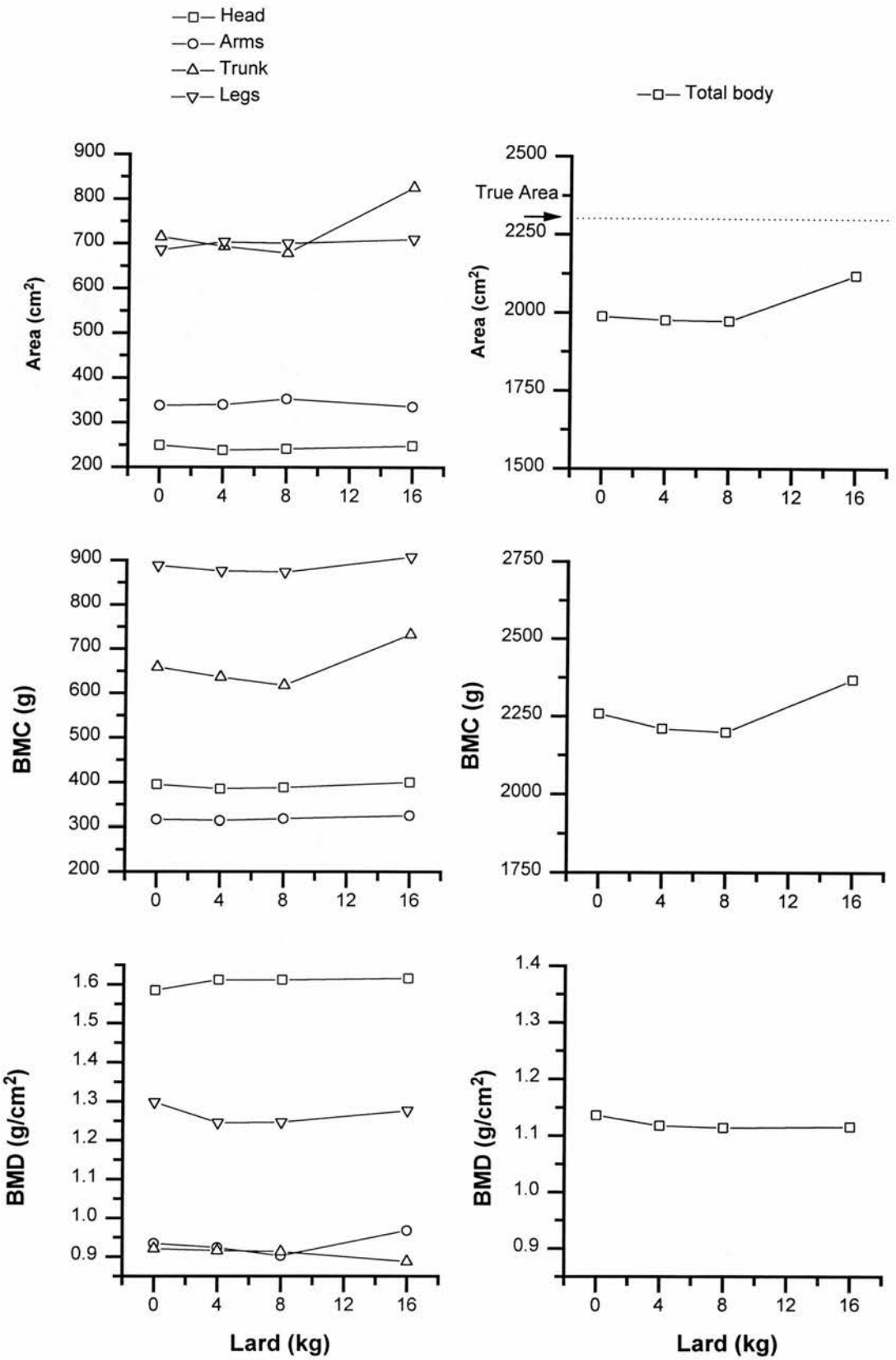

Figure 5.4 The in-vitro effect of the distribution of lard on part body and total body bone mineral measurements.

Figure 5.5 illustrates the effect of soft tissue (hardboard) thickness on bone mineral measurements, with the two different phantoms' BMDs of normal (1.14 g/cm^2) and low (0.988 g/cm^2). The error bars represent ± SDs. The Figure shows the bone area for normal phantom BMD increased significantly ($t = 4.2$, $P = 0.001$) as the soft tissue thickness decreased by 15%. There was no change in BMD with a further 15% reduction in soft tissue thickness. The low BMD phantom showed the same trend. BMC did not change significantly ($t = -1.3$, $P = 0.2$) for the normal BMD phantom when the soft tissue thickness decreased by 15%. Even when the soft tissue thickness was removed by a further 15% no variation in BMC was observed. The low BMD phantom showed a similar pattern with the soft tissue thickness alterations. BMD changed significantly ($t = -8.4$, $P = 0.001$) for the first 15% reduction in soft tissue thickness. The low BMD phantom followed the same trend as the normal BMD phantom for the first 15% reduction in the soft tissue thickness and the BMD was kept constant for a further 15% of soft tissue thickness removal.

5.3.2 Part-body bone threshold and position dependency

Variations in the bone mineral measurements with the thickness of aluminium in the skeleton and the bone threshold for each region of the body are illustrated in Figure 5.6. The Figure shows a plot of BMD against aluminium sheet thickness for the various regions of the whole body phantom.

It can be seen that for some regions like the ribs and thoracic vertebrae some bones have been detected, though there was no aluminium. When one aluminium sheet was placed in the position of the legs, pelvis and lumbar vertebrae, no bone was recognised. When the same number of aluminium sheets were placed in different regions, different sites showed different BMDs, i.e. they were position dependant. A true phantom bone area of 2305 cm^2 has been shown by a dashed line (Figure 5.4).

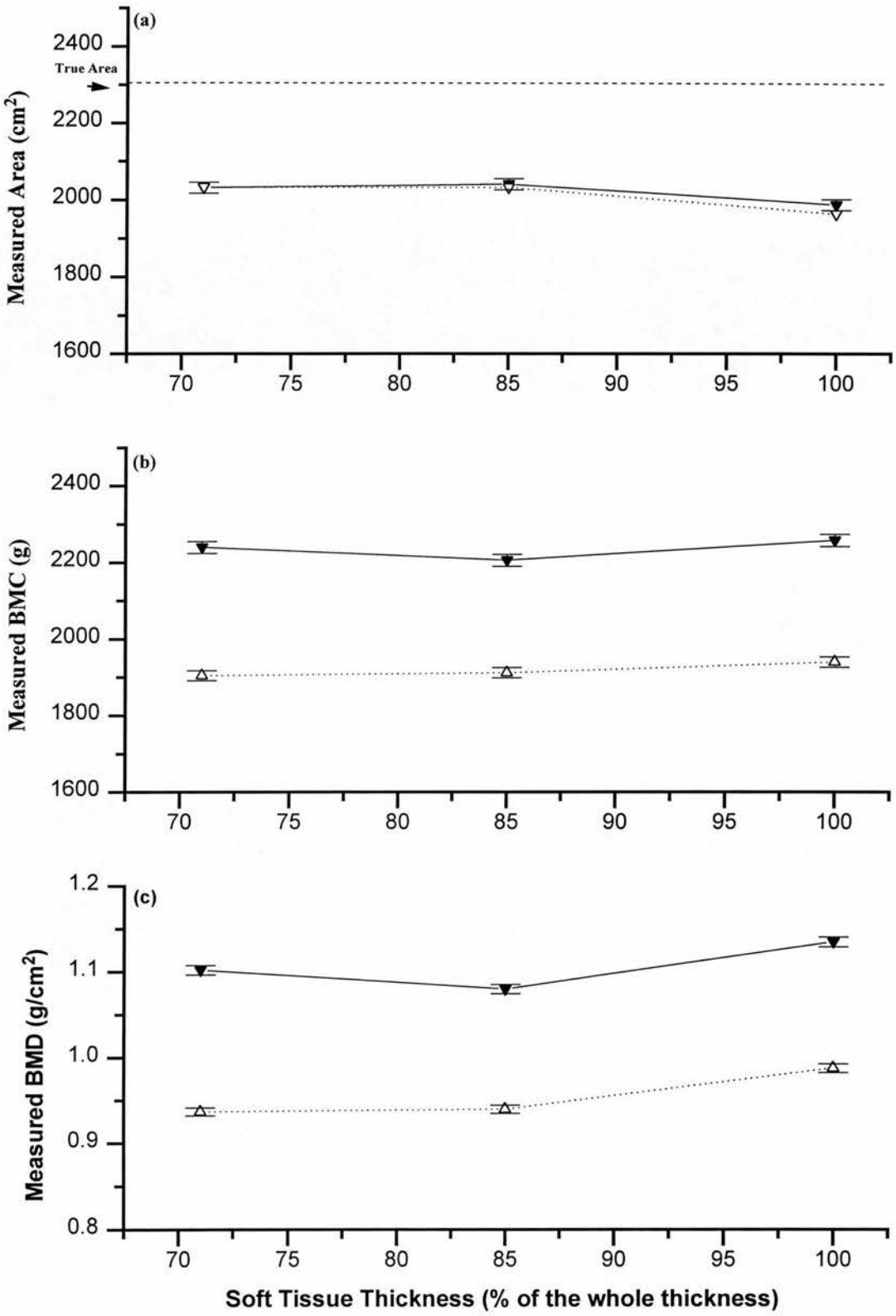

Figure 5.5 The in-vitro effect of soft tissue thickness variation on whole body bone mineral measurements. Solid and open symbols denote the normal and low bone density phantom, respectively. Error bars (using SDs of the data) are added.

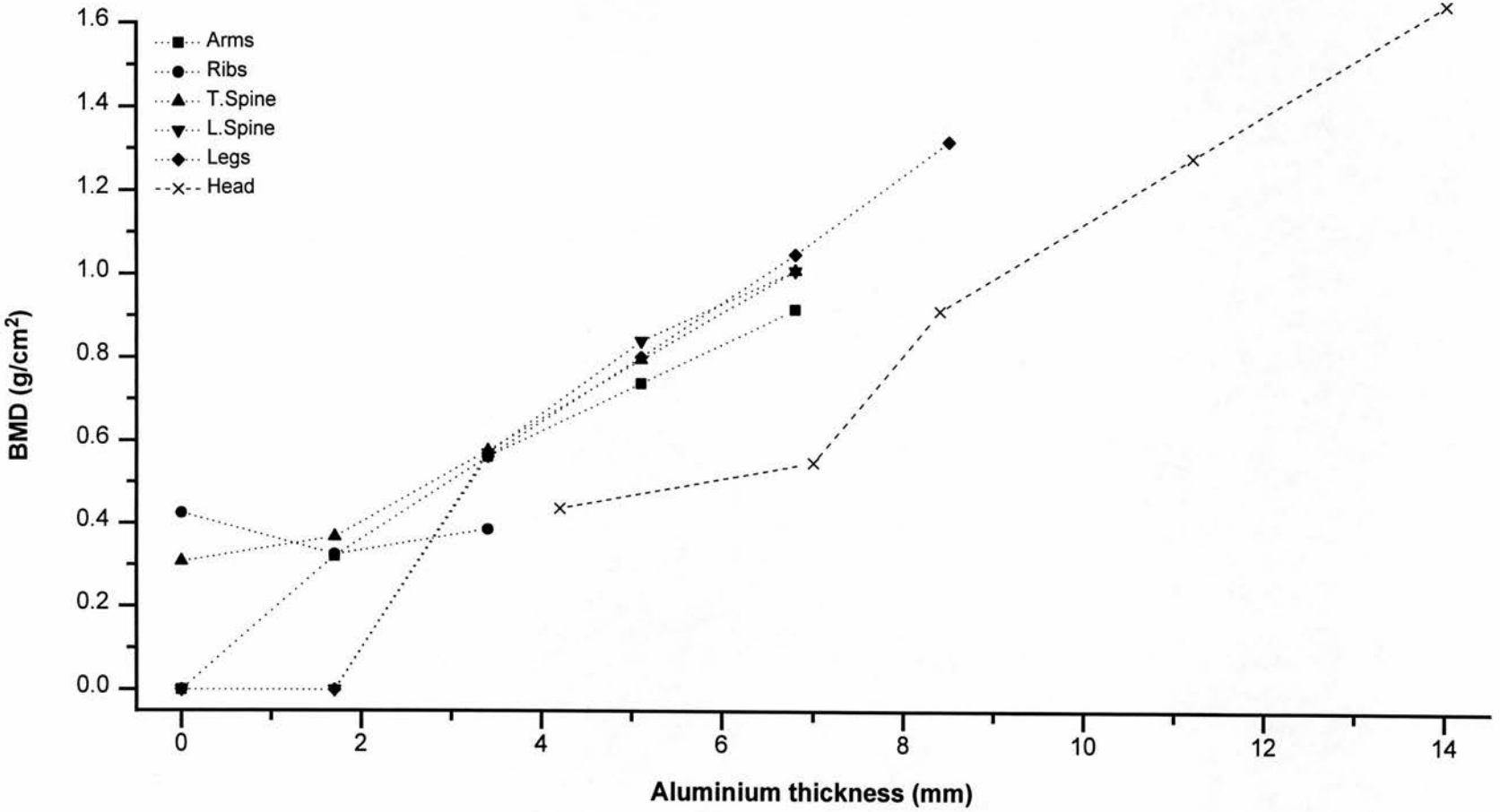

Figure 5.6 BMD as a function of aluminium thickness (using the phantom). BMD threshold and the difference in BMD (position dependency) for the same thicknesses of aluminium can be seen.

However, there was a significant under-estimation of the area (Figure 5.2), which was largely due to an under-estimation of the pelvis area (true value = 500 cm^2). The bone detection thresholds for those sites were higher and, therefore, they were not fully estimated.

5.3.3 The effect of the rotation of the legs

Figure 5.7 illustrates the effect of the rotation of the legs on total body area, TBBMC and TBBMD for 3 subjects. As can be seen, there were significant changes of up to approximately 4% in the measured TBBMC and TBBMD for two of the subjects.

5.3.4 Normalisation of total body bone mineral measurements

The DXA manufacturers supply normal data and express the subject's BMD in terms of a Z and T-score. However, TBBMD is a function of weight and stature (Table 5.3). Therefore, normalisation of total body bone mineral content by size was performed.

Table 5.3 Correlation (r) of TBBMD with weight and stature for the normal subjects (n = 39).

	Weight	Area	Height	SW	APt
r	*0.53	*0.54	0.20 NS	*0.42	*0.49

Area = total body bone area, SW = shoulder width and APt = anterior-posterior thickness.
NS = not significant *P < 0.01

Figure 5.8 shows plots of TBBMC and TBBMD as functions of age for the normal females with the following linear regression equations.

TBBMC = 2386 + 0.460 × Age, R = 0.01, P = 0.9, SD = 336 and N = 39

TBBMD = 1.138 - 0.00051 × Age, R = -0.06, P = 0.72, SD = 0.0765 and N = 39

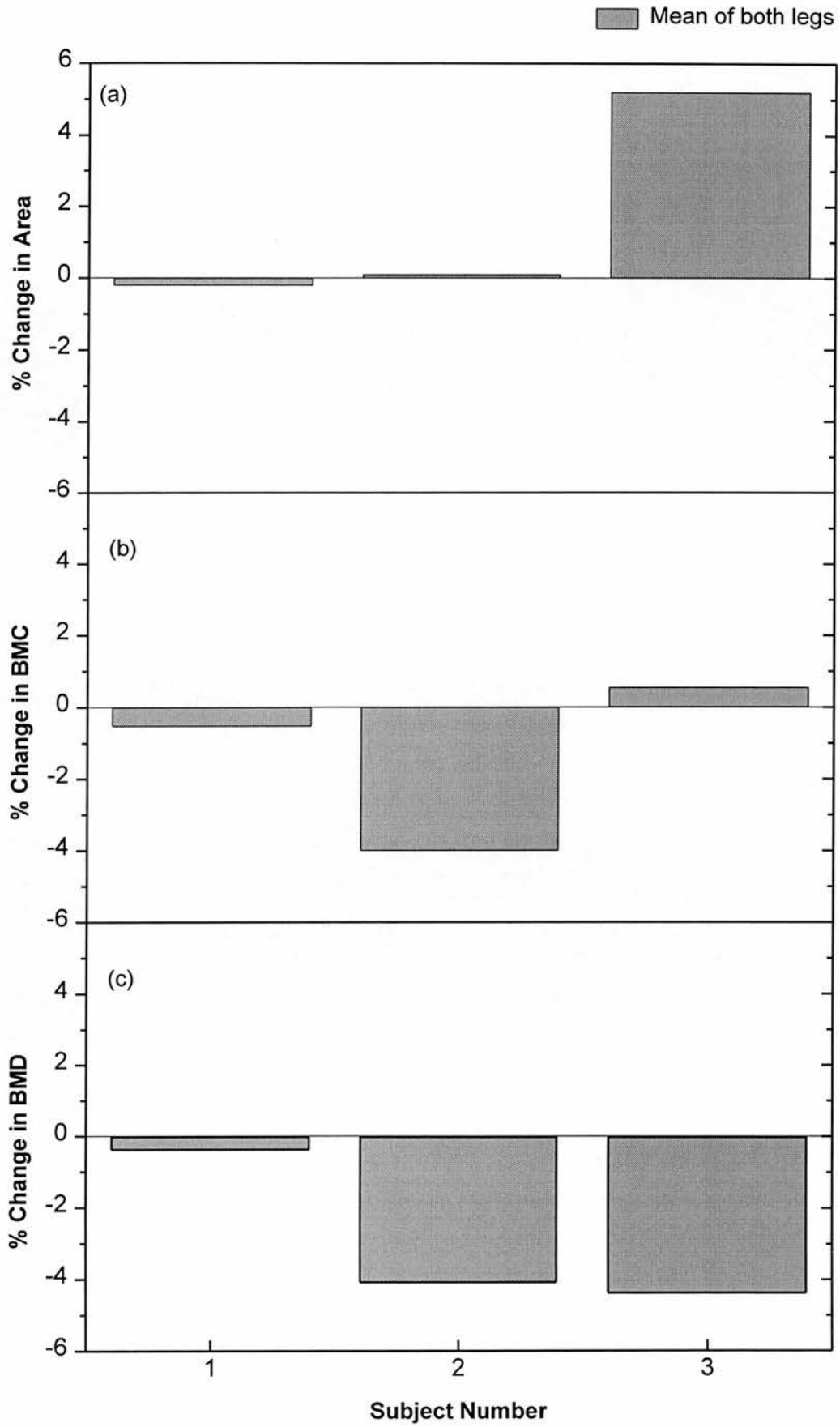

Figure 5.7 The effect of extreme rotation (26 ± 9 degrees) of the legs on the total body bone mineral measurements.

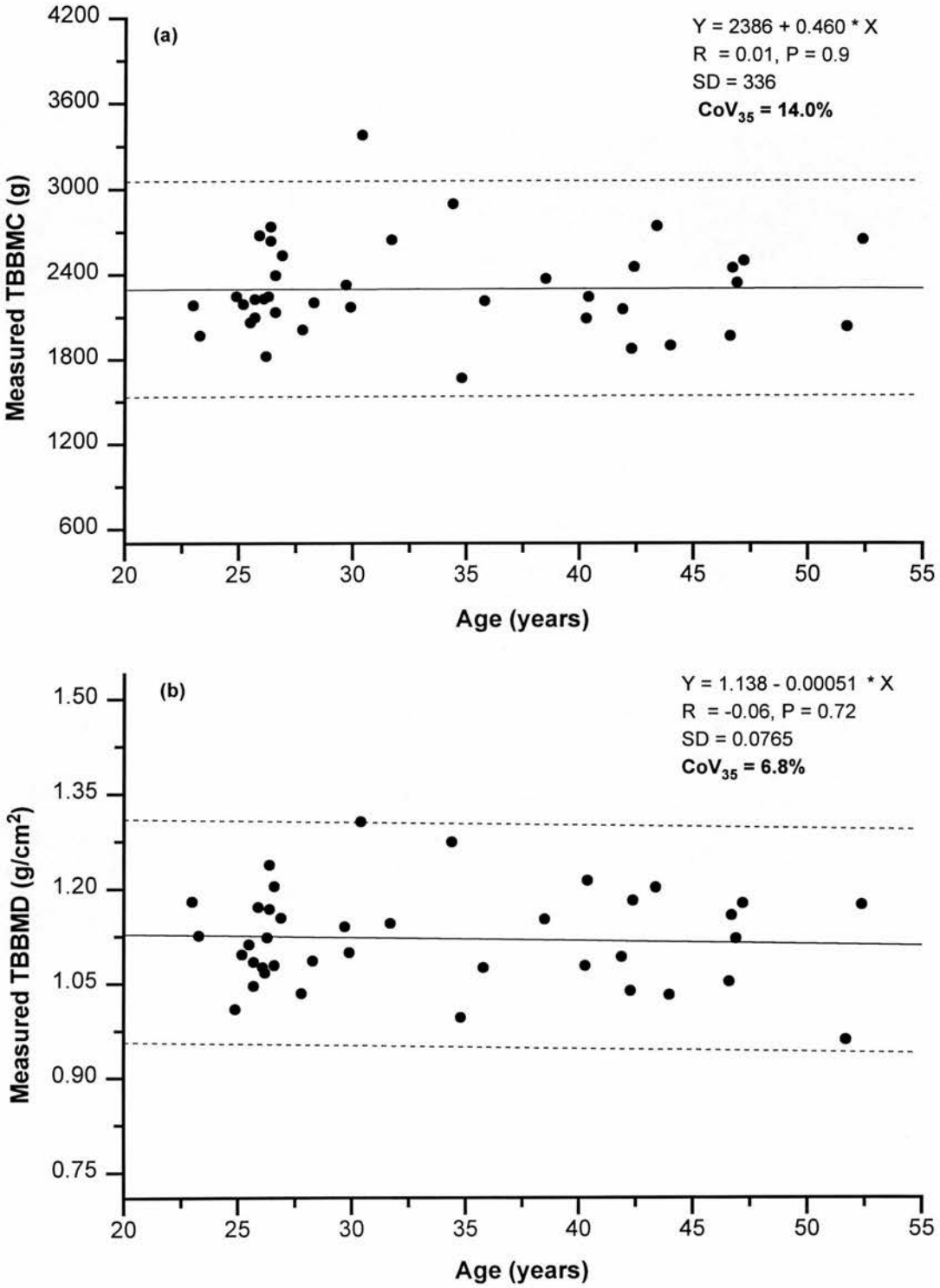

Figure 5.8 The variation of TBBMC (a) and TBBMD (b) with age in the normal subjects (n = 39). The least square fits and the 95% confidence intervals are shown.

Coefficients of variation (at 35 years age) of 14.0% and 6.8% for TBBMC and TBBMD were found, respectively. Table 5.4 shows the prediction equations for TBBMC based on various body habitus parameters. The variables are listed in the order in which they contribute to the prediction equation. In each case a significant reduction in the error of prediction was obtained by including body habitus parameters in the prediction equation. Indeed, the age was not selected as one of the important variables and hence it was not included in the stepwise regression analysis except in part III. Table 5.4 shows that TBBMC is best predicted from the weight and height of the subjects. However, for the prediction of TBBMC for weight changing subjects, weight was not used as a variable (II). Therefore, for eating disorder patients (anorexia nervosa, bulimia nervosa) height and shoulder width provided an alternative predictive equation. For the prediction of TBBMC for patients with established osteoporosis, height was not used as a variable because height might be altered due to spinal compression (or presence of one or more vertebral fractures) (III). For these patients an alternative prediction equation based on weight and age was derived.

Table 5.4 The prediction of TBBMC in women from body size. Variables are listed in the order in which they contribute to the predictive equation.

Variable	Predictive equation	SE	r
TBBMC			
I.			
W	0.9948 + 0.0196 W	214	0.82
W, H	-1.583 + 0.0162 W + 0.0172 H	185	0.87
II.			
S	-2.188 + 0.1207 S	262	0.71
S, H	-4.472 + 0.0929 S + 0.0203 H	230	0.79
III.			
W	0.9948 + 0.0196 W	214	0.82
W, A	1.200 + 0.0206 W - 0.0078 A	204	0.84

A = age (years), W = weight (kg), H = height (cm), S = shoulder width (cm), SE = standard error of prediction (g) and r = multiple correlation.

Figure 5.9a shows a plot of the total body index (TBI) defined as TBI = measured TBBMC/predicted TBBMC (from weight) as a function of age (Table 5.4I.). It was not appropriate to use the height as a variable for the prediction of TBBMC for patients suffering from severe osteoporosis. Therefore, TBI was not plotted as a function of age when TBBMC was predicted from the weight and height. A COV (at age 35 years) of 7.3% was calculated. Figure 5.9b illustrates a plot of TBI as a function of age when TBBMC was predicted from shoulder width and height, calculating a $CoV_{35} = 8.5\%$. Linear regression analysis confirmed that TBI (predicted from stature) was no longer correlated ($P \geq 0.2$) with the shoulder width or height.

Figure 5.10a shows the regression of TBI on age for the normal subjects, where the predicted TBBMC was derived from the height and shoulder width. The anorexic patients' values for comparison with the normal subjects are shown on the same graph. Figure 5.10b shows the normals and patients spine BMD as a function of age, for visual comparison. However, to find the significance of bone loss in the anorexic patients, the T-scores were calculated and un-paired t-test was performed.

The results of TBBM in the anorexic and normal females are tabulated in Table 5.5. The difference between the two groups for TBI was higher than TBBMD and as high as the spine BMD.

5.3.5 Precisions of TBBMC, TBBMD and TBI

The precisions of TBBMC/TBBMD and TBI are tabulated in Table 5.6. As can be seen, TBI measurements were as precise as TBBMC/TBBMD measurements.

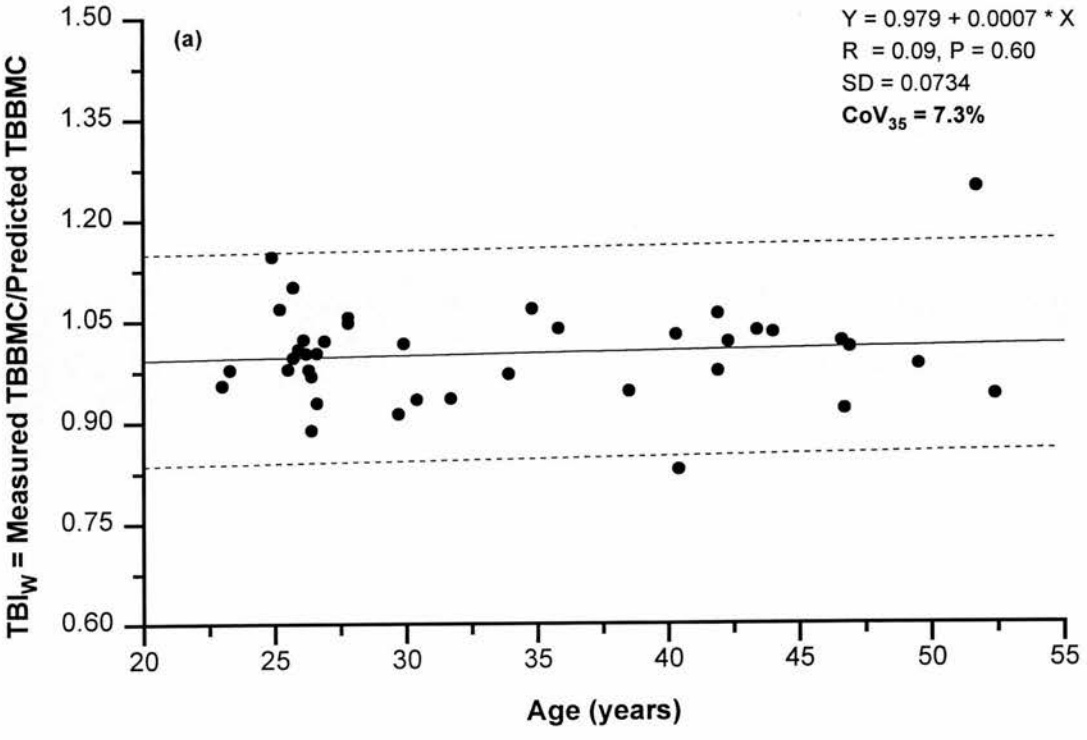

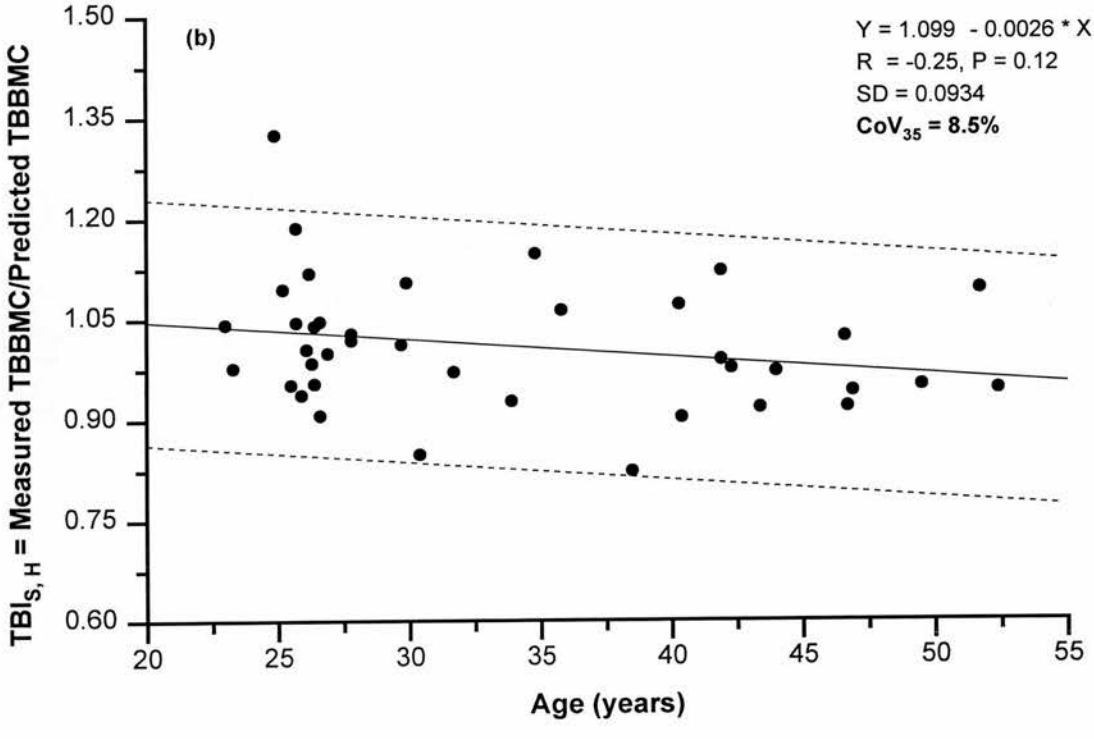

Figure 5.9 The variation of TBI with age in the normal subjects (n = 39). Weight was used as the only variable (a), shoulder width and height were used as variables (b) to calculate the predictive equations based on stature. The least square fits and the 95% confidence intervals are also shown.

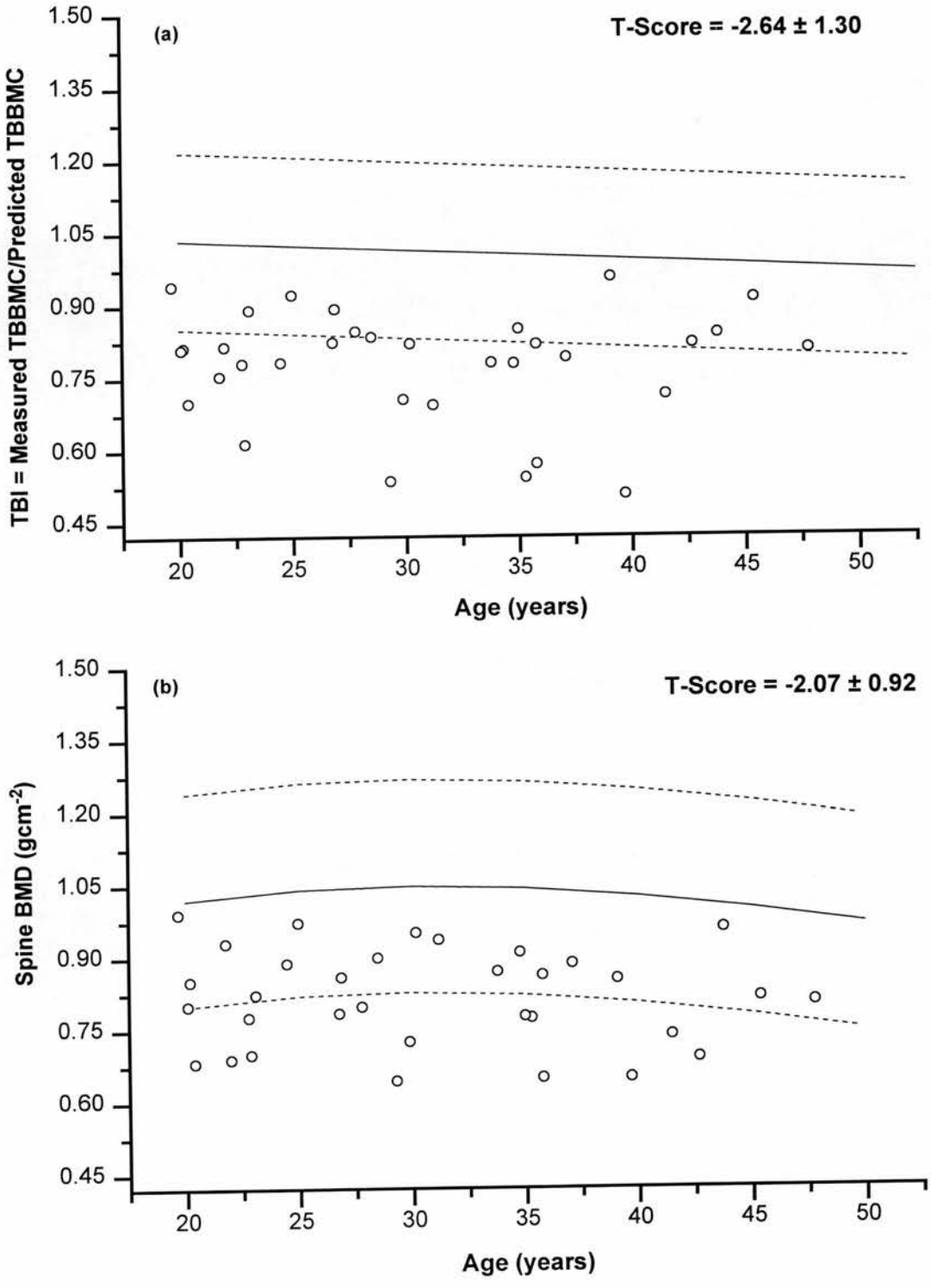

Figure 5.10 The variation of TBI (a) and spine BMD (b) with age for the anorexic patients (n = 34). TBBMC was predicted from the shoulder width and height. The least square fits and the 95% confidence intervals for the normals are also shown.

Table 5.5 Comparison of total body and spine bone mineral values in the two groups of anorexic patients and normal subjects.

	Patients (n = 34)	Normals (n = 39)	P-value	(Patients value) ÷ (Normals value)
TBBMD (gcm^{-2})	1.00 ± 0.080 (0.849 - 1.21)	1.13 ± 0.083 (0.961 - 1.32)	1.55×10^{-12}	88.5 %
TBI	0.773 ± 0.11 (0.517 - 1.00)	1.02 ± 0.092 (0.745 - 1.26)	1.36×10^{-20}	75.8%
BMD_{Spine} (gcm^{-2})	0.812 ± 0.094 (0.644 - 0.991)	1.08 ± 0.16 (0.823 - 1.55)	5.05×10^{-18}	75.2%

Results are expressed as mean ± SD. TBI = Total body index, measured TBBMC/predicted TBBMC (from shoulder width and height).

Table 5.6 The in-vivo precision of TBBMC, TBBMD and TBI (n =11).

	TBBMC	TBBMD	TBI
CV (%)	1.12	1.26	1.33

5.3.6 The in-vivo effect of soft tissue thickness variation

Table 5.7 shows the paired t-test results for the in-vivo effect of lard on the total and part body bone mineral measurements. The Table shows that distribution of lard on the volunteers' trunks and thighs has no significant effect on any body part/total body bone mineral measurements.

Table 5.7 Paired t-test results on the in-vivo effect of lard on part/total body bone mineral measurements (n = 6).

Site		Without lard Mean	With lard Mean	t-value	P-value
Head	Area, cm^2	235.3	235.4	0.08	0.94NS
	BMC, g	449.0	450.1	0.38	0.72NS
	BMD, gcm^{-2}	1.908	1.912	0.06	0.96NS
Arms	Area	431.5	432.4	0.17	0.87NS
	BMC	333.1	341.6	1.45	0.21NS
	BMD	0.7673	0.7900	2.01	0.10NS
Trunk	Area	660.8	707.2	2.59	0.05NS
	BMC	574.1	605.7	2.28	0.07NS
	BMD	0.8688	0.8565	-1.70	0.19NS
Legs	Area	745.3	749.7	0.48	0.65NS
	BMC	954.8	958.2	0.30	0.78NS
	BMD	1.285	1.281	-0.32	0.76NS
Total	Area	2073	2125	2.31	0.07NS
	BMC	2311	2356	1.79	0.13NS
	BMD	1.115	1.109	-2.60	0.05NS

S = significant NS = non-significant. 12 to 20 kg of fat (lard) equal to 22% - 25% of the subject's weight was placed over the trunk. 2/3 of the fat was distributed over the trunk and 1/3 over the thighs equally.

5.4 Discussion and conclusions

Measurement of bone mass at multiple sites in the skeleton allows a more general evaluation of skeletal integrity. Although many cross sectional studies have been published previously, most have measured selected local sites either in the peripheral skeleton or in the axial skeleton, or both. It is becoming increasingly clear that different skeletal regions, even those that have similar quantities of cancellous or cortical bone, may respond differently to age, estrogen deficiency, or other stimuli (Silverberg et al., 1989 and Riggs et al., 1990).

However, with the current DXA scanners, Tothill et al. (1997) found anomalies in the measurement of changes in whole body BMD using a Hologic QDR 1000W. They observed an apparent increase of BMD with decreased weight, while BMC decreased. This was certainly unexpected and was caused by an apparent decrease of area, although anatomical, physiological and radiological evidence suggest that the true projected area does not vary with changes of weight in adult women.

When the phantom was used in order to investigate the effect of soft tissue alterations, and 15% of the soft tissue thickness was removed, only the trunk bone area was increased significantly ($P = 0.02$) and, therefore, the total bone area ($P = 0.01$). BMC of no region and , therefore, the total did not change significantly, and because there was an increase in total body bone area, TBBMD reduced significantly ($P = 0.001$). For phantom measurements the areas increased with a decrease in soft tissue thickness, only for the first 15% thickness reduction in the hardboard. When different amounts of lard were distributed on the trunk and thighs, although significant variations in the measured trunk area and BMC were found, no significant change in BMD measurement was found. However, significant changes in the measured legs bone mineral values (of up to 4%, $P = 1 \times 10^{-6}$) were found. The other body sites, such as the head and arms, showed significant variations in one or more measured bone mineral parameters, when lard was distributed on the phantom.

Therefore, a significant reduction in TBBMD was found. When the same thickness of soft tissue (on the trunk) was replaced with lard, no change was observed in TBBMC. However, significant variations were found for area and TBBMD. The discrepancy between the direction of the hardboard and lard thickness variation and TBBMD variation might be due to differences of fat content between the lard and the hardboard.

The influence of fat on measurements of BMC by DPA (Hassager et al., 1989 and Hangartner et al., 1990) and DXA (Hanssen et al., 1990; Charles et al., 1990 and Hangartner et al., 1990) has been reported as a consistent over or under-estimation. In these reports this local effect was re-produced by covering bone with a suitable amount of alcohol or fat, implying that the over or under-estimation was caused by fat adjacent to bone influencing the measurements. Using a DXA scanner (Hologic 1000W), Jensen et al. (1994) reported only minor changes in TBBMC when volunteers were scanned with varying layers of lard. The TBBMC losses were much larger in their patient group (51 obese patients). The patients went on a low calorie diet and were re-scanned after 15 weeks. The authors concluded that the bone loss in the patients could not be explained as an error in the method. They found on average a 5.9% loss of TBBMC during the 15 week period. Malnutrition was not likely, as the patients were on a recommended healthy diet. However, in their study they did not mention the effect of lard on the area and TBBMD of the normal group, or changes in those measured bone parameters for the patient group.

In the present study when lard was placed on the control volunteer's trunk and thighs, in order to investigate the soft tissue influence, there were no significant variations in the measured bone mineral parameters of any site. Our study confirms the results of Jensen et al. (1994). The inconsistency between our in-vivo and in-vitro results might be due to the construction of the semi-anthropomorphic phantom. However, the in-vitro magnitudes of error was far less than the observed anomaly in the subjects whose weight changed, and we found no valid explanation for the observed

anomaly.

Another deficiency of the scanner was when bone densities of the various sites of the body were measured with the various thickness of the aluminum, different sites registered different bone densities for the same aluminum thickness. At higher skeletal densities, the relationship between BMD and aluminum thickness was linear for the various regions. However, at lower densities, BMDs of the various sites reduced quite sharply and non-linearly. The measured bone densities were position dependant. In addition the bone density thresholds were different for the various sites. When the phantom was re-scanned without the aluminium, surprisingly the thoracic spine and ribs registered some bone. When the legs rotated inwards, TBBMC/TBBMD was under-estimated by about 4%. Therefore, there is a crucial need for a consistent method of patient positioning in order to avoid the effects of leg rotation shown in Figure 5.7. When the soft tissue thickness was altered the in-vivo results showed no significant change in the measurement of any region. However, the in-vitro measurements on the other hand, showed significant change in the measurements of some regions/total with a change in soft tissue thickness and composition. Therefore, errors may be introduced in regional body measurements when the subjects undergo a weight change.

Using a DPA scanner (Lunar DP3) for total body bone mineral measurements, Lindsay et al. (1992) confirmed results of Gallagher et al. (1987), showing no reduction in TBBMC before the onset of the menopause (n = 74, 17-54 years). The present study did not find any significant bone loss before the menopause either.

In order to overcome the anomaly observed in the measurement of total body bone mineral, and also to reduce the biological variance in total body bone mineral content, predictive equations based on structure size were derived. The SE of the predictive equations were significantly reduced as a second variable was considered in the multiple stepwise regression analysis. As an example for the prediction of

TBBMC for subjects whose weight changed, the SE was significantly reduced from 262 g to 230 g, when a second variable, i.e. height was added to the only variable (shoulder width). A CoV of 7% for TBI similar to the CoV of TBBMD measurements was achieved. The difference between the anorexic patients and the normal subjects for TBI was as significant as the difference in the spine BMD between the two groups and more significant than the TBBMD. In addition, TBI measurements were assessed as precise as TBBMC and TBBMD measurements.

In summary, the following conclusions may be drawn:

1. In normal subjects TBBMD showed significant correlations ($P \leq 0.01$) with area, weight and stature (Table 5.3).

2. However, TBI derived from TBBMC when normalised for body habitus parameters no longer showed any significant correlation ($P \geq 0.2$) with body size.

3. TBI showed a higher difference between the anorexic and normal groups than TBBMD and as high as the spine BMD (Table 5.5).

4. Precisions of TBI and TBBMD measurements (Table 5.6) as well as their CoVs (Figures 5.8 and 5.9) were comparable.

Therefore, studies of changes should be based on TBI measurements. Further studies are recommended using the latest versions of DXA systems.

Chapter 6

Summary and Conclusions

6.1 Osteoporosis and the role of DXA for bone mineral measurement

Osteoporosis is so common in older women that for many years it was accepted as an inevitable result of aging. Many thought that its early detection was of little value, based upon the assumption that nothing could be done at that time. However, recently increasing effort is being made to improve early detection, because early changes in life style and therapeutic interventions may reduce the ultimate incidence of fractures. The incidence of osteoporosis has almost doubled in the past 30 years. In 1990, according to the WHO, 1.7 million osteoporotic hip fractures occurred in the west. Osteoporosis is estimated to cause around 200,000 fractures in Britain alone each year and it costs the national health service around £750 million per year to care for those people.

DXA could potentially offer many advantages for the assessment of the various sites of the skeleton. The equipment is widely available and the precision obtained for the conventional sites of measurement suggested that precise measurements for the other sites of the body could be achieved to allow progression and treatment of osteoporosis to be monitored. Although DXA is widely used to assess bone mineral of the spine and hip little use of the technique has been made to investigate other sites of the body. Therefore, in this thesis appropriate measurers were made to use DXA in the hand, os calcis and tibia. Total body DXA is generally available but anomalies have been reported. These anomalies were investigated and an alternative method of assessing total body bone mineral was developed.

6.2 Development of hand measurement

Rheumatoid arthritis (RA) is a progressive disease characterised by inflammation and

swelling of the joints and the hand may become progressively more deformed. It was therefore important to assess how changes in soft tissue and hand posture may affect the measured bone mineral. However, there were various problems associated with the measurement of hand bone mineral in RA patients which were thoroughly investigated.

The conventional protocols differ in terms of pixel size, scan speed, linearity correction factors and bone density threshold. Therefore, four DXA protocols as well as new software were evaluated to establish the optimum method of measuring hand bone mineral in RA patients. The linearity factors for the range of bone density and tissue thickness appropriate to the hand, which are used to correct the effects of beam hardening, were established for the Forearm and Spine acquisition protocols. The effects of using a build up plate were evaluated. The effects of bone density threshold, soft tissue thickness and hand posture on BMC and BMD were investigated using aluminum tubes embedded in perspex. The most appropriate threshold was established.

A hand phantom was constructed and used to assess the precision of the various methods as well as examining the suitability of threshold selection, by comparing the known hand phantom area with the values determined by different bone density thresholds. The hand phantom provides a convenient means of investigating various protocols and assessing long term precision. In-vitro precision of the methods and, therefore, their abilities to monitor changes with disease progression or treatment were also assessed. Each method was allocated a score for the linearity, effects of soft tissue, angles of deviation/inclination and height with respect to the scanner couch. Precision and the time required to acquire a hand image were the two important factors for the selection of the most appropriate method. The best score for the time factor was given to two methods: (a) A method based on the Spine acquisition protocol, (b) the recent software which was referred to as the Hologic Hand protocol. Both methods allowed measurements in fast mode. The fast mode took half the time required for a performance mode scan. The longer the scan time the more possibility of hand movement during the imaging which had a direct adverse effect on the precision. Therefore, the various

methods achieved similar scores.

In-vivo effects of bone density threshold were examined in order to minimise the variations in hand bone mineral with posture alterations. In-vivo precision and the effect of hand posture were assessed in a group of normal subjects. Prediction equations for hand BMD and BMC in normal subjects were used to derive indices of hand bone mineral which were then used to compare normal subjects and RA patients.

Excellent correlations between the measured parameters using the fast and performance Hand method were found. Paired t-test on BMD measurements by the different speed of fast and performance also revealed no significant difference between the two means. Bland and Altman (1986) statistical method also confirmed a good agreement between the performance and fast modes over the entire required BMD range. It is therefore possible to perform scans in fast mode.

For the assessment of hand bone mineral, BMD measurement is recommended. Since DXA measurements of other skeletal sites are expressed as an area density, it is more appropriate to apply the same approach to the hand, and to normalise hand BMC for the projected hand area ($r = 0.90$ $P < 0.0001$) giving an areal bone mineral density. This was because of the following reasons:

(a) No significant difference between the precision of BMC and BMD was observed.
(b) No BMD variation with respect to the distance from the reference point (distal ulna radius junction) was observed.
(c) Better separation between the RA and normals was observed.
(d) Use of BMC normalised by size, such as body height or weight, could also be affected by disease related progression.

The Hologic Hand and the optimum 'developed' method show no significant difference in terms of precision, linearity, soft tissue or posture dependency or separation of RA

and normal subjects. Since the Hologic Hand protocol is becoming widely available its use is therefore, recommended (Salamat, 1996). Both the RA males and females had significantly lower hand BMC and BMD ($P \leq 0.01$) than the normal people.

6.3 Assessment of os calcis

This study developed a technique for the measurement of os calcis (Salamat, 1998). In order to compensate for the low soft tissue and bone equivalent of the os calcis compared with the spine and forearm sites, appropriate linearisation values for the methods of spine and forearm were established. A build up plate was used to obtain the linearisation values for the spine method. The effect of soft tissue thickness was found to be negligible. An os calcis phantom was constructed and used to assess precision and the effect of size of region of interest (ROI) on the precision. In-vitro precise measurements (CV = 0.4%) were achieved independent of the size of ROI.

The os calcis is a non-homogeneous bone, i.e. it is a bone with non-uniform density, which may considerably affect the precision. It was therefore important to select region(s) of interest with less variation in BMD. Therefore, a measurement point with minimum variation in BMD with distance from the sole of the foot and the end of the heel was established. This region is in the centre and flat part of the os calcis. Two different ways of subject positioning were established for the patients' comfort. In-vivo precise BMC and BMD measurements ($CV \leq 1.1\%$) for two different regions of the site which were referred to as "total os calcis" and "trabecular os calcis" were established. To assess if the measurements of the different regions of the os calcis were reproducible and not operator-dependent, the scans were analysed by two different operators. The time required for an os calcis measurement was one-third of that for a spine/femur measurement.

The reference values for total femur/neck of femur BMD, provided with the QDR scanner, differed significantly from that observed in the National Health and Nutrition

Examination Survey (NHANES) (Looker et al., 1995) . Therefore, recent NHANES data supplied by the manufacturer were used to calculate the total femur/neck of femur T-score. The T-score for the two ROIs of the os calcis were also established. Patient's BMD was classified according to the WHO criteria. In the present study high correlations were found between the spine, neck of femur and the total femur with the trabecular and total os calcis. However, despite moderate correlation between ultrasound (US) parameters and femoral neck (Lees et al., 1993), US measurements at os calcis predict hip fracture as accurately as femoral neck BMD does (EPIDOS) (Hans et al., 1996). It has also been found in a large epidemiological study that os calcis BMD was better than BMD of spine for the prediction of hip fractures (Glüer et al., 1996). Therefore, it seems that the os calcis DXA measurement may have significant value for the prediction of fractures and monitoring of therapy.

Using the T-score values, the number of patients defined as osteoporotic varied from site to site. In addition, a combination of the total femur and spine diagnosed a higher number of patients at risk of fracture. Therefore, a combination of the os calcis, total femur and the spine measurements may identify a further number of osteopenic/osteoporotic patients. Therefore, assessment of os calcis may predict risk of fracture at other sites at an earlier stage. Moreover, ANOVA also confirmed that there was no significant difference between the osteopenic/osteoporotic patients' T-scores for the spine, os calcis and the femur.

In this chapter a number of previous published works using the various techniques were compared with the present study. Except for the US technique, the main drawbacks of the other techniques were either the long measurement time, poor reproducibility and the requirement of a waterbath when the SPA technique was used.

Due to the following facts, it can be concluded that although it might have seemed that os calcis measurement had limited value, this study suggests that a prospective study is required to assess the DXA value of the os calcis for the prediction of risk of fracture

at femur and spine:

(a) Short measurement time is required.
(b) Linear and precise results were achieved independent of soft tissue.
(c) A combination of the total os calcis, total femur and the spine measurements can identify a higher number of osteopenic/osteoporotic sufferers.

Fan beam systems that allow lateral measurements with a better image quality can significantly reduce the required imaging time and may further assure the patients' comfort.

6.4 Assessment of lower leg

The assessment of the various regions of the lower leg (tibia/fibula), which contain different proportions of trabecular and cortical bone was done by developing a method which was based on the Whole Body acquisition protocol. The linearity of the method was as good as the linearity of the Forearm and Spine methods. The effect of soft tissue on BMD measurements was minor (less than precision) and the change in BMD per centimetre soft tissue thickness variation was $\leq 0.41\%$. Using the Whole Body protocol for the measurement of the lower leg showed high correlations ($r > 0.995$, $p < 0.001$) for BMC and BMD measurements with the methods of Forearm and Spine.

The effects of the rotation of the legs on the measured bone mineral parameters of the various regions of the lower leg were assessed; the minimum change in BMD with the rotation of the legs was observed for the proximal lower leg. Precise BMD measurements (CV $\leq 1.4\%$) were achieved for the proximal and total lower leg.

In this study excellent correlation ($r = 0.92$, $p < 0.0001$) was found between the proximal lower leg T-score and the total femur T-score (Table 4.4). This correlation was as strong as the correlation between the femur neck/total femur and the proximal/distal lower leg

BMD T-score. The correlation of the proximal lower leg T-score with the spine or femur neck was very high and as close as the correlation between the spine and femur neck. The diaphysis lower leg, which is predominantly cortical bone, showed a moderate correlation with the spine, but a good correlation with the femur neck and a very good correlation with the total femur (Table 4.4). Correlation of the total lower legs with the spine and femoral neck was similar and agreeable with the report of Nordin et al. (1996).

The difference between the normals and osteopenic/osteoporotic patients was more significant at the spine. However, the bone loss at the proximal/distal lower leg was as significant as the bone loss at the femur neck/total femur. The least difference between the two groups was observed at the predominantly cortical section of the lower leg and the total body when normalised for age and weight.

The assessment of the proximal lower leg appears to be valuable due to the following factors:

(a) Measurements were precise, linear and soft tissue independent.
(b) High correlations were observed for BMD measurement of the site between the Whole Body/Forearm and Whole Body/Spine acquisition methods.
(c) A strong correlation was found between BMD T-score of the proximal leg and the spine, and in particular between BMD T-score of the proximal leg and the total femur.
(d) A similar difference in BMD T-score was observed between the normal and osteopenic/osteoporotic group for the proximal lower leg, neck of the femur and total femur.

6.5 Assessment of total body measurement

A method was developed by establishing an alternative index for total body bone measurement. The study was designed to overcome anomalies in the measurement of

changes in total body bone mineral during weight change. In subjects who underwent a weight change, a change in total body BMC was related to a change in weight, but a loss of weight was related to an increase in total body BMD. This observation was quite unexpected and, therefore, various experiments were performed in order to find an explanation.

In-vitro effects of changes in weight and soft tissue composition were investigated using a whole body phantom. When the soft tissue was reduced by 15% in thickness, the BMCs of the regions were unchanged and therefore the total did not change significantly; due to a significant increase in the measured area, TBBMD was reduced significantly ($P = 0.001$). Similar results were found when a low density phantom was used. When different amounts of lard were distributed on the trunk and thighs, no significant change in the trunk BMD measurement was found. However, significant changes in the measured bone mineral values of the legs (up to 4%, $P = 1 \times 10^{-6}$) were found resulting in a significant reduction in TBBMD. When the same thickness of the trunk soft tissue was replaced with lard, no change in TBBMC was observed. However, significant variations were found for TBBMD due to the variations in area. The discrepancy between the direction of the hardboard and lard thickness variation and TBBMD variation may be due to the difference in fat content of the lard and the hardboard.

In order to investigate the effects of changes in weight and soft tissue composition, lard was placed on the control volunteer's trunk and thighs, but no significant variations in the measured bone mineral parameters of any site were observed. Therefore, we found no valid explanation for the observed anomaly. The inconsistency between our in-vivo and in-vitro results may be due to the construction of the semi-anthropomorphic phantom.

Other deficiencies associated with the method were that: (a) When bone densities of the various sites of the body were measured with the various thickness of the aluminum,

different sites registered different bone densities for the same aluminum thickness. (b) At higher skeletal densities, the relationship between BMD and aluminum thickness was linear for the various regions; however, at lower densities, BMDs of the various sites reduced quite sharply and non-linearly. (c) The measured bone densities were position dependant; in addition the bone density thresholds were different for the various sites. (d) When the legs were rotated inwards, TBBMC or TBBMD was under-estimated by 4% (therefore, it is important to have a consistent method of patient positioning). Furthermore, when a change in weight and soft tissue composition was investigated, in-vitro measurements showed significant variations in the measurements of some regions/total with a variation in soft tissue thickness and composition. Therefore, errors may be introduced in regional body measurements when the subjects undergo a weight change.

Using a DPA system for total body bone mineral measurements Lindsay et al. (1992) confirmed results of Gallagher et al. (1987), showing no reduction in TBBMC before the onset of the menopause. The present study did not find any significant bone loss before the menopause either.

In order to overcome the anomaly observed in the measurement of total body bone mineral, and also to reduce the biological variance in total body bone mineral content, predictive equations based on structure size were derived. The SE of the predictive equations were significantly reduced as a second variable was considered in the multiple stepwise regression analysis. Two groups of anorexic and normal subjects were compared for the spine BMD, TBBMD and TBI. The difference between the anorexic patients and the normal subjects for TBI was as significant as the difference in the spine BMD and more significant than the TBBMD (Table 5.5). Moreover, TBI measurements were assessed as precise as TBBMC and TBBMD measurements (Table 5.6).

In summary, for total body bone mineral measurement the following conclusions may be drawn:

(a) In normal subjects TBBMD showed significant correlations with area, weight and stature.
(b) TBI derived from TBBMC normalised for body habitus parameters no longer showed any significant correlation with body size.
(c) TBI showed a higher difference between the anorexic and normal groups than TBBMD and as high as the spine BMD.
(d) Precisions of TBI and TBBMD measurements were comparable.

Therefore, due to the above reasons, studies of changes should be based on TBI measurements.

6.6 Future studies

The main advantages of fan beam systems are reduced scanning time and improved image resolution; precise hip and spine images can be acquired in about 1 minute. However, some fan beam systems also allow lateral imaging of the supine spine. These systems allow a faster and more convenient imaging than conventional pencil beam systems; therefore, studies of the hand, os calcis and tibia can more thoroughly be pursued. The values established for threshold and linearity corrections, and the conclusions relating to optimum protocols, should also apply to fan beam systems. Fan beam systems also can be assessed for the measurement of total body bone mineral.

References

Anderson J, Osborn S B, Tomlinson R W S, Newton D, Rundo J, Salmon L, Smiths J W 1964 Neutron activation analysis in man in-vivo. Lancet 2:1201 - 1205.

Bachrach L K, Guido D, Katzman D K, Litt I F, Marcus R 1990 Decreased bone density in adolescent girls with anorexia nervosa. Paediatrics 86:440 - 447.

Baumgartner R N, Stabuer P M, McHugh D, Keohler K M, Garry P J 1995 Cross-sectional age differences in body composition in persons 60+ years of age. J Gerontol 5OA:307 - 316.

Beshyah S A, Freemantle C, Thomas E, Rutherford O, Page B, Murphy M, Johnston D G 1995a Abnormal body composition and reduced bone mass in growth hormone deficient hypopituitary adults. Clin Endocrinol 42:179 - 189.

Beshyah S A, Freemantle C, Thomas E, Page B, Murphy M, Johnston D G 1995b Comparison of measurements of body composition by total body potassium, bioimpedance analysis, and dual energy x-ray absorptiometry in hypopituitary adults before and during growth hormone treatment. Am J Clin Nutr 61:1186 - 1194.

Bjarnason K, Nilas L, Hassager C, Christiansen C 1995 Dual energy x-ray absorptiometry of the spine-decubitus lateral versus anterorposterior projection in the osteoporotic women: comparison to single energy x-ray absorptiometry of the forearm. Bone 16:255 - 260.

Black D M, Cummings S R, Genant H K, Nevitt M C, Palermo L, Browner W 1992 Axial and appendicular bone density predict fracture in older woman. J Bone Miner Res 4:633 - 38.

Blake G M, Tong, C M, Fogelman A 1991 Intersite comparison of the Hologic QDR-1000 dual energy x-ray bone densitometer. Br J Radiol 64:440 - 446.

Bland J M, Altman D G 1986 Statistical methods for assessing agreement between two methods of clinical measurement. Lancet 1:307 - 311.

Butz S, Wüster C, Scheidt-Nave C, Götz M, Ziegler R 1994 Forearm BMD as measured by peripheral quantitative computed tomography (pQCT) in a German reference population. Osteoporosis Int 4:179 - 184.

Bywaters E G L 1960 The early radiological signs of rheumatoid arthritis. Bull Rheum Dis 11:231 - 234.

Cameron J R, Sorensen J 1963 Measurement of bone mineral in-vivo: an improved method. Science 142:230 - 236.

Cameron J R, Mazess R B, Sorenson J A 1968 Precision and accuracy of bone mineral determination by direct photon absorptiometry. Invest Radiol 3:141 - 150.

Cann C E, Genant H K 1980 Precise measurement of vertebral mineral content using computed tomography. J Comput Assist Tomogr 4:493 - 500.

Casez J P, Fischer E, Stüssi H, Stalder A, Gerber A, Delmas P D, Colombo J P, Jaeger P 1995 Bone mass at lumbar spine and tibia in young males impact of physical fitness, exercise, and anthropometric parameters: a prospective study in cohort military recruits. Bone 17(3):211 - 219.

Catto G R D, McIntosh J A R, MacLeod M 1973 Partial body neutron activation analysis in-vivo: a new approach to the investigation of metabolic bone disease. Phys Med Biol 18:508 - 517.

Chamberlain M J, Fremlin J H, Peters D K and Philip H 1968 Total body calcium by whole body neutron activation: new technique for study of bone disease Br Med J 2:581 - 585.

Charles P H, Richard W K, Mitchell B S, Sartoris D J 1990 Accuracy of dual energy radiographic absorptiometry of the lumbar spine: cadaver study. Radiology 176:171 - 173.

Checovich M M, Kiratli B J, Smith E L 1989 Dual photon absorptiometry of the proximal tibia. Calcif Tissue Int 45:281 - 284.

Christiansen C 1982 Bone mineral measurements with special reference to precision accuracy normal values and clinical relevance. Non-invasive Bone Measurements: Methodological Problems. In: Dequeker J V and Jonston C C editors (Oxford: IRL Press):95 - 104.

Cohn S H, Shukla K K, Dombrowski C S, Fairchild R G 1972 Design and calibration of a 'broad beam' ^{238}Pu, Be neutron source for total body neutron activation analysis J Nucl Med 13(7):487 - 492.

Compston J E, Cooper C, Kanis J A 1995 Bone densitometry in clinical practice. Br Med J 310:1507 - 1510.

Consensus Development Conference 1993 Diagnosis, prophylaxis, and treatment of osteoporosis. Am J of Med 94:646 - 650.

Cooney L M, Marottoli P A 1993 Functional decline following hip fracture. In Osteoporosis. Proceedings of IV International Symposium on Osteoporosis and Consensus Development Conference. Hong Kong. In: Christiansen C and Riis B Rodovre editors. Denmark:480 - 481.

Cooper C, Atkinson E J, Jacobsen S J et al 1993 Survival following vertebral fractures: a population-based study. Am J Epidemiol 86:247 - 253.

Cummings S R, Kelsey J L, Nevitt M C et al 1985 Epidemiology of osteoporosis and osteoporotic fractures. Epidemiol Rev 7:178 - 208.

Cummings S R, Black D M, Nevit M C, Browner W, Cauley J, Ensurd K, Genant H K, Palermo L, Scott J, Vogt T M 1992 Bone density at various sites for prediction of hip fracture. Lancet 341:72 - 75.

Deodhar A A, Akhtar N, Woolf A D 1992 Hand assessment in rheumatoid Arthritis (RA) by bone densitometry. Arthritis and Rheumatism 35(9):S195.

Deodhar A A, Brabyn J, Jones P W, Davis M J, Woolf A D 1994 Measurement of hand bone mineral content by dual energy x-ray absorptiometry: development of the method and its application in normal volunteers and in patients with rheumatoid arthritis. Annals of Rheumatic Diseases 53:685 - 690.

Durand E P, Rüegsegger P 1991 Cancellous bone structure: analysis of high resolution CT images with the run-length method. J Comp Assist Tomogr 15:133 - 139.

Evans W D 1988 Broadband ultrasonic attenuation of the os calcis. Current research in osteoporosis and bone mineral measurement. In: Ring E F J, Elvins D M, Bhalla A K, editors. The Institute of Physical Sciences in Medicine:127.

Fromm G A, Vega E, Plantaleach L E et al 1991 Differential action of pamidronate on trabecular and cortical bone in women with involutional osteoporosis. Osteoporosis Int 1:129 - 133.

Funke M, Kopka L, Fey T, Grabbe E 1993 Broadband ultrasound attenuation (BUA) in the diagnosis of osteoporosis. Radiologe 33(8):462 - 465.

Gallagher J C, Godgar D, Moy A 1987 Total body calcium in normal women: effect of age and menopause status. J Bone Miner Res 2(6):491 - 496.

Gallagher J C, Kable W T, Goldgar D 1991 Effect of progestin therapy on cortical bone and trabecular bone: comparison with estrogen. Am J Med 90:171 - 178.

Gasperino J A, Wang J, Pierson R N, Heymsfield S B 1995 Age-related changes in musculoskeletal mass between black and white women. Metabolism 44:30 - 34.

Genant H K, Boyd D P 1977 Quantitative bone mineral analysis using dual energy computed tomography. Invest Radiology 12(6):545 - 551.

Genant H K, Steiger P, Block J E, Glüer C C, et al 1987 Quantitative computed tomography. Calcif Tissue Int 41:179 - 186.

Genant H K, Ettinger B, Harris S T, Block J E, Steiger P 1988 Quantitative Computed Tomography in the assessment of osteoporosis: etiology diagnosis and measurement. In: Riggs B L and Melton L J Editors. Raven Press New York: 221 - 249.

Genant H K, Engelke K, Fuerst T, Glüer C C, Grampp S, Harris S T, Jergas M, Lang T, Lu Y, Majumdar S, Mathur A and Takada M 1996 Noninvasive assessment of bone mineral and structure state of art. J Bone Miner Res 11:707 - 730.

Glüer C C, Vahlensieck M, Faulkner K G, Engelke K, Black D, Genant H K 1992 Site-matched calcaneal measurements of broadband ultrasound attenuation and single x-ray absorptiometry: do they measure different skeletal properties? J Bone Miner Res 7:1071 - 1079.

Glüer C C, Cummings S R, Bauer D C, Stone K, Pressman A, Mathur A, Gennant H K 1996 Osteoporosis: association of recent fractures with quantitative US findings. Radiology 199:725 - 732.

Gutin B, Litaker M, Islam S, Manos T, Smith C, Treiber F 1996 Body-composition measurement in 9 - 11 -y-old children by dual energy x-ray absorptiometry, skinfold-thickness measurements, and bioimpedance analysis. Am J Clin Nutr 63:287 - 292.

Hangartner T N, Johnston C C 1990 Influence of fat on bone measurements with dual energy absorptiometry. Bone Miner 9:71 - 81.

Hannan W J, Cowen S J, Freeman C P, Wrate R M, Barton J 1993 Evaluation of dual energy x-ray absorptiometry for the assessment of body composition in anorexic females. Basic Life Sciences 60:169 - 172.

Hannan W J, Cowen S J, Wrate R M and Barton J 1995 Improved prediction of bone mineral content and density. Archives of disease in childhood 72:147 - 149.

Hans D, Dargent-Molina P, Schott A M, Sebert J L, Cormier C, Kotzki P O, Delmas P D, Pouilles J M, Breart G, Meunier P J 1996 Ultrasonographic heel measurements to predict hip fractures in elderly women: the EPIDOS prospective study. Lancet 348:511 - 514.

Hanssen M A, Hassager C, Overgaard K, Marslew U, Riis B J, Christiansen C 1990 Dual energy x-ray absorptiometry: a precise method of measuring bone mineral density in the lumbar spine. J Nucl Med 31(7):1156 - 1162.

Hansen T B, Vahl N, Jorgensen J O L, Christiansen J S, Hagen C 1995 Whole body and regional soft tissue changes in growth hormone deficient adults after one year of growth hormone treatment: a double-blind, randomized, placebo-controlled study. Clin Endocrinol 43:689 - 696.

Hassager C, Christiansen C 1989 Influence of soft tissue body composition on bone mass and metabolism. Bone 10:415 - 419.

Heaney R P, Avioli L V, Chesnut C H 1989 Osteoporotic bone fragility-detection by ultrasound transmission velocity. JAMA 261:2986 - 2990.

Henderson B E, Ross R K, Lobo R K, Pike M C, Mack T M 1986 Re-evaluating the role of progestogen therapy after the menopause. The American Fertility Society. Fertil Steril 49(suppl):9 - 15.

Herd R J M, Ramalingham T, Ryan P J, Fogelman I, Blake G M 1992 Measurement of broadband ultrasound attenuation in the calcaneus in premenopausal and postmenopausal women. Osteoporosis Int 2: 247-251.

Herd R J M, Blake G M, Parker J C, Ryan P J 1993 Total body studies in normal British women using dual energy x-ray absorptiometry. Br J Radiol 66:303 - 308.

Hodsman A B, Drost D J 1989 The response of vertebral bone mineral density during the treatment of osteoporosis with sodium fluoride. J Clin Endocrinol Metab 69:932 - 938.

Hologic DXA systems 1987 Waltham, Massachusetts, USA.

Hosie C J, Smith D A, Deacon A D, Langton C M 1987 Comparison of broadband ultrasonic attenuation of the os calcis and quantitative computed tomography of the distal radius. Clin Phys Physiol Meas 8(4) 303 - 308.

Jensen L B, Quaade F, Søremsen O H 1994 Bone loss accompanying voluntary weight loss in obese humans. J Bone Miner Res 9(4):459 - 463.

Jonson R 1992 Determination of bone mineral content in the heel bone using a gamma camera. Nuclear Medicine Communications 3:256 - 260.

Kalender W A, Klotz E, Süss C 1987 Vertebral bone mineral analysis: an integrated approach. Radiology 164:419 - 423.

Kalender W A 1992 Effective dose values in bone mineral measurements by photon absorptiometry and computed tomography. Osteoporosis Int 2:82 - 87.

Kanis JA, Meltonn, LJ, Christiansen C Johnston CC, Khaltaev N 1994 The diagnosis of osteoporosis. J Bone Miner Res 9:1137 - 41.

Kelly T, Slovick D, Schoenfield D, Neer R 1988 Quantitative digital radiography versus dual photon absorptiometry of the lumbar spine. J Clin Endocr Metab 67:839 - 844.

Korczyk P, Hoszowski K, Jaworski M, Tatajka A, Lorence R S 1993 Clinical precision and accuracy of ultrasound measurement of the calcaneus in diagnosis of osteopenia. Presented at Fourth International Symposium on Osteoporosis Hong Kong:59.

Kotzki P O, Buyck D, Leroux J L, Thomas E, Rossi M, Blotman F 1993 Measurement of the bone mineral density of the os calcis as an indication of vertebral fracture in women with lumbar osteoarthritis. Br J Radiol 66:55 - 60.

Krolner B, Pors Nielsen S, Lund B J, Sorenson O H, Uhrenholdt A 1980 Measurement of bone mineral content (BMC) of lumbar spine. II. Correlation between forearm BMC and lumbar spine BMC. Scan J Clin Lab Invest 40:665 - 670.

Langton C M, Palmer S B, Porter R W 1984 The measurement of broadband ultrasounic attenuation in the cancellous bone. Eng Med 13:89-91.

Laval-Jeantet A M, Bergot C, Carroll R, Garcia, Shaefer F 1983 Cortical bone senescence and mineral bone density of the humerus. Calcif Tissue Int 35:268 - 272.

Lees B, Stvenson J C 1993 Preliminary evaluation of new ultrasound bone densitometry. Calcif Tissue Int 53(3):149 - 152.

Leichter I, Margulies J Y, Weinreb A, et al 1982 The relationship between bone density, mineral content and mechanical strength in the femoral neck. Clin Orthop 163:272 - 281.

Lindsay R, Cosman F, Herrington B S, Himmerlstien S 1992 Bone mass and body composition in normal women. J Bone Miner Res 17(1):55 - 63.

Looker A C, Wahner W H, Dunn W L, Calvo M S, Harris T B, Heyes S P, Johnston C C, Lindsay S L 1995 Proximal femur bone mineral levels of US adults. Osteoporosis Int. 5:389 - 409.

Lunar DXA systems 1988 Madison, Wisconsin, USA.

Lunar News June 1994 Ultrasound densitometry: a new consensus:10 - 11.

Lunar News April 1996 Ultrasound: good sensitivity and precision for stiffness:19 - 20.

Lunar News July 1996 QDR reference values: potential for misdiagnosis:14.

Lunar News December 1996 QDR femur BMD: misdiagnosis can be corrected:13 - 15.

Matsumoto C, Kushida K, Yamazaki K, Imose K, Inoue T 1994 Metacarpal bone mass in normal and osteoporotic Japanese women using computed x-ray densitometry. Calcif Tissue Int 54:324 - 329.

Mazess R B, Barden H S 1987 Single and dual photon absorptiometry for bone measurement in osteoporosis. Genant H K editor. Radiology Research and Education Foundation, San Francisco California. USA: 73 - 80.

Mazess R B 1990 Fracture Risk: a role for compact bone. Calcif Tissue Int 47:191 - 193.

Maziere B, Kuntz D, Comar D, Ryckewaert A 1979 In-vivo analysis of bone calcium by local neutron activation of the hand: results in normal and osteoporotic subjects. J Nucl Med 20:85 - 91.

Melton L J III, Atkinson E J, O'Fallen W M, Wahner H W, Riggs B L 1993 Long-term fracture prediction by bone mineral assessed at different skeletal sites. J Bone Miner Res 8:1227 - 33.

Miller C G, Herd R J M, Ramalingam T, Fogelman I, Blake G M 1993 Ultrasonic velocity measurements through the calcaneus: which velocity should be measured? Osteoporosis Int 3:31 - 35.

Miller P D, Neal P J, Mcintyre D O et al 1991 Effect of cyclical therapy with phosphorus and etidronate on axial bone mineral density in postmenopausal osteoporotic women. Osteoporosis Int 1:171 - 176.

Minister of Health 1987 Personal communication to the National Osteoporosis Society. PO Box 10, Radstock, Bath BA3 3YB UK.

Morgan D B, Spires F W, Pulvertaft C N, Fourman P 1967 The amount of bone in the metacarpal and phalanx according to age and sex. Clin Radiol 18:101 - 108.

Mottet J J, Horber F F, Casez J P, Descoeudres C, Jaeger P 1996 Evidence for preservation of cortical bone mineral density in patients on continuous ambulatory peritoneal dialysis. J Bone Miner Res 11(1):96 - 104.

NOS 1994a Osteoporosis in men: a guide to its causes, prevention and treatment. PO Box 10, Radstock, Bath BA3 3YB UK.

NOS 1994b Priorities for prevention: osteoporosis a decision-making document for diagnosis and prevention. PO Box 10, Radstock, Bath BA3 3YB UK.

NOS 1995a Exercise and physiotherapy in the prevention and treatment of osteoporosis. PO Box 10, Radstock, Bath BA3 3YB UK.

NOS 1995b Osteoporosis: a guide to its causes, treatment and prevention. PO Box 10, Radstock, Bath BA3 3YB UK.

Nicoll J J, Smith M A, Reid D, Law E, Brown N, Tothill P, Nuki G 1987a Measurement of hand bone mineral content using photon absorptiometry. Phys Med Biol 32:697 - 706.

Nicoll J J, Tothill P, Smith M A, Reid D, Kennedy N S J, Nuki G 1987b In-vivo precision of total body calcium and sodium measurements by neutron activation analysis. Phys Med Biol 32:243 - 6.

Nordin B E C, Chatterton B E, Schultz C G, Need A G, Horowitz M 1996 Regional bone mineral density interrelationships in normal and osteoporotic postmenopausal women. J Bone Miner Res 11(6):849 - 856.

Norland DXA systems 1988. Norland of Fort Atkinson, Wisconsin, USA.

North J, Situnayake R D, Tikly M, Cremona, A, Nicoll J, Kumaratne, Nuki G 1994 Interleukin 1 beta, hand and foot bone mineral content and the development of joint erosions in rheumatoid arthritis. Annals of the Rheumatic Diseases 53:543 - 546.

Ogle G D, Alien J R, Humphries I R J, Lu P W, Briody J N, Morley K, Howman-Giles R, Cowell C T 1995 Body-composition assessment by dual-energy x-ray absorptiometry in subjects aged 4 - 26 y. Am J Clin Nutr 1995:746 - 753.

Origin™ Scientific and technical graphics in windows 1994. 1 Roundhouse Plaza, Northampton, MA 01060 USA.

Ouyang X, Lang P, Selby K, Zucconi F, Gindele A, Klifa C, Engelke K, Majumdar S, Genant H K 1995 Analysis of high resolution MRI images of calcaneus: gray-level thresholding and trabecular qualification. Society of Magnetic Resonance. Third Scientific Meeting, Nice, France.

Peel N F A, Spittlehouse A J, Bax D E, Eastell R 1994 Bone mineral density of hand in rheumatoid arthritis. Arthritis and Rheumatism 37(5):983 - 991.

Pouilles J M, Tremollieres F, Causse E, Louvet J P, Ribot C 1991 Fluoride therapy in postmenopausal osteopenic skinfolds and hydrostatic weighing. Med Sci Sports Exerc (25):528 - 535.

Pye D W, Law A 1990 The measurement of total hand bone mineral by QDR. Current research in osteoporosis and bone mineral measurement. In: Ring E F J, editor. London The British Institute of Radiology: 20 - 21.

Pye D W, Blaze M, Wright C E, Vincent R M, Jones P R M, Lyons A 1994 Dual x-ray absorptiometry of the calcaneus using a Lunar DPX-L bone densitometer. In: Ring E F J, Elvins D M, Bhalla A K, editors. Current research in osteoporosis and bone mineral measurement. London. The British Institute of Radiology:73.

Reid D M, Kennedy N S J, Nicol J, Smith M A Tothill P, Nuki G 1986 Total and peripheral bone mass in patients with psoriatic arthritis and rheumatoid arthritis. Clin Rheumatol 5:372 - 378.

Reid D M, Nicol J J, Brown N, Tothill P, Nuki G 1988 Measurement of hand bone mass by single photon absorptiometry in rheumatoid arthritis and asthma: comparison with metacarpal indices. In: Ring E F J, Evans W D, Dixon A S editors. Current research in osteoporosis and bone mineral measurement. The Institute of Physical Sciences in Medicine:224.

Rice S, Blimkie C J, Webber C E, Levy D, Martin J, Parker D, Gordon G L 1993 Correlates and determinants of bone mineral content and density in healthy adolescent girls. Can J Physiol Pharmacol 71:923 - 930.

Riggs B L, Melton L J III 1983 Evidence of two distinct syndromes of involutional osteoporosis. Am J of Med 75:899 - 901.

Riggs B L, Hodgson S F, O'Fallon W M, Chao E Y, Wahner HW, Muhs J M 1990 Effect of fluoride treatment on the fracture rate in postmenopausal women with osteoporosis. N Engl J Med 322:802 - 809.

Rockoff S D, Sweet E, Bleustein J 1969 The relative contribution of trabecular and cortical bone to the strength of human lumbar vertebrae. Calcif Tissue Res 3:163 - 75.

Rüegsegger P, Dambacher M A, Ruegsegger E, Fisher J A, Anliker M 1984 Bone loss in premenopausal and postmenopausal women. J Bone Jt Surg 66-A:1015 - 1023.

Rüegsegger P, Durand E, Dambacher M A 1991 Localization of regional forearm bone loss from high resolution computed tomographic images. Osteoporosis Int 1:76 - 80.

Ruff C B, Hayes W C 1988 Sex differences in age related remodelling of the femur and tibia. J Orthop Res 6:886 - 96.

Ryan P J, Blake G M, Fogelman I 1992 Measurement of forearm BMD by dual energy x-ray absorptiometry. Br J Radiol 65:127 - 131.

Salamat M R 1996 Evaluation of various DXA protocols for hand bone mineral. In: Ring E F J, Elvins D M, Bhalla A K, editors. Current research in osteoporosis and bone mineral measurement. London. The British Institute of Radiology:64.

Salamat M R 1998 Assessment of bone mineral of the os calcis by DXA. In: Ring E F J, Elvins D M, Bhalla A K, editors. Current research in osteoporosis and bone mineral measurement. London. The British Institute of Radiology:31.

Salmone L M, Krall E A, Harris S, Dawson Hughes B 1994 Comparison of broadband ultrasound attenuation to single x-ray absorptiometry measurements at the calcaneus in postmenopausal women. Calcif Tissue Int 54:87 - 90.

Scothern S, Tikly M, Cremona A, Hannan J, Tothill P, Nuki G 1993 Studies of hand bone mineral in patients with rheumatoid arthritis: the influence of hand dominance and hand function. Presented at Fourth International Symposium on Osteoporosis, Hong Kong:178.

Sievänen H, Oja P, Uori I 1992 Precision of dual energy x-ray absorptiometry in determining bone mineral density and content of various skeletal sites. J Nucl Med 33:1137 - 1142.

Silverberg S J, Shane E, De La Cruz L 1989 Skeletal disease in primary hyperparathyrodism. J Bone Miner Res 4(3):283 - 291.

Slosman D O, Rizzoli R, Donath A, Bonjour J 1990 Vertebral bone mineral density measured laterally by dual energy x-ray absorptiometry. Osteoporosis Int 1:23 - 29.

Smith M A, Tothill P 1979 Development of apparatus to measure calcium changes in the forearm and spine by neutron activation analysis using californium-252. Phys Med Biol 24:319 - 29.

Sopha 1988 Sopha medical systems, 105 Avenue Morane Saulnier, 78530 BUC, France.

Sogaard C H, Hermann A P, Hasling C, Mosekilde L 1994 Spine deformity index in osteoporotic women: Relations to forearm and vertebral bone mineral measurements and to iliac crest ash density. Osteoporosis Int 4:211 - 19.

SoundScan 2000 1994, Myriad Ultrasound System, Ltd., Israel.

Spardo J A, Werner FW, Brenner R A 1992 The contribution of cortical bone to osteopenic distal radius strength. 38th Annual Meeting, Orthopaedic Research Society, Washington D C:31.

Stein J A, Lazewatsky J L, Hochberg A M 1987 Dual energy x-ray bone densitometer incorporating an internal reference system. Radiology 165:313.

Stewart A, Reid D M, Porter R W 1994 Broadband ultrasound attenuation and dual energy x-ray absorptiometry in patients with hip fracture: which technique discriminates fracture risk. Calcif Tissue Int 54:466 - 469.

Suleiman S, Moniz C, Buxton-Thomas M 1994 Bone mineral density of the os calcis and lifestyle factors. In: Ring E F J, Elvins D M, Bhalla A K, editors. Current research in osteoporosis and bone mineral measurement. London. The British Institute of Radiology:27.

Svendsen O L, Hassager C, Christiansen C 1995a The response to treatment of overweight in postmenopausal women is not related to fat distribution. Int J Obese 19:496 - 502.

Svendsen O L, Hassager C, Christiansen C 1995b Age- and menopause-associated variations in body composition and fat distribution in healthy women as measured by dual energy x-ray absorptiometry. Metabolism 44:369 - 373.

Thompson D D 1980 Age changes in bone mineralization, cortical thickness, and haversian canal area. Calcif Tissue Int 31:5 - 11.

Tothill P 1986 Total body calcium and other bone mineral studies at Edinburgh. Proceeding of International Symposium held at Brookhaven National Laboratory New York on in-vivo body composition studies:213 - 220.

Tothill P 1989 Methods of bone mineral measurement. Phys Med Biol 34:543 - 572.

Tothill P, Pye D W 1992 Errors due to no-uniform distribution of fat in dual x-ray absorptiometry of the lumbar spine. Br J Radiol 65:807 - 813.

Tothill P, Avenell A, Reid D M 1994 Precision and accuracy of measurements of whole-body bone mineral: comparison between Hologic, Lunar and Norland dual energy x-ray absorptiometers. Br J Radiol 67:1210 - 1217.

Tothill P, Hannan W J, Cowen S, Freeman C P 1997 Anomalies in the measurement of changes in total body bone mineral by dual energy x-ray absorptiometry during weight change. J Bone Miner Res 12(11):1908 - 1921.

Uebelhart D, Duboeuf F, Meunier P F, Delmas P D 1990 Lateral dual-photon absorptiometry: a new technique to measure the bone density at the lumbar spine. J Bone Miner Res 5:525 - 531.

Unistat[R] Statistical Package 1995. Unistat Ltd, PO Box 383, Highgate, London N6 5UP.

Van Berkum F N R, Birkenhager J C, Van Veen L C P 1989 Non-invasive axial and peripheral assessment of bone mineral content: A comparison between osteoporotic women and normal subjects. J Bone Miner Res 4:679 - 85.

Venkataraman P S, Ahluwalia B W 1992 Total bone mineral content and body composition by x-ray densitometry in newborns. Paediatrics 90:767 - 770.

Vesterby A, Ullerup R, Bayer I et al 1991 Cortical bone: a major determinant for fracture risk in vertebral osteoporosis. J Bone Miner Res 6, Suppll:S274.

Vogel J M, Cline J R, Ulloa G A, McDonald R J 1979 Microcomputer based dual energy photon absorbtiometric bone mineral analyzer (VCH). IEEE Transact. Nucl Sci NS-26:576.

Vogel J M, Wasnich R D, Ross P D 1988 The clinical relevance of calcaneus bone mineral measurement. Bone mineral 535 - 538.

Wahner H W, Dunn W L, Riggs B L 1984 Assessment of bone mineral. Part 2. J Nuc Med 25(11):1241 - 1253.

Wahner H W, Fogelman H 1994 The evaluation of osteoporosis: dual energy x-ray absorptiometry in clinical practice.

Wark J D 1993 Osteoporosis: pathogenesis, diagnosis, prevention and management. In: Burger H G, editor. Baillieres Endocrinol and Metab 7:15 - 81.

Wasnich R D, Ross P D, Heilbrun L K, Vogel J M 1985 Prediction of postmenopausal fracture risk with use of bone mineral measurements. Am J Obstet Gynacol 153:745 - 51.

Wasnich R D, Ross P D, Heilbrun L K, Vogel J M 1987a Selection of the optimal skeletal site for fracture prediction. Clinical Orthopaedics 216:262 - 269.

Wasnich R D Ross P D Maclean C J et al 1987b A prospective study of bone mass measurement and spine fracture incidence in osteoporosis. In: Christiansen C Johnson J S and Riss B J editors (Osteopress APS Copenhagen) 1:377 - 378.

Waud C E, Lew R, Baran D T 1992 The relationship between ultrasound and densitometric measurements of bone mass at the calcaneus in women. Calcif Tissue Int 51(6):415 - 418.

Wellens R, Chumlea W C, Guo S, Roche A F, Reo N V, Siervogel R M 1994 Body composition in white adults by dual energy x-ray absorptiometry, densitometry, and total body water. Am J Clin Nutr 59:547 - 555.

Yamada M, lto M, Hayasahi K, Nakamura T 1993 Calcaneus as a site for assessement of bone mineral density: evaluation in cadavers and healthy volunteers. American Journal of Roentgenology 161(3):621 - 627.

Yang S-O, Hagiwara S, Engelke K, Dhillon M S, Guglielmi G, Bendavid E J, Soejima O, Nelson D, Genant H K 1994 Radiographic absorptiometry for bone mineral measurements of the phalanges: precision and accuracy study. Radiology 192:857 - 859.